

# UC Santa Barbara

## UC Santa Barbara Electronic Theses and Dissertations

### Title

Essays on the Distributional Effects of Environmental Policy

### Permalink

<https://escholarship.org/uc/item/8r34b29r>

### Author

Hernandez Cortes, Danae

### Publication Date

2021

Peer reviewed|Thesis/dissertation

University of California  
Santa Barbara

# **Essays on the Distributional Effects of Environmental Policy**

A dissertation submitted in partial satisfaction  
of the requirements for the degree

Doctor of Philosophy  
in  
Economics

by

Danae Hernández Cortés

Committee in charge:

Professor Kyle C. Meng, Chair  
Professor Kelsey Jack  
Professor Christopher Costello

June 2021

The Dissertation of Danae Hernández Cortés is approved.

---

Professor Kelsey Jack

---

Professor Christopher Costello

---

Professor Kyle C. Meng, Committee Chair

June 2021

Essays on the Distributional Effects of Environmental Policy

Copyright © 2021

by

Danae Hernández Cortés

A mis padres, Jorge Luis Hernández Mortera y Leticia Cortés  
Castillo, por todo su apoyo y amor incondicional.

## Acknowledgements

I have been very fortunate to have a large number of people that have provided their support and encouragement during my doctoral work. I would like to thank my dissertation committee, Kyle Meng, Kelsey Jack, and Christopher Costello for their support and patience. I would like to thank Kyle Meng for all of his advice and support throughout my Ph.D., I have learned a lot from him in the last few years and his excellent advice helped me become the researcher I am today. I would like to thank Kelsey Jack for all her detailed feedback that shaped my research, her generous mentorship during all the steps of my Ph.D., and for being my role model. I would also like to thank Christopher Costello for his guidance, for always encouraging me to think about big ideas, and for believing in me since I was a second-year student trying to start research in environmental economics. I would also like to thank:

Lint Barrage, Kelly Bedard, Javier Birchenall, Mark Buntaine, Olivier Deschenes, Rober Heilmayr, Peter Kuhn, Meera Mahadevan, Antony Millner, Andrew Plantinga, Dick Startz, Gonzalo Vazque-Bare, and Paige Weber for their feedback on my ideas and dissertation chapters at different stages of the work.

My wonderful coauthors, Eva Arceo-Gomez, Alejandro Lopez-Feldman, Paulina Oliva, Christopher Severen, Margaret Walls, and Erick Rosas-Lopez, for allowing me to learn from you. Our work has allowed me to learn from exciting projects and our discussions have helped me grow as a researcher.

Hazem Alshaikhmubarak, Juliana Helo, and Maria Kogelnik, without whom I would have not passed my first year. Thank you for all the great moments in Santa Barbara and for your friendship.

My cohort friends, Antoine Deeb, Dave Hales, Hongyuan Jin, Jason Maier, Ganghua Mei, Jaime Ramirez-Cuellar, Molly Schwarz, Ryan Sherrard, Kent Strauss, and Richard

Uhrig, for our shared laughs and for all your help throughout the years.

All the members of the Environmental Reading Group, in particular, Jeffrey Cross, Jimena Rico, and Emily Robertson, for reading my work over and over again and offering your thoughtful comments.

Mark Patterson for his help through all the administrative procedures, his commitment to graduate students is outstanding.

My parents, for all their love and support. No matter the distance you have always made me feel at home.

And Matthew Fitzgerald, for holding my hand through every significant and insignificant result. For always believing in me and giving me his unconditional love and support. This dissertation could not have been finished without him.

# Curriculum Vitæ

## Danae Hernández Cortés

### EDUCATION

- 2021 Ph.D. in Economics, University of California, Santa Barbara.  
2017 M.A. in Economics, University of California, Santa Barbara.  
2015 B.A. in Economics, Centro de Investigación y Docencia Económicas (CIDE), Mexico City.

### PUBLICATIONS

Arceo-Gómez, E., Hernández-Cortés, D. & López-Feldman, A. Droughts and rural households' wellbeing: evidence from Mexico. *Climatic Change*. Vol. 162. September 2020, pp. 1197-1212.

Chakraborti, L., Heres, D. & Hernández-Cortés, D. "Are Land Values Related to Ambient Air Pollution Levels? Hedonic Evidence from Mexico City". *Environment and Development Economics*. Vol. 24, Issue 3. June 2019, pp. 252-270.

López-Feldman, A. & Hernández-Cortés, D. "Cambio Climático y Agricultura: Una Revisión de la Literatura con Énfasis en América Latina" [*Climate Change and Agriculture: A Literature Review for Latin America*] *El Trimestre Económico*, 2016, 332:459-496.

### WORKING PAPERS

"The Distributional Consequences of Incomplete Regulation"

"Do Environmental Markets Cause Environmental Injustice? Evidence from California's Carbon Market" with Kyle Meng [NBER WP 27205]

"The Environmental Justice Dimension of the Mexican Emissions Trading System" with Erick Rosas López

### WORK IN PROGRESS

"Modal Choice and Income in Mexico City" with Paulina Oliva and Christopher Severen



“Migration as Adaptation? U.S. Relocations in Response to Hurricanes” with Margaret Walls.

## **CHAPTERS AND POLICY REPORTS**

Enhancing equity while eliminating emissions in California’s supply of transportation fuels with emLab Carbon Neutrality project team.

Carbon Neutrality and California’s Transportation Fossil Fuel Supply with emLab Carbon Neutrality project team.

“Mexican Rural Households’ Vulnerability and Adaptation to Climate Change” with Alejandro López-Feldman, Antonio Yúnez-Naude, J. Edward Taylor and Alan Hernández. White Paper for the Environmental Working Group of the UC-Mexico Initiative. August 11, 2017.

“The link between clean air policy and climate change policy in Mexico: Building an agenda for evaluation and research” with Paulina Oliva, Marco Heredia, Victor H. Paramo, Teresita Romero, Jose A. Ortinez, Giovanna Montagner, and Karla J. Lopez. White Paper for the Environmental Working Group of the UC-Mexico Initiative. October 23, 2017.

“MRV Blueprint for Road Freight Transport NAMA in Mexico” with Georg Schmid and Miriam Frisch. MRV Blueprint, German Ministry for the Environment, Nature Conservation and Nuclear Safety. 2015.

## **PRESENTATIONS**

**2021:** ASSA Virtual Meeting (discussant), University of Illinois Urbana Champaign (pERE Seminar), UCSB Grad Slam Competition, Microsoft Research Seminar, ASU College of Global Futures, UCSB Pacific Views Public Lecture, ZEW, University of Oregon, OSWEET, AERE 2021.

**2020:** UC Berkeley Climate Economics Workshop, UCSB Labor Lunch, IETA Webinar, Bren Environmental Justice Symposium, AERE 2020, NBER Summer Institute (egg-timer), Montana State University, 2020 Virtual UEA, Claremont McKenna College, SOCAE, CIDE, RIDGE Environmental Economics Workshop.

**2019:** TWEEDS, EAERE Summer School, UCLA-Institute of the Environment & Sustainability, Occasional Workshop in Environmental and Resource Economics (egg-timer).

**2018:** Resources for the Future’s research seminar, UCSB Environmental Lunch Series.

**2016:** Third Annual Congress of Economics and Public Policy at IBERO.

## FELLOWSHIPS, GRANTS, AND AWARDS

Winter 2021	UCSB Grad Slam Finalist and Winner of People's Choice Award.
Spring 2020	Economics UCSB Outstanding Undergraduate Course Teaching Assistant Award.
Spring 2019	UCSB Economics Research Quarter Competition.
Spring 2019	UCSB Economics Travel Grant.
Fall 2018	UCSB Economics Data Purchase Grant.
Spring 2016	UC MEXUS-CONACYT Doctoral Fellowship 2016-2021.
Spring 2014	Grant for visiting students by the Grants Committee of the Philosophical Faculties, Gothenburg, Sweden.

## RESEARCH POSITIONS

2017-Current	Graduate Student Researcher, Environmental Market Solutions Lab (emLab), UCSB.
Fall 2019	Research Assistant for Kelsey Jack, UCSB.
Summer 2018	Research Intern for Margaret Walls, Resources for the Future, Washington, D.C.
Summer 2016	Research Assistant for Paulina Oliva, UC-Mexus Initiative.
2014-2016	Research Assistant for Alejandro Lopez-Feldman and David Heres, CIDE, Mexico City.

## TEACHING

Winter 2021	Environmental Economics (Prof. Kyle Meng).
Spring 2020	Environmental Economics (Prof. Antony Millner).
Winter 2018	Probability and Statistics 109: Statistics for Economics (Prof. Michael Nava).
Fall 2017	Economics 9: Introduction to Economics (Prof. Cindy Benelli).
Spring 2016	Microeconomics I for Ph.D. students (Prof. Luciana Moscoso).
Fall 2015	Econometrics III: Microeconometrics (Prof. Florian Chavez-Juarez).
Fall 2014	Introduction to Economics (Prof. Eva O. Arceo-Gómez).

## SERVICE

2021	Undergraduate Honor's Thesis Advisor, UCSB.
2019-2020	Co-chair of WeSB, <i>We Are Economics at Santa Barbara</i> : Group aimed at promoting diversity in the Economics Department at UCSB.

2019 Undergraduate and Master's Thesis Committee Member, CIDE,  
Mexico City.

## **REFEREE**

*Journal of the Association of Environmental and Resource Economists, Science Advances,  
SAGE Open.*

## **COMPUTER SKILLS**

Stata, R, Python, ArcGIS, Amazon Web Services.

## **LANGUAGE SKILLS**

English (fluent), Spanish (native) and Swedish (basic).

## Permissions and Attributions

1. The content of Chapter 1 and Appendix A benefited from data shared by Noé Aguilar Rivera and CONADESUCA officials, José Fernández Betanzos and Pedro Aquino Mercado.
2. The content of Chapter 2 and Appendix B is the result of a collaboration with Kyle C. Meng. Use was made of computational facilities purchased with funds from the National Science Foundation (CNS-1725797) and administered by the Center for Scientific Computing (CSC). The CSC is supported by the California NanoSystems Institute and the Materials Research Science and Engineering Center (MRSEC; NSF DMR 1720256) at UC Santa Barbara.
3. The content of Chapter 3 is the result of a collaboration with Eva O. Arceo-Gómez and Alejandro López-Feldman, and has previously appeared in Arceo-Gómez, E. O., Hernández-Cortés, D., & López-Feldman, A. (2020). Droughts and rural households' wellbeing: evidence from Mexico. *Climatic Change*, 162(3), 1197-1212. The published version is available at: <https://doi.org/10.1007/s10584-020-02869-1>. The journal permits re-use of material in student's thesis with proper citation.
4. This dissertation was partially funded by CONACYT's Fellowship for Doctoral studies and UC-Mexus. I appreciate their support and funding during my doctoral studies.

## Abstract

Essays on the Distributional Effects of Environmental Policy

by

Danae Hernández Cortés

This dissertation consists of three essays that explore the distributional consequences of environmental policy and the impacts of environmental phenomena on vulnerable populations. These chapters use causal inference methods together with pollution transport models and remote sensing data to explain some of the causes of environmental inequities and analyze how environmental policy affects existing environmental disparities.

The first chapter studies the distributional consequences of incomplete regulation. Environmental policies that do not regulate all sources of pollution can be ineffective if firms are able to shift production processes from regulated to unregulated sources. Such incomplete regulation could affect the spatial distribution of pollution and who bears its burden. I study the consequences of incomplete regulation in the context of a policy intended to reduce pollution from mills that process sugarcane in Mexico. In response of the regulation, I show that mills shifted some processing to the fields where sugarcane is grown. I find that following the policy, sugarcane fields linked to regulated facilities increased fires by 14% which increased  $PM_{2.5}$  exposure by 6%. This pollution increase is associated with worse birth outcomes for nearby populations: I estimate decreases in birth weight associated to pollution from fires. Pollution increases were unevenly distributed across communities: agricultural fields tend to be located near poorer populations, and therefore the increase in fires increased their pollution burden. These results highlight that incomplete regulations can create environmental inequality when the unregulated sector is located near disadvantaged populations.

The second chapter, based on joint work with Kyle C. Meng, analyzes the environmental justice consequences of environmental markets. Environmental markets have been increasingly used to address environmental problems. By lowering the cost of regulation, markets are widely adopted for their allocative efficiency. However, there are growing concerns that these markets can reallocate pollution exposure, increasing pollution exposure in disadvantaged communities. We combine causal inference methods together with a pollution transport model to estimate whether California’s carbon market increased the pollution concentration gap between disadvantaged and other communities (the environmental justice gap). We find that the environmental justice gap was increasing prior to the introduction of the cap and trade program but it has since decreased after the introduction of the program. This finding suggests that market-based climate policies can have environmental justice co-benefits for disadvantaged communities.

The third chapter, based on joint work with Eva O. Arceo-Gómez and Alejandro López-Feldman, explores the effects of extreme weather events on rural welfare in Mexico. We study the poverty and labor effects of one of the worst droughts in Mexico in the past 70 years. We find that droughts have negative effects on rural households’ wellbeing: households that experienced a drought had lower per capita earnings and were 5 percentage points more likely to experience poverty than households that did not experience a drought. We also find that droughts have negative impacts on employment and schooling and these effects vary by gender: droughts reduce female employment and male school attendance. In addition, households with more experience with water scarcity are less likely to be affected by droughts. Given that climate change will increase the frequency and duration of droughts, our paper suggests that these extreme weather events are likely to become an additional threat to rural households in low and middle income countries.

# Contents

Curriculum Vitae	vii
Permissions and Attributions	xi
Abstract	xii
<b>1 The Distributional Effects of Incomplete Regulation</b>	<b>1</b>
1.1 Introduction . . . . .	1
1.2 Background . . . . .	7
1.3 Conceptual framework . . . . .	11
1.4 Data . . . . .	16
1.5 Empirical Specification . . . . .	23
1.6 Results . . . . .	29
1.7 Internalizing the costs of burning . . . . .	40
1.8 Conclusion . . . . .	42
<b>2 Do Environmental Markets Cause Environmental Injustice? Evidence from California’s Carbon Market</b>	<b>45</b>
2.1 Introduction . . . . .	45
2.2 Background . . . . .	50
2.3 Data . . . . .	55
2.4 Empirical Approach . . . . .	56
2.5 Results . . . . .	65
2.6 Discussion . . . . .	80
<b>3 Droughts and rural households’ wellbeing: Evidence from Mexico</b>	<b>82</b>
3.1 Introduction . . . . .	82
3.2 Data and methods . . . . .	85
3.3 Results and discussion . . . . .	95
3.4 Conclusions . . . . .	100

<b>A</b>	<b>Appendix to Chapter 1</b>	<b>102</b>
A.1	Mathematical Appendix . . . . .	102
A.2	Appendix Figures . . . . .	104
A.3	Appendix Tables . . . . .	105
<b>B</b>	<b>Appendix to Chapter 2</b>	<b>125</b>
B.1	Mathematical Appendix . . . . .	125
B.2	Appendix Figures . . . . .	129
B.3	Appendix Tables . . . . .	130
	<b>Bibliography</b>	<b>146</b>



# Chapter 1

## The Distributional Effects of Incomplete Regulation

### 1.1 Introduction

Environmental policies regulate productive activities that generate pollution. However, production can be reallocated across locations and within supply chains, escaping the reach of regulation. In such circumstances, the regulation may be “incomplete” and a firm may substitute production from a regulated to an unregulated activity, generating more pollution than absent regulation (i.e. leakage). Incomplete regulation has well established efficiency consequences [1, 2, 3]. Much less attention has been paid to how incomplete pollution policies can create winners and losers. It is possible that individuals living near regulated activities experience relative decreases in pollution while individuals near unregulated activities experience higher pollution levels.

This paper provides evidence of supply chain leakage and its distributional consequences in the context of the sugarcane industry in Mexico. Mexico is the world’s sixth largest sugarcane exporter and the sugarcane industry is an important part of the econ-

omy in southern and central Mexico. However, sugarcane harvest is a heavily polluting activity: it often requires fires in order to clean and cut the sugarcane. These fires have been found to affect in-utero health outcomes for affected populations [4].

The sugarcane sector in Mexico is an interesting setting for studying the distributional consequences of incomplete regulation. Sugar mills have two technological options for harvesting sugarcane: either mechanical or manual cut. When sugarcane is cut manually, it must also be burned since fires clean excess vegetation on the sugarcane plant. If sugarcane is not cleaned in the field using fires, it needs to go through an additional cleaning process that uses industrial boilers. Starting in 2014, the Mexican government implemented a policy aimed at decreasing sulfur dioxide emissions from industrial boilers (NOM-085-SEMARNAT-2011), requiring industrial facilities in all sectors of the economy using oil as fuel to reduce emissions each year by either substituting to less polluting boilers or acquiring abatement technologies. Facilities using biofuels were exempt from complying. Using rich data on sugar mills operations, technology, and production inputs and outputs, I show that regulated mills (facilities not using biofuels) shifted some of their processing to fields where sugarcane is grown, increasing the amount of agricultural fires. Furthermore, I show that sugar mills shifted the type of inputs used, altering the spatial distribution of pollution and the populations exposed to pollution.

The first part of the paper provides a conceptual framework to provide intuition for the expected effects under the Mexican regulation. A producer decides the optimal amount of inputs, and generates pollution associated with the use of either input. There are two types of households: low-wealth and high-wealth households. Households choose consumption goods, leisure, and medical expenditures to maximize utility but are affected by pollution via damages in health. A social planner implements an emissions tax to only one input, therefore the regulation being incomplete. This simple framework has three main predictions: 1) regulation to one input decreases the use of this input, 2)

regulation to one input increases the use of the other input (and its emissions) conditional on being gross substitutes, and 3) incomplete regulation will be regressive, affecting low-wealth households unless medical treatment goods are relatively low compared to the ratio of non-labor income and wages. Therefore, incomplete regulation can create distributional damages via pollution exposure to low-wealth households when pollution of the unregulated input increases.

The second part of the paper provides an empirical analysis of the effects of incomplete regulation in Mexico's sugarcane sector. I analyze whether the regulated facilities (using non-biofuel boilers) substituted cleaning sugarcane in the mills using regulated boilers with cleaning in the fields using agricultural fires, as well as the resulting pollution consequences. Using a difference-in-differences approach, I compare regulated and exempt facilities before and after the policy was implemented. I find that fields linked to regulated mills increased the number of sugarcane fires by 14% following the regulation and ambient concentrations of  $PM_{2.5}$  over these fields increased by 6%. I then analyze input substitution responses to the regulation using detailed data on various inputs and outputs used in sugarcane mills and fields. Consistent with an increase in fires, I find that fields linked to regulated mills increased manual cut workers by 5% and that the amount of sugarcane harvested using manual cut increased by 9%. I find no evidence of a change in the quantity of sugar produced as a result of the regulation and suggestive evidence of a decrease in processing efficiency.

The third part of the paper examines whether this change in pollution disproportionately affected vulnerable rural areas. Similar to other developing countries, the agricultural fields in Mexico are located near rural areas that have higher levels of poverty and socioeconomic vulnerability. Given my findings that fires and pollution in the sugarcane fields increased, groups living near the sugarcane fields could experience an increase in pollution as a result of the regulation. I use the results from my empirical analysis to

predict pollution exposure in the fields as a result of the policy and link this to exposed populations. Populations with greater socioeconomic vulnerability experienced relatively lower pollution prior to the policy but experienced a larger share of the pollution increases due to the policy. I find that the most vulnerable households experienced the largest increases in pollution relative to less vulnerable populations. These results highlight an important finding that has not been previously empirically documented in the literature: incomplete regulation can contribute to environmental inequality by altering the spatial distribution of pollution.

Finally, this paper estimates whether the increase in pollution from fires caused by input substitution is associated with worse health outcomes in affected areas. I use individual birth records for the period 2012-2017 obtained from the Mexican Health Ministry to estimate the impacts of pollution exposure on birth outcomes such as birth weight, gestational length, very low birth weight (<1,500 g), and very preterm birth (< 32 weeks). I link the fires location to the mother's locality of residence (rural village or city) and estimate the impact of pollution exposure associated with fires caused by the policy on birth outcomes. I find that an additional  $\mu\text{g}/\text{m}^3$  increase in pollution is associated with a decrease in birth weight of 1 gram, a 2% increase in the incidence of very low birth weight, a 3% increase in the incidence of very preterm birth, and an insignificant decrease in gestational length. These results add to the extensive literature examining the impacts of air pollution on health [5], and in particular, the impact of pollution on birth outcomes [6]. Consistent with [7], I find that increases in pollution caused by sugarcane fires are associated with worse birth outcomes for impacted localities. These results further document the negative impacts of incomplete regulation when producers can substitute the inputs they use and these create higher pollution to nearby communities.

Using the estimates found, I calculate that a tax of \$39 USD per ton of sugarcane (average ton of sugarcane is \$650 USD) would internalize the impacts of sugarcane burning

on affected populations caused by the regulation of pollution emissions in the mill.

This paper provides two main contributions. First, it contributes to the leakage literature by documenting a specific mechanism through which firms substitute pollution from regulated to unregulated sources: input substitution. If these substitution patterns increase emissions or generate additional social costs, environmental regulation can backfire, creating more pollution than otherwise absent regulation. Others have found that the amount of leakage induced by a regulation depends on the structure of the sector and the producers' responses to the regulation [2, 8]. Firms can substitute pollution to unregulated media [1], sectors [9], other facilities [10], and countries with laxer regulations [11, 12]. By focusing on one sector and using detailed individual production data, I am able to unravel how leakage can alter the production processes to adjust to the regulation. This paper highlights a previously overlooked mechanism through which incomplete regulation can create leakage: firms can shift towards dirtier, unregulated inputs. In addition, this paper provides evidence of leakage from point sources (industry) to non-point sources (agricultural fires). Shifting pollution from point sources to non-point sources could be particularly problematic since non-point sources are harder to regulate due to their dispersed nature [13]. In so doing, I contribute to another literature that explores the role of regulation in incentivizing firms or individuals to adjust margins to avoid regulation [14, 15].

Second, I contribute to the literature on environmental justice and inequality in the distribution of pollution. Agricultural fields are mainly located in rural areas, that are on average poorer and face higher socioeconomic vulnerability than their urban counterparts. By increasing the number of fires and pollution in these areas, regulation aimed at point sources with the potential to reallocate production to non-point sources could increase pollution in already disadvantaged areas. The environmental justice literature has long studied the unequal distribution of environmental hazards finding that minority

and poor populations face higher pollution levels than other communities [16, 17, 18, 19]. Studies have found that high polluting facilities and toxic waste sites are mostly located in poor and minority communities in the United States [20, 21]. Recent literature highlights the potential of environmental regulations to have distributional consequences across sectors in the economy [22] and other studies have found that gains from environmental regulation are unevenly distributed across demographic groups [23, 24, 25]. In the case of Mexico, studies have found that larger polluters tend to be located near poor, marginalized populations [26, 27]. This paper suggests another source of environmental injustice: incomplete regulation can cause pollution leakage to vulnerable populations.<sup>1</sup> Given that pollution damages could be higher in low income communities due to low access to health care and defensive investments, regulations that increase agricultural burning could generate disproportionate pollution damages to rural populations.

This paper also finds that despite increasing pollution in rural areas, input relocation can have positive employment benefits. Some studies have documented the tradeoff between health and local economic outcomes in developing countries. For instance, [29] show the wealth-health tradeoff due to mining activities in Africa, where mines increase asset wealth in nearby communities coexist with increases on anemia and stunting for young children. [4] shows that the increase in economic activity during the sugarcane harvest is also accompanied by worsening health outcomes for newborns in Brazil. By showing that local employment for manual work increases together with increases in pollution, this paper adds to the literature examining this health-local economic outcomes tradeoff. However, other studies have shown that regulation of polluting technologies might not need be accompanied by labor losses. In the case of sugarcane production, Costa and Lima (2020) show that harvest mechanization in Brazil decreased employment

---

<sup>1</sup>Other studies have analyzed additional mechanisms of environmental injustices in the case of the U.S, such as incomplete information about pollution damages and hidden pollution [28] and mergers (Jacqz, 2020).

in the agricultural sector but increased employment in the manufacture and services sectors.

The results of this paper extend beyond the sugarcane industry in Mexico. For instance, several other studies have found supporting evidence of the “pollution haven effect” which highlights that environmental damage might be shifted towards places with less strict regulation or unregulated places [11, 30]. Other examples of where this could occur are global chains for processed food when regulation is incomplete between two countries. My results suggest that regulators attempting to regulate one input need to be aware of firms’ responses in unregulated sectors and the location of these sectors relative to disadvantaged communities.

The rest of the paper proceeds as follows. Section 1 describes the sugarcane sector and boiler regulation. Section 2 provides a simple conceptual framework of input substitution when regulation is incomplete. Section 3 describes the data. Section 4 presents the empirical specification. Section 5 explains the effects of regulation-induced pollution redistribution towards non-point sources and its distributional consequences as well as the health effects of incomplete regulation. Section 6 calculates a tax that would internalize the social costs caused by sugarcane burning. Section 7 concludes.

## 1.2 Background

### 1.2.1 Sugarcane harvest and production in Mexico

Sugarcane is the main input of sugar production, which is processed in nearly 60 mills across Mexico. The high demand for sugar in Mexico (on average 80 pounds of sugar per capita consumption per year) makes sugarcane among the 10th highest demanded crops in Mexico and Mexico is the 6th largest global sugar exporter. Sugar mills have

two technological options for harvesting sugarcane: either mechanical or manual cut. When sugarcane is cut manually, it must also be burned. These fires facilitate harvest by cleaning the excess of vegetation in the sugarcane plant. If sugarcane is not cleaned in the field using fires, it would need to go through an additional cleaning process that uses machines powered by industrial boilers.

Sugarcane is first harvested in the field and then sent to process at the mill. Given that there are only 60 active mills in Mexico that process nearly 865,000 hectares of sugarcane, the harvest needs to be staggered from mid-November to late May.<sup>2</sup> The fields are usually located within driving distance from the mills and mills in general own the fields where they source the sugarcane.<sup>3</sup> This also means that mill management has a decision power over the type of harvesting technique used. Important to note, there is no quality difference between sugarcane cut using controlled fires and sugarcane cut using machines. After sugarcane has been cut, the sugarcane is transported to the sugar mill where it is then processed. Sugarcane cut using machines goes through an additional process of cleaning the plant that uses equipment fueled by boilers. These boilers can either use diesel, fuel oil, biofuels, or natural gas. After the sugarcane is clean, the sugarcane goes through another process to grind the sugarcane and extract its caloric content to then crystalize and refine the sugar in the mill.

The sugar producing industry is an important part of the sugarcane regions. The Mexican Agricultural Agency estimates that sugarcane production has approximately 440,000 direct employees and 2,000,000 indirect employees.<sup>4</sup> Although the harvest season

---

<sup>2</sup>Sugarcane needs to be processed within the same week after harvest or it might lose its caloric content, creating less sugar. However, after sugarcane has been converted into sugar, sugar can be stored for long periods. After sugar has been produced, mills send the sugar to individual packaging facilities that would distribute them for retail.

<sup>3</sup>Mills also report part from their production coming from private small landowners. However, the smallholders have contracts with specific mills. The mills are responsible of providing inputs to these smallholders such as machines to harvest sugarcane in the case of mechanical cut and trucks to transport the sugarcane to the mills.

<sup>4</sup>Studies have documented the importance of sugar production for local employment and development.



brings employment to these regions, it comes with a cost: according to [32], sugarcane fires are harmful because they raise particulate matter concentrations (96% of these particles are respirable), CO and NO<sub>x</sub> which have many adverse health consequences. Moreover, sugarcane-harvest fires have been associated with negative health outcomes to nearby communities. For instance, [4] found that in utero exposure to pollution from sugarcane fires reduces birth weight and gestational age at birth in Brazil.<sup>5</sup> Sugar processing after sugarcane has been harvested is also heavily polluting. For instance, the average sugar mill generates, on average, 2,427.65 tons of NO<sub>x</sub> per year which makes it one of the most heavily polluting industries in the country. To put in context, the average California cement facility generates 1,364.2 tons of NO<sub>x</sub> per year.<sup>6</sup>

### 1.2.2 Regulating pollution from sugar mills

In 2011, the Mexican government strengthened the maximum pollution limits of all stationary sources via the NOM-085-SEMARNAT-2011. The regulation targeted many sectors including cement production, chemical manufacturing, and general industrial activities. The regulation stated that beginning in 2014-2015 all pollution sources must decrease the emissions related to the combustion process.<sup>7</sup> The regulation stipulated that starting in 2011, the emissions from new and existing equipment must be reported to the environmental agency in Mexico and after 2015, the new emission standards need to be attained for all the combustion sources. The regulation stated an annual reduction

---

For example, [31] show that households living within a few kilometers of historical sugar factories have 10% higher per-capita consumption than other households living further away.

<sup>5</sup>Other studies have shown that exposure to smoke from fires also increases early-life mortality [33, 34] and affects children's human capital outcomes such as exam performance [35]. Agricultural burning can also increase deaths from respiratory problems for adults [36].

<sup>6</sup>Data on mills emissions are available for 2017 via the National Registry of Emissions (RENE) and data on California's cement emissions are available in CARB pollution mapping tool.

<sup>7</sup>The regulation in 2011 stipulated that the beginning of the compliance period should be 2014. However, in 2012 the beginning of the compliance period was extended by one year. Therefore, the beginning of the compliance period is 2015.

of 1,000 ppmv of SO<sub>2</sub> in 2015 relative to pre-existing levels and a reduction of additional 100 ppmv per year until 2019. In case of non-attainment at the facility level, the facilities will have to pay a fee to the environmental agency depending on the exceeding emissions. Facilities that used biofuels as the main source of energy were exempt from the policy.

In the case of the sugarcane industry, the regulated equipments were mainly used as a substitute in the cleaning process. This meant regulating the boiling of (unburnt) sugarcane for facilities that are not using biofuels in their operations. As a result of the policy, non-exempt facilities could respond by either complying with the regulation, lowering the amount produced. or by shifting technologies in the field to decrease the emissions coming from the regulated technology.

The regulation is enforced by the Mexican Environmental Protection Agency's regulator entity, PROFEPA. However, in the case of the sugarcane industry, the Mexican Agriculture Agency through the sugarcane regulator entity, the *Comité Nacional para el Desarrollo de la Caña de Azúcar*, CONADESUCA, also monitors annual compliance. At the time of the regulation, biofuels were not regulated. However, there have been some recent efforts to extend environmental regulation to cover sugar mills using biofuels. For instance, the PROY-NOM-170-SEMARNAT-2017 is expected to regulate mills using biofuels once it is approved by the Mexican government.

Sugarcane burning is not regulated in Mexico.<sup>8</sup> Regarding agricultural fires, the NOM-015-SEMARNAT/SAGARPA-2007 specifies a few rules for agricultural burning. For instance, farmers can only burn one plot if they do not have contiguous fires in an adjacent plot. Farmers should notify neighboring plots in case of wishing to use a controlled fire and notify local authorities if the fire grows uncontrollably. However, sugarcane harvest fires are not regulated.

---

<sup>8</sup>Other countries have started regulating sugarcane burning. For example, Brazil's sugarcane growing regions have started adopting mechanical harvesting methods in the last decades and has nearly complete adoption by 2013 (Davis, 2016).

In this paper, I leverage variation induced by the regulation to compare regulated and unregulated facilities before and after the regulation was introduced.<sup>9</sup> The following section provides a simple model of input decision with incomplete regulation and households' welfare. The objective of the following section is to provide intuition on the possible producer responses under the new regulation.

### 1.3 Conceptual framework

This section presents a conceptual framework of incomplete pollution regulation and its welfare effects to nearby populations. The objective of this section is to explain under which conditions incomplete regulation can create input substitution. Similarly, I derive conditions under which incomplete regulation can be regressive, affecting poor households via pollution damages more than when no regulation exists.

*Producer maximization problem:* A producer decides between labor ( $l$ ) and capital ( $k$ ) that are used in the production of a homogeneous good that is competitively produced. The producer is a price taker in both the labor and capital markets (input prices are  $w$  and  $r$ , respectively, and both are competitive input markets) and faces a Constant Elasticity of Substitution (CES) production function.

$$Y = [k^\sigma + l^\sigma]^{1/\sigma}$$

The use of each technology produces pollution emissions ( $\gamma_l$  and  $\gamma_k$ ) that are an increasing

---

<sup>9</sup>One concern using this specification is that non-exempt facilities could change regulation status after the policy started in order to be exempt of the policy (i.e. regulation-induced technology adoption) which changes the composition of the control and treatment groups. This is an unlikely concern in this setting. In general, the decision to invest in boilers for the facility operations/electricity generation is a long-run decision, whereas this paper focuses in the three years (short run) of the policy. Moreover, I obtained data on all of the mills' industrial investments in the recent years and electricity generation permits and only one mill invested in a new boiler in 2016 (Ingenio San Francisco Ameca that acquired a biofuel boiler), most of the studied mills' last investment was done during 1980-2000.

function of input use.

$$\gamma_k = f(k) \quad \text{and} \quad \gamma_l = f(l)$$

The representative producer chooses  $l$  and  $k$  to maximize:

$$\pi = p[k^\sigma + l^\sigma]^{1/\sigma} - rk - wl \quad (1.1)$$

The optimal share between  $l$  and  $k$  is given by:

$$l^* = \left(\frac{w}{r}\right)^{\frac{1}{\sigma}} k^* \quad (1.2)$$

Optimal use of  $l$  and  $k$  is given by:

$$l^* = \bar{y} \left[ \frac{w^{\frac{\sigma}{\sigma-1}}}{r^{\frac{\sigma}{\sigma-1}} + w^{\frac{\sigma}{\sigma-1}}} \right]^{1/\sigma} \quad \text{and} \quad k^* = \bar{y} \left[ \frac{r^{\frac{\sigma}{\sigma-1}}}{r^{\frac{\sigma}{\sigma-1}} + w^{\frac{\sigma}{\sigma-1}}} \right]^{1/\sigma}$$

*Households' maximization problem:* There are two types of households: low-wealth households ( $L$ ) and high-wealth ( $H$ ) households. Low-wealth households' utility is a function of consumption goods  $x_L$ , leisure  $(1 - l_L^s)$ , where  $l_L^s$  is labor supplied, and health  $H_L$ , where  $H_L = \mathcal{H} + \beta M_L(\gamma_l) - D_L(\gamma_l)$ .<sup>10</sup>  $\mathcal{H}$  is a health stock that is determined by external and genetic factors,  $M_L(\gamma_l)$  denotes medical care, and  $D_L(\gamma_l)$  is pollution exposure created by emissions linked to the use of  $l$ .<sup>11</sup> Low wealth households decide the amounts of consumption goods, the labor to supply for the production of the good explained in the producers' maximization problem, and the amount of medical care to consume taking prices ( $c_M$  and  $c_x$ ) as exogenous.<sup>12</sup> Low-wealth households obtain wages  $w$  associated with labor supplied and other non-labor sources of income,  $I_L$ . High-wealth

<sup>10</sup>This health expression is similar to [5], however, their health function also depends on avoidance behavior and the marginal productivity of labor also depends on pollution ( $w(\gamma_l)$  for this case).

<sup>11</sup> $\beta$  is the share of medical expenses used, which means that  $0 < \beta \leq 1$

<sup>12</sup>I also assume that damages  $D(\gamma_l)$  are an increasing function of pollution exposure  $\gamma_l$  and the demand for medical care also increases in  $\gamma_l$ .

households' utility depends on consumption goods,  $x_H$ , and health,  $H_H$ , where  $H_H = \mathcal{H} + \beta M_H(\gamma_k) - D_H(\gamma_k)$ .  $D_H(\gamma_k)$  are the damages caused by emissions associated with the use of  $k$  and  $M_H(\gamma_k)$  is the medical care, which depends on pollution emissions associated with  $k$ . High-wealth households receive a constant share of total output produced  $\phi\bar{Y}$  and non-labor sources of income,  $I_H$ .

Low wealth households' maximization problem is given by:

$$\begin{aligned} \max_{x_L, l_L^s, M_L} \{ & u_L(c_L, l_L^s, M_L) = \log(x_L) + \log(1 - l_L^s) + \log(\mathcal{H}_L + \beta M_L(\gamma_l) - D_L(\gamma_l)) \} \\ \text{s.t. } & c_x x_L + c_m M_L(\gamma_l) = w l_L^s + I_L \end{aligned}$$

High wealth households' maximization problem is given by:

$$\begin{aligned} \max_{x_H, M_H} \{ & u_H(x_H, M_H) = \log(x_H) + \log(\mathcal{H}_H + \beta M_H(\gamma_k) - D_H(\gamma_k)) \} \\ \text{s.t. } & c_x x_H + c_m M_H(\gamma_l) = I_H + \phi\bar{Y} \end{aligned}$$

The optimal  $l_L^s$ ,  $x_L$ , and  $M_L(\gamma_l)$  demanded are given by:

$$\begin{aligned} l_L^s &= \frac{w(c_M + \beta) - \beta I_L + c_M(D_L(\gamma_l) - \mathcal{H})}{w(c_M + 2)} \\ x_L &= \frac{1}{c_x} \left[ \frac{w(2 - \beta) + \beta I_L + c_M(\mathcal{H} - D_L(\gamma_l))}{c_M + 2} \right] \\ M_L(\gamma_l) &= \frac{\beta(I_L + w) + 2(w + D_L(\gamma_l) - \mathcal{H})}{\beta(c_M + 2)} \end{aligned}$$

The optimal  $x_H$  and  $M_H(\gamma_k)$  demanded are given by:

$$M_H(\gamma_k) = \frac{1}{2c_M} \left[ I_H + \phi\bar{Y} + \frac{1}{\beta}(D(\gamma_k) - \mathcal{H}) \right]$$

$$x_H = \frac{1}{c_x} [I_H + \phi \bar{Y}]$$

*The effect of incomplete regulation on technology use and households' welfare:* Exogenous variation from the regulation establishing pollution limits to industrial boilers allows me to quantify the effects of incomplete regulation on input substitution between  $k$  and  $l$  empirically. Mechanical cut implies higher use of boilers, therefore this technology is capital intensive and is considered as  $k$ . Manual cut, on the other hand, is labor intensive and therefore is considered as  $l$ . Given that both technologies co-exist in the sugar production process, I model the choice between each technologies under incomplete regulation. The following paragraphs describe the predicted effects of incomplete regulation on labor, capital use, emissions, and wages.

**Prediction 1:** a tax on capital emissions decreases the demand for capital-intensive technology.

For this prediction, let's assume that a regulator who aims at decreasing the production of emissions coming from capital introduces a tax ( $\tau$ ) for emissions generated by capital such that the new producers' maximization problem becomes:

$$\pi = p[k^\sigma + l^\sigma]^{1/\sigma} - rk - wl - \tau\gamma(k) \quad (1.3)$$

$$\frac{\partial k^\tau}{\partial \tau} = -\bar{y} \left[ 1 + \left( \frac{w}{r + \tau\gamma'_k(k)} \right)^{\frac{\gamma}{\gamma-1}} \right]^{\frac{1-\gamma}{\gamma}} \left( \frac{w}{r + \tau\gamma'_k(k)} \right)^{\frac{\gamma}{\gamma-1}} \left( \frac{w\gamma'_k(k)}{(r + \tau\gamma'_k(k))^2} \right) < 0$$

**Prediction 2:** a tax on capital emissions increase (decrease) the demand for labor-intensive technology if labor and capital are substitutes (complements).

Expression (1.2) becomes:

$$l^\tau = \left( \frac{w}{r + \tau\gamma'_k(k)} \right)^{\frac{1}{\sigma}} k^\tau \quad (1.4)$$

The optimal demand of  $l$  is given by:

$$l^\tau = \bar{y} \left[ \frac{w^{\frac{\sigma}{\sigma-1}}}{(r + \tau\gamma'_k(k))^{\frac{\sigma}{\sigma-1}} + w^{\frac{\sigma}{\sigma-1}}} \right]^{1/\sigma} \quad (1.5)$$

Taking the derivative of (1.5) with respect to  $\tau$ :

$$\frac{\partial l^\tau}{\partial \tau} = - \left( \frac{\bar{y} w^{\frac{1}{\sigma-1}}}{\sigma - 1} \right) \left[ \frac{(r + \tau\gamma'_k(k))^{\frac{1}{\sigma-1}} \gamma'_k(k)}{\left[ (r + \tau\gamma'_k(k))^{\frac{\sigma}{\sigma-1}} + w^{\frac{\sigma}{\sigma-1}} \right]^{\frac{1+\sigma}{\sigma}}} \right]$$

By the CES properties, gross complements ( $\sigma > 1$ ) implies  $\sigma - 1 > 0$ , which means that  $\frac{\partial l^\tau}{\partial \tau} < 0$ . Conversely, gross-substitutes implies that  $\frac{\partial l^\tau}{\partial \tau} > 0$ . Therefore, regulating the emissions from capital when labor and capital are gross-substitutes means a higher use of the labor intensive technology and increased emissions from its use.

**Prediction 3:** low-wealth households will be worse off under incomplete regulation on  $k$  unless  $\frac{I_L}{w} > \frac{c_M(2-\beta)}{\beta}$ . High-wealth households will only be worse off under regulation on  $k$  if  $\beta(I_R + \phi Y(\tau)) < 2D(\gamma_k)c_M$ . For this derivation, see Appendix A.

The conceptual framework predicts that under incomplete regulation, the emissions from the regulated technology decrease whereas the use of the unregulated technology and its emissions increase, conditional on being substitutes in the production process. This increase in pollution is regressive, affecting low-wealth households utility unless the ratio between non-labor income sources,  $I_L$ , and labor wages,  $w$  is larger than the price of medical treatment discounted by  $\beta$ .<sup>13</sup>

These results have implications for the setting studied in this paper. Under the new regulation of sugar mills, we can expect that regulating the technology used to process sugarcane in the mill translates into higher use of its substitute: manual cut.

<sup>13</sup>Note that this condition only holds in the case that pollution does not affect productivity, (i.e.  $w$  does not depend on  $\gamma_l$ ).

This prediction implies a shift from the capital intensive technology towards the labor intensive technology, increasing its associated pollution emissions. The following sections examine the impact of the policy on input substitution and its consequences for pollution emissions.

## 1.4 Data

This paper uses a combination of remote sensing data and administrative data. The remote sensing data allows me to measure fires, land use, and pollution. The administrative data from sugarcane producers in Mexico allows me to document input-use responses to the regulation. Combining these data sources, I created an exhaustive dataset of weekly inputs use and outputs, and daily associated fires and pollution from 2012 to 2017. This section provides a description of the data sources and the construction of all the relevant variables.

### 1.4.1 Fires data

I obtained data on the universe of daily fires in Mexico from the Active Fire Data product based on the NASA's Visible Infrared Imaging Radiometer Suite (VIIRS). This product provides data on all fires occurrences starting in February 2012. NASA detects fires in a  $375 \text{ m} \times 375 \text{ m}$  grid and provides the centroid of the pixel with a fire event.<sup>14</sup> I restricted the fires to the months November to May to cover the sugarcane harvest season because sugar mill operations are concentrated in these months.<sup>15</sup>

---

<sup>14</sup>The average size of sugarcane fields in Mexico is approximately 4.7 hectares [37]. This means that the VIIRS pixel covers approximately two average fields.

<sup>15</sup>CONADESUCA reports the start and end of the harvesting season. For the years in the sample, the harvest begins around the third week in November and finishes at the end of May.



### 1.4.2 Sugarcane coverage data

In order to identify the extent of sugarcane fields in Mexico, I used data from Mexico's National Committee for Sugarcane Sustainable Development (CONADESUCA). The data include confidential information of sugarcane plots in Mexico. CONADESUCA used Landsat 8 images from 2014-2015 to map the sugarcane plots in Mexico. To do so, they classified sugarcane fields using the Normalized Difference Vegetation Index (NDVI) and revalidated using Landsat data and field visits.<sup>16</sup> Given the confidentiality of the data, CONADESUCA linked the fires centroids from VIIRS with the sugarcane fields polygons for this project. Therefore, I am able to identify whether a particular fire event occurred inside a sugarcane polygon. I obtained a total of 23,106 sugarcane fires for the study period 2012-2017.<sup>17</sup> These fires are classified as sugarcane-harvest fires.

### 1.4.3 Mill characteristics

The geographic location of all sugar mills was obtained from the National Statistical Directory of Economic Units from INEGI that is based on the Economic Census 2009 performed by INEGI. The location information about the mills was then linked with detailed mill-level production data provided by the Sinfocaña system updated by CONADESUCA.<sup>18</sup> Figure A.1 shows the geographic coverage of the sugar mills along with their exempt classification based on fuel use pre-policy. The fuel use pre-policy was

---

<sup>16</sup>After processing the NDVI, CONADESUCA calculated the average lifetime of sugarcane to estimate the plant's maximum growth in order to correctly monitor the NDVI changes. They estimated the month with the highest sugarcane height and cross-validated with other SPOT images from Landsat. Furthermore, they performed field visits to sugarcane fields in Mexico to cross-validate the information.

<sup>17</sup>In order to correct for measurement error between the VIIRS resolution and the sugarcane fires provided by CONADESUCA, I also created a 50 m buffer around the fires and classified as sugarcane fires other fires in the VIIRS dataset that were not classified as a sugarcane fire but that were captured at the same date, time, and within the 50 meters of the sugarcane fires. This was done in order to account for fires that are not classified as sugarcane fires. This procedure yielded a total of nearly 200 additional sugarcane fires.

<sup>18</sup>Source: <https://www.siiba.conadesuca.gob.mx/infocana/>

obtained from CONADESUCA sustainability annual reports. A mill is considered to be part of the non-exempt group if it did not use biofuels in their production process or if it did not use biofuels for co-generate electricity for its production activities during 2010 and 2011.<sup>19</sup> Table A.1 shows descriptive statistics for facilities using biofuels (exempt) and oil (non-exempt). Exempt facilities have on average lower daily fires and lower mechanical and manual sugarcane harvested. The empirical specification accounts for underlying differences in these facilities by using a difference-in-differences design.

#### 1.4.4 Sugarcane and sugar production data

Detailed weekly administrative data of inputs and outputs at the mill level was obtained from CONADESUCA's Sinfocaña system. The data includes information on inputs and outputs for each mill and its associated fields. Information on inputs includes the total number of field workers, total harvested sugarcane (tons and hectares), total sugarcane cut used manual and mechanical cut, hours worked, among other information from the fields.<sup>20</sup> The outputs information includes raw processed sugarcane, processed sugarcane per day, total sugar produced, total sugar produced per day of operation, sugar-by products like alcohol and molasses, and indicators of sugar production efficiency. The sugar mills also provide information on energy and production efficiency as well as compliance to the NOM-085-SEMARNAT-2011 (previously known as NOM-085-ECOL-1994).<sup>21</sup>

I also obtained agricultural wages per day for sugarcane workers at the municipality

---

<sup>19</sup>I obtained information on biofuel use for 50 mills. I obtained information of the 10 additional mills that used oil either for generating electricity or oil-fueled boilers in their production using CONADESUCA annual reports, therefore being regulated by the NOM-085-SEMARNAT-2011. I cross-validated the exempt vs. non-exempt definition using a list of compliance at the mill level provided by PROFEPA.

<sup>20</sup>This information includes information on the fertilizers, the number of days of active production, pests in fields, and observed temperature and precipitation.

<sup>21</sup>Source: <https://www.siiba.conadesuca.gob.mx/sicostossustentabilidad/consultapublica/IndicadoresPublico.aspx?app=sustenta>

level. The data is based in payroll contributions to the Social Security Institute (*Instituto Mexicano del Seguro Social*, IMSS). The data contains total workers by sector, age, and gender at the district (municipality) level. IMSS covers mainly formal workers and might not be a good representation of agricultural workers in subsistence agriculture areas. However, in the case of sugarcane production, sugarcane harvest workers are among the workers with social security access. The data is reported at the municipality level, not at the mill level like the rest of the results from mills, therefore, for the analysis of wages I drop the municipalities that have more than one mill within the municipality with different regulation status (two municipalities, four sugar mills total).

### Linking fires and sugar mills

I linked sugar mills to their distribution fields by calculating the distance from the sugarcane fires to all existing mills and associated the fires to the closest mill. Distance to the mill is likely a good indicator on property: sugarcane needs to be processed within a week of being harvested or it can lose caloric content and produce less sugar.<sup>22</sup> Indeed, Figure A.2 shows that most of the sugarcane is processed within 48 hours after being cut. Furthermore, sugar mills usually own the sugarcane fields that supply to them and incur in the transportation costs from the fields using their own trucks and lend mechanical harvest technologies to smallholders.<sup>23</sup> To the extent that there are not consistent differences between non-exempt and exempt facilities in misassignment on the fires, measurement error linking facilities and mills is likely to downward bias my estimates.

I corroborated the link by obtaining information on a random sample of the sup-

---

<sup>22</sup>Within this week, sugarcane needs to be transported from the mill to the field, wait to be weighted by mill workers, cleaned, and processed.

<sup>23</sup>In some cases small landholders or *Ejidors* own fields of sugarcane and eventually sell the sugar to a mill. These individual transactions are very hard to track and there is no consistent record of it. However, I performed interviews to sugar mill workers and they mentioned that this is a small percentage.

ply fields for the mills in the state of Veracruz, Mexico and calculated the overlap of the sugarcane harvest fires definition with these fires. The sample was obtained by the Mexican government in collaboration with the Universidad Veracruzana and contains sampling points of sugarcane fields in the state of Veracruz, the largest sugarcane producer state.<sup>24</sup> I created a buffer of 300 and 500 meters surrounding the sampling sites and compared the mills association of these fires. I found that I correctly classified 80% of the fires based on 2009 data. Figure A.3 shows an example of the geographic extent of this data and the sugarcane fires data. Figure A.4 shows the classification (either matched or missassigned) of the mills in this sample, showing that most fires and mills are assigned correctly, except two mills where their missassigned fires are a larger share of total fires.<sup>25</sup> Section 4 shows the results of the empirical specification only considering the fires inside the buffers of the sampling sites. The results show higher magnitudes and significance level compared to the full set of fires.

Figure A.5 shows the distance distribution of the sugarcane fires with respect to mills. As a comparison, I also show the distance to other fires, most of the sugarcane fires are within 20-70 kilometers from a sugar mill, which is consistent with field interviews to sugar mill administrative staff. Important to note, sugar mills sell the sugarcane that they harvest to other mills when they do not have enough capacity to process it within the week it was harvested. This could be a problem since I would be miscalculating the amount of sugarcane processed with either biofuels or oil/coal. Figure A.6 shows the total sugarcane harvested by the own mill and the amount either sold or received from other

---

<sup>24</sup>The data was obtained with support from Noe Aguilar Rivera who shared the data of the project “Digitalización del Campo Cañero en México para Alcanzar la Agricultura de Precisión de la Caña de Azúcar”. This was a sampling effort from part of the Mexican government and the Universidad Veracruzana to collect data of a random sample of the sugar mills and their corresponding sugarcane fields in the state of Veracruz in 2009.

<sup>25</sup>One limitation of this study is the lack of data on field ownership for other states. However, the distance assignment is likely a smaller problem in states where sugar mills are located farther away from each other, given the biological and production characteristics of sugarcane processing.

mills. The vast majority of sugarcane processed by the mills is originally harvested either in their plots or in fields owned by small landholders that sold the sugarcane directly to the mills.

### Other agricultural fires

To perform a falsification test, I obtained the number of agricultural fires that are not associated to sugarcane areas in order to obtain a fires “placebo” group. I used the rest of the non-sugarcane fires in the VIIRS data not classified as belonging to a sugarcane polygon by CONADESUCA. I classified them as agricultural fires (NSHF) if they were within an agricultural land pixel using 2012 land use data from the Mexican Land Use data series V (*Serie V de Uso de Suelo y Vegetación*) from INEGI. I followed the same procedure to classify each fire in the mill “catchment” area than for the sugarcane fires. Figure A.5 shows the distance distribution between these agricultural fires and the mills. Compared to the sugarcane fires, these fires are located further away from the mills, which is what we would expect if these plots were not used as sugarcane fields. As another robustness check, I also classified fires as “non-harvest sugarcane fires” if these fires occurred within a sugarcane field but during the months June-October, outside the usual harvest window for sugarcane.<sup>26</sup>

### 1.4.5 Pollution data

I obtained daily pollution data from NASA’s MERRA-2 aerosol optical depth product.<sup>27</sup> The daily pollution data has a  $0.5^\circ \times 0.625^\circ$  resolution. This reanalysis AOD product has information of  $\text{SO}_2$  and I calculated  $\text{PM}_{2.5}$  following [38]. This methodology

---

<sup>26</sup>These fires are usually related to sugarcane residue burning post-harvest activity and occur after the main harvesting season.

<sup>27</sup>In specific, we used the diurnal, time-averaged, single level assimilation, Aerosol Diagnosis V5.12.4 (M2TUNXAER).

is analogous to other work that uses satellite data to measure pollution in areas that are remote and without a close pollution monitoring station [39]. I linked the fires and mills coordinates to the pollution pixels and calculated the pollution associated to the mill or the fire in that pixel during the day of the event (in the case of the sugarcane fires) or the day of the production season (in the case of the mills).

One limitation of the data from MERRA-2 is the spatial resolution, especially for obtaining pollution for small areas such as the location of mills. In order to address this problem, I used data from [40] that estimates global annual surface fine particulate matter (PM<sub>2.5</sub>) for 2012-2017. These data have a resolution of  $0.01^\circ \times 0.01^\circ$ . The dataset provides measurements of PM<sub>2.5</sub>  $\mu\text{g}/\text{m}^3$  from aerosol optical depth and accounts for transport of pollutants using the GEOS-Chem chemical transport model. The data has been used in other contexts for the U.S. [41] and its spatial definition is desirable to analyze detailed spatial units such as mills. The downside of the data is the temporal scale since it only provides annual estimates of particulate matter.

#### 1.4.6 Birth outcomes data

Data on birth outcomes was obtained from the Mexican Health Ministry (*Secretaria de Salud*) that collects data from individual birth certificates and has information on all birth records and mother's demographic and residency information such as number of doctor visits, age, education, employment, and locality of residence. I am able to link the locality of the mother's residence to the sugarcane fire catchment areas by obtaining all the rural villages and cities located within 10 km from sugarcane fields and associating the average pollution exposure in the last pregnancy trimester given the literature findings linking pollution exposure and negative birth outcomes for the last pregnancy trimester [42, 7]. I merged average daily birth outcomes at the locality (city or rural village) to

the average monthly pollution exposure in each month of the last pregnancy trimester. This approach is similar to [7], however, I am not able to observe some of the outcomes the authors examine such as hospitalizations or fetal and neonatal mortality.

### 1.4.7 Socioeconomic characteristics

In order to analyze the distributional consequences of incomplete regulation policies and pollution leakage, I used data from the Mexican National Marginalization index constructed by the Mexican government and used to classify the socioeconomic vulnerability of urban and rural areas. The index uses several variables to calculate the marginalization level, among them the percentage of people older than 15 without education, percentage of households without piped water, bathroom, electricity, and refrigerator, and average number of people living in a household. The index uses data at the locality<sup>28</sup> level and classifies the localities in five levels of marginalization: very low, low, medium, high, and very high. I also use data from 2010 census in order to calculate poverty levels at the locality level in order to analyze whether poorer communities experienced a higher increase in fires.

## 1.5 Empirical Specification

### 1.5.1 Impact of incomplete regulation on within supply chain leakage

The first objective of this paper is to estimate the impact of regulation on within-supply chain leakage and pollution redistribution. I take advantage of the introduction

---

<sup>28</sup>In terms of urban areas a locality is analogous to a city and in terms of rural areas is analogous to a village. A caveat with this classification is that I am not able to disentangle within-city variation in urban areas (i.e. neighborhood). However, I plan to extend this in future work.

of the regulation in 2015 to point-sources, comparing two groups: non-exempt facilities (oil) and exempt facilities (biofuels). In order to analyze whether non-exempt facilities substitute from cleaning sugarcane in the mills using regulated boilers to cleaning in the fields using controlled fires, I use a difference-in-differences approach:

$$SHF_{idm} = \alpha + \beta_1 D_i \times \mathbf{1}[t \geq 2015] + \gamma_i + \mu_t + \rho_m + W_{id} + \epsilon_{idm} \quad (1.6)$$

Where  $SHF_{idm}$  is the sugarcane harvest fires in day  $d$  associated to mill  $i$  as described in section 3.4.1,  $D_i$  equals one if the sugar mill is a non-exempt facility,  $\gamma_i$  are mill fixed effects,  $\mu_t$  are year fixed effects,  $\rho_m$  are month fixed effects to control for seasonality in harvesting activities,  $W_{id}$  are weather controls, and  $\epsilon_{idm}$  are two-way clustered standard errors at the municipality and year level following [43].  $\beta_1$  shows the difference-in-difference estimate of the impact of being non-exempt from the new emission limits after 2015.

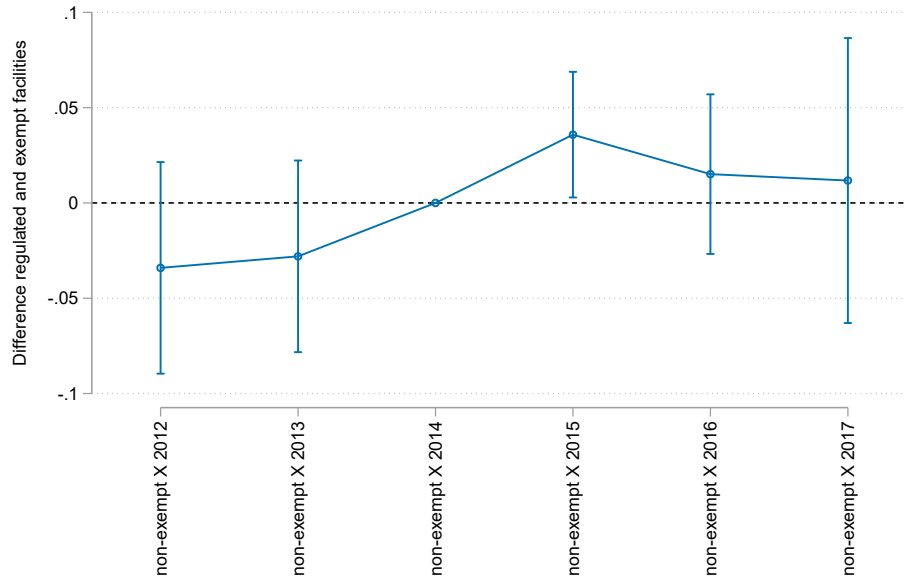
The identifying assumption of equation 1.6 is that in the absence of treatment, fires in both exempt and non-exempt facilities would have followed the same trend. Testing this assumption is not possible but showing parallel trends in the outcomes of interest allows me to informally test for differences in the groups prior to the introduction of the policy.<sup>29</sup> Figure 1.1 shows that pre-treatment, both exempt and non-exempt facilities follow similar trends in the number of daily fires. This figure suggests that prior to the start of the program, fires in exempt and non-exempt facilities followed a similar trend. I performed two falsification tests. First, I replaced the dependent variable for  $NSHF_{it}$  that denotes the number of agricultural fires in non-sugarcane plots associated to mills. Second, I restricted the timeframe of the fires to the months of June through October, outside of the harvesting season. There is no significant increase in NSHF after

<sup>29</sup>Figure A.7 shows the total number of fires by exempt and non-exempt facilities. In general, regulated mills have a higher number of associated harvest fires than exempt facilities.



the policy and there is no increase in SHF outside the harvesting season. Figure A.8 shows the parallel trends controlling for international sugar prices and Mexican crude oil prices.<sup>30</sup>

Figure 1.1: Effect on total daily sugarcane fires:



**Notes:** This figure shows the differences in differences-year specific coefficients for the total number of daily fires following equation 1.6. The regulation started in 2015. 95% confidence intervals calculated using two-way fixed effects at the municipality and year level.

In a similar way, I examine whether the changes in the number of fires are associated with the substitution of inputs related to the fire use. Following a similar approach to equation 1.6, I estimate the following difference-in-differences specification:

$$Y_{ist} = \alpha + \beta_1 D_i \times \mathbf{1}[t \geq 2015] + \gamma_i + \mu_t + \rho_s + \epsilon_{ist} \quad (1.7)$$

Where  $Y_{ist}$  denotes the variables of interest at the sugar mill level such as number of

<sup>30</sup>I obtained monthly sugar prices from the Federal Reserve Economic Data (FRED) of St. Louis Fed. I used the nominal sugar prices (PSUGAUSAUSDM) and the US CPI (CPALTT01USA6615) to obtain the real sugar price. I obtained daily Mexican crude oil prices from the Mexican Central Bank (SI744, *Precios del Petróleo: Mezcla Mexicana, Dolares por barril, PMI* and obtained the monthly average.)

tons harvested using manual and mechanical cut, total manual workers, total sugarcane harvested, total sugarcane processed, and total sugar.  $s$  is the week with respect to the beginning of the harvest,<sup>31</sup> and  $\rho_s$  are week with respect to harvest fixed effects. Figure A.10 shows parallel trends for each of the inputs: sugarcane harvested by mechanical and manual cut, total tons harvested, and number of manual workers. Figure A.11 shows parallel trends for outputs such as total sugarcane processed and total sugar produced. These two figures show that there are no striking differences between regulated and exempt facilities at the start of the policy in terms of inputs used or total sugarcane harvested or sugar produced except for the amount of mechanical cut. Any differences in mechanical cut associated with the policy will not be interpreted as causal.

Finally, in order to examine whether there are differences in air pollution concentrations due to changes in the number of fires or production patterns, I use a similar specification than equation 1.6:

$$P_{idm} = \alpha + \beta_1 D_i \times \mathbf{1}[t \geq 2015] + \gamma_i + \mu_t + \rho_m + W_{id} + \epsilon_{idm} \quad (1.8)$$

Where  $P_{idm}$  is the ambient pollution concentration of PM<sub>2.5</sub> and SO<sub>2</sub> at the daily level in  $\mu g/m^3$  obtained using the pollution level described in the Data section. I ran two separate versions of equation 1.8: one for the pollution associated with the pollution level in the fires polygons and another for the pollution associated with the mills' location. Figure A.12 shows the parallel trends for the pollution associated with the fields and Figure A.13 shows the pollution parallel trends associated with the mills.

---

<sup>31</sup>The administrative data is reported by sugar mills directly in a weekly basis and they start reporting it at the beginning of each harvesting cycle. However, information on the date of the beginning of the harvest for each mill is not available.

## 1.5.2 Distributional effects of incomplete regulation

The second objective of this paper is to analyze the distributional consequences of within supply chain leakage. A large body of literature has documented negative effects of pollution on health outcomes [7, 44, 45] and how the damages of pollution could vary across income levels [46]. Other studies have analyzed whether the damages of environmental policies are distributed unevenly across populations [47, 48]. However, studies that document emissions leakage caused by a policy have not examined the extent of which the emissions are distributed across populations.<sup>32</sup> Understanding how the damages of environmental policy are distributed across populations and the determinants of the environmental damages is important for welfare analysis [23] and environmental justice [19]. Analyzing the distributional damages of incomplete regulation in the context of this paper is important because of the characteristics of the underlying population living close to the sugarcane fields. Figure A.14 shows the characteristics of the populations exposed to mills and fields. In general, poorer households tend to live in rural areas that are exposed to sugarcane fires.

In order to explore the distributional consequences of incomplete regulation, I calculated the catchment areas of all localities (either urban or rural) by creating a buffer of 10 km surrounding the centroid of the locality.<sup>33</sup> I then merged these catchment areas to pollution concentrations by predicting the pollution exposure coming from the policy in equation 1.8, obtaining the predicted  $PM_{2.5}$  and  $SO_2$  from the policy,  $\hat{P}_{idm}$ , and modifying the empirical specification of [49]:

<sup>32</sup>Important to clarify, many studies that have documented leakage have done it in terms of GHG emissions where emissions occur is not as worrying due to the nature of GHG emissions.

<sup>33</sup>I assigned pollution from fires and mills by calculating a receptor catchment area of 10km from the centroid of the urban or rural locality. A caveat of this analysis is that pollution can follow non-uniform transport and dispersion patterns. In future work I aim to characterize this using prevailing wind approaches. The total people in the buffer area of fires originated in sugarcane fields is 9,834,436 and the total people in the buffer area of the mills is 5,723,850.

$$\hat{P}_{idm} = \gamma_0 + \gamma_1 \mathbf{1}[DAC_i] + \gamma_2 DAC_i \times \mathbf{1}[t \geq 2015] + \tau_i + \mu_t + \epsilon_{idm} \quad (1.9)$$

Where  $\hat{P}_{idm}$  is the predicted pollution exposure coming from the policy calculated in equation 1.8 and DAC is an indicator variable that equals one if the locality is disadvantaged (high or very high marginalization index),  $\tau_i$  are mills fixed effects,  $\mu_t$  are year fixed effects. Standard errors are clustered at the locality level.  $\gamma_2 > 0$  implies that disadvantaged communities have experienced a higher burden of the pollution change due to the incomplete regulation than other disadvantaged localities,  $\gamma_1 + \gamma_2$  is the total effect of the pollution exposure gap between disadvantaged communities and non-disadvantaged communities. I also further divide localities into the marginalization categories to examine heterogeneity across different marginalization levels. I weighted equation 1.9 by population to account for differences in population in disadvantaged and non disadvantaged areas.

### 1.5.3 Health impacts of incomplete regulation

The paper also analyzes whether the pollution exposure caused by incomplete regulation translate into negative outcomes for the populations located within the catchment area described in the previous section. In particular, I use the predicted pollution exposure derived in equation (1.8) to explain changes in birth outcomes:

$$H_{jd} = \alpha + \beta_1 \hat{P}_{i(d-w)m} + X_{id} + \lambda_i + \mu_t + \epsilon_{id} \quad (1.10)$$

Where  $H_{jd}$  denotes average birth outcomes such as birth weight, gestation length, very low birth weight, and very preterm births at the locality and day level.  $\hat{P}_{i(d-w)m}$  is the predicted exposure coming from the policy calculated in equation (1.8) associated

with the weeks  $w$  before the birthdate in the last trimester of the pregnancy, where  $w \in \{4, 8, 12\}$ .  $X_{id}$  are controls such as mother age and total doctor visits averaged at the locality and day level.  $\mu_t$  denotes year fixed effects. Standard errors are clustered at the locality level. This specification differs from [7] since the authors explore the differences between upwind and downwind fires from the mother’s municipality in order to isolate the impacts of pollution from the economic activity derived from the harvesting season. To the extent that  $\hat{P}_{i(d-w)m}$  is obtained using variation that exploits the introduction of regulation to sugarcane mills with a rich set of controls and fixed effects, my specification is likely capturing pollution and not economic activity.<sup>34</sup>

## 1.6 Results

### 1.6.1 Effects on upstream fires

This section discusses the effects of incomplete regulation on within supply chain leakage. Given that fires are a production substitute for cleaning in the plant, we would expect the amount of fires to increase after the boiler regulation for regulated facilities (non-biofuel users). Column (1) of Table 1.1 shows the difference-in-differences estimator,  $\beta_2$ , of interest. This shows that there is an approximate 14% increase in the number of daily fires after the policy began. Column (2) shows the impact on the number of fires using a Poisson model and the results are similar to column (1), the increase in the count of fires is around 13.5% after the policy began.

As robustness tests, Table A.2 shows the results using the monthly number of fires at the mill level. The effect is similar in magnitude considering the number of monthly fires. These results are robust to controlling for oil and sugar prices: Table A.3 shows

---

<sup>34</sup>Exploring the upwind and downwind specification like [7] is one of the priorities for future work.

Table 1.1: Effect of emission limits on daily fires

	(1)	(2)
	Total SHFs	Total SHFs
After 2015 $\times$ non-exempt	0.04120** (0.01429)	0.13506** (0.06518)
Pre 2015 mean	0.286	0.292
Obs.	71,535	70,280
R-squared	0.091	
Year FE	Yes	Yes
Month FE	Yes	Yes
Mill FE	Yes	Yes
Weather controls	Yes	Yes
Cluster level	Mun-year	Robust
Poisson	No	Yes

**Notes:** Column (1) shows the difference-in-differences estimator of the impact of being regulated by the emission limits after the policy started on the number of fires using equation 1.6. Column (2) estimates the same specification in equation 1.6 using a Poisson model with robust standard errors. Standard errors for column (1) and (2) using two way clusters (municipality and year) in parenthesis.

these results. Table A.4 shows the results from equation 1.6, analogous to column (1) of Table 1.1 with bootstrap standard errors. Table A.5 shows the results for the first falsification test: other agricultural fires not related to sugarcane. There is no difference in the number of non-sugarcane agricultural daily fires after the policy for the non-exempt facilities compared to the exempt facilities. I conducted another falsification test where I restricted the sample to the fires outside the sugarcane harvest season. Table A.6 shows these results, showing no effect in the increase of fires outside the harvest season. Table A.7 shows a stronger effect when restricting the dataset to the fires inside of the mills' distribution areas using the sampling points of several mills in the state of Veracruz. Results in Table A.7 show that the link using distance to the mills seem appropriate: most mills usually harvest their sugarcane from the nearest fields. As a robustness test, Table A.8 shows the results for the mills known to be under compliance by CONADESUCA.<sup>35</sup>

<sup>35</sup>CONADESUCA verifies compliance by doing inspections to the mills every two years. Important to mention, the regulation is enforced by the Mexican Environmental Protection Agency, PROFEPA.

The results are stronger when restricting the data to the compliant facilities which is what we would expect if mills are actually substituting for more manual cut. Table A.9 shows the results doing two additional sample selections. Sample restriction 1 estimates the results without the only mill that invested in a biofuel-powered boiler in 2016 who could have changed fuel use as a response to the policy. Sample restriction 2 estimates the results without the mill that shows a higher rate of mismatched fields based on the minimum distance definition according to Figure A.4.

### 1.6.2 Effects on input substitution

Next, I turn to analyze whether the change in the number of fires is reflected in input substitution across firms. Consistent with the finding of an increase in the number of fires used during the harvest, Column (1) of Table 1.2 shows that there is an increase of 9% in the total sugarcane harvested using manual cut. In the opposite direction, I find that the amount of sugarcane harvested decreases although this result is not statistically significant. Given that the use of fires is consistent with an increase on manual cut, I also find that the number of field workers increase by 5%, as column (3) of Table 1.2 shows. The results of table 1.1 and 1.2 show that incomplete regulation generates within supply chain leakage and changes in the inputs used. Using data on payroll for formal sugarcane agricultural workers at the municipality level, Table A.10 shows that there is no change in wages for agricultural workers throughout the period of study, even dividing by different age categories. I cannot find a discernable impact on wages with the data available.<sup>36</sup>

---

However, CONADESUCA verifies mills' inventory every two years and reports its compliance in order to build the Sugarcane Sustainability Index.

<sup>36</sup>Other papers have investigated whether proximity to industrial facilities have positive employment effects despite the negative pollution exposure impacts on nearby communities. [50] found that the share of pollution risk accruing to minority groups located near polluting facilities exceeds their share of employment and wages.

Table 1.2: Effects on inputs substitution

	(1)	(2)	(3)
	Manual cut (tons)	Mechanical cut (tons)	Total field workers
After 2015 $\times$ non-exempt	2,913.460** (1,188.58879)	-274.228 (814.47535)	81.893** (34.54865)
Mean	30,971.456	6,915.284	1,453.505
Obs.	6,095	6,102	5,640
R-squared	0.749	0.727	0.913
Year FE	Yes	Yes	Yes
Week FE	Yes	Yes	Yes
Mill FE	Yes	Yes	Yes
Cluster level	Mun and year	Mun and year	Mun and year

**Notes:** Column (1) shows the difference-in-differences estimator of the impact of being regulated by the emission limits after the policy started on the amount of sugarcane harvested using manual cut (tons) following specification 1.7. Column (2) shows the difference-in-differences estimator of the impact of being regulated by the emission limits after the policy started on the amount of sugarcane harvested using mechanical cut (tons) following specification 1.7. Column (3) shows the difference-in-differences estimator of the impact of being regulated by the emission limits after the policy started on the number of manual labor workers following specification 1.7. Standard errors using two way clusters (municipality and year) in parenthesis.

Although there is an increase in manual cut, I do not find evidence of an increase in total sugar produced. Table A.11 shows that there is no increase in the total amount of sugarcane processed in the mill (column 1) and no increase in the total amount of sugar produced in the mill (column 2). These results suggest that there is redistribution between input use but this does not imply that final output increased.<sup>37</sup> I find suggestive evidence that the non-increase in total sugar produced is due to changes in production efficiency. I estimate that changes in production efficiency by using three indicators such as (1) the total kilograms of sugar obtained by ton of harvested sugarcane, (2) total kilograms of sugar obtained by ton of processed sugarcane, and (3) sugar extraction efficiency. Table A.12 show these results which suggest that there is a non-significant

<sup>37</sup>A potential problem conflicting event influencing the total amount of produced sugar is the soda tax that started in 2014. This tax was a flat rate per liter of soda and it was uniform across the country. However, it is not clear why this would affect my main identification strategy. (1) There is no a priori reason why a soda tax would have affected biofuel facilities differently from non-biofuel facilities. (2) Moreover, the Mexican sugar tax was levied in the consumers directly and thus any effect would be driven by sugar demand not total production.



decrease in overall sugar production efficiency, consistent with the fact of non-positive effects in production due to the change in inputs.

### 1.6.3 Effects on ambient pollution

What does supply chain leakage mean in terms of total pollution generated? Table 1.3 shows the implications of an increase of fires in terms of local ambient pollution level around the sugarcane fields (columns 1-4) and mills (columns 5-6). Columns (1)-(4) and columns (5)-(6) are estimated using different datasets, given the spatial resolution of the data: columns (1)-(4) are estimated using data from MERRA 2.0 with calculations following [38] and columns (5)-(6) are estimated using [40] that includes  $PM_{2.5}$  only. I find that there is an increase of  $1.05 \mu g/m^3$  of  $PM_{2.5}$  or of 6% increase in pollution coming from the fields associated to the 2015 regulation. I do not find a change in the  $SO_2$  levels in the fields region.

Columns (5)-(6) of Table 1.3 show the results of pollution from the mills, suggesting a decrease of pollution near the mills following the introduction of the new regulation. These results translate into a decrease of 3% on  $PM_{2.5}$  pollution coming from mills.<sup>38</sup> Table A.13 shows the results of pollution exposure in the mills area using MERRA 2.0. These results are less precise and have different sign than the results in 1.3 columns (5)-(6), which is likely due to the coarse spatial resolution of the data.

The magnitudes of my results are consistent with existing studies. I find that as a response to the regulation, regulated mills increased fires by 14%. [1] finds that regulated facilities under the Clean Air Act increase their production in unregulated facilities by 11% and [11] finds that regulated facilities under the Clean Air Act increased foreign output by 9%. In terms of increase in pollution, I find that incomplete regulation in-

<sup>38</sup>Important to note, the data from [40] is annual pollution concentrations at  $1km \times 1km$ , while the MERRA 2.0 is daily data at resolution of approximately  $50km \times 50km$  at the latitude of the fields.

Table 1.3: Effect on pollution

	(1)	(2)	(3)	(4)
	Pollution in fields		Pollution in mills	
	PM2.5	Log(PM2.5)	PM2.5	Log(PM2.5)
After 2015 $\times$ non-exempt	1.05187**	0.04638*	-0.38421**	-0.05121
	(0.37124)	(0.01972)	(0.09956)	(0.02569)
Mean	17.549	2.608	12.566	2.455
Obs.	20,489	20,489	295	295
R-squared	0.466	0.566	0.827	0.967
Year FE	Yes	Yes	No	No
Month FE	Yes	Yes	Yes	Yes
Mill FE	Yes	Yes	Yes	Yes
Weather controls	Yes	Yes	Yes	No
Cluster level	Mun&year	Mun&year	Mun&year	Mun&year

**Notes:** Columns (1)-(4) shows changes in pollution concentrations in the fields associated to mills. Columns (5)-(6) shows changes in pollution concentrations in the mills, data of SO<sub>2</sub> at the small-scale mill resolution is not available. Column (1) and (2) show the difference-in-differences estimator of the impact of being regulated by the emission limits after the policy started on the ambient pollution level of PM<sub>2.5</sub> and log(PM<sub>2.5</sub>), respectively following specification 1.8 using [38]. Column (3) and (4) show the difference-in-differences estimator of the impact of being regulated by the emission limits after the policy started on the ambient pollution level of SO<sub>2</sub> and log(SO<sub>2</sub>), respectively following specification 1.8 using [38]. Column (5) and (6) shows the difference-in-differences estimator of the impact of being regulated by the emission limits after the policy started on the ambient pollution level of PM<sub>2.5</sub> following [40] (SO<sub>2</sub> data for this data product is not available). Standard errors using two way clusters (municipality and year) in parenthesis.

creased pollution exposure by 6% in rural areas located near the agricultural fields. This increase in pollution is higher than the documented by [51], who find an increase of 1.25% in PM<sub>2.5</sub> exposure as a result of increasing agricultural fires due to labor exits in India.

#### 1.6.4 Who experiences the increased pollution?

This section analyzes whether vulnerable communities experienced a larger increase in pollution coming from sugarcane fires after the policy. I classified vulnerable communities using the marginalization index provided by the Mexican government. In this section I will use the official index that classifies communities from “very low” to “very high” marginalization and a classification of “disadvantaged” if the community has “very

high” and “high” marginalization levels. Given the spatial distribution of vulnerable communities in Mexico, we could expect that there are differences in baseline characteristics between disadvantaged communities and non-disadvantaged localities. These differences are captured by  $\gamma_1$  in equation 1.9. Table 1.4 shows that before the policy, disadvantaged localities have lower levels of  $PM_{2.5}$  and slightly insignificant, higher levels of  $SO_2$  levels. However, after the policy the total pollution exposure in disadvantaged localities increased, meaning that total pollution exposure in disadvantaged localities increased after the policy compared to non-disadvantaged localities. Exposure to  $SO_2$  in the other hand, decreased but the difference is not significant. I estimate that by the end of the policy, disadvantaged localities experienced 12% more pollution exposure than non-disadvantaged localities.

Table 1.4: Distribution of the effects of pollution coming from fires

	(1)
	Predicted $PM_{2.5}$ (fires)
DAC=1	-0.13900*** (0.04193)
DAC=1 $\times$ After 2015=1	0.27055*** (0.08194)
Obs.	3,627,238
R-squared	0.717
Year FE	Yes
Month FE	Yes
Mill FE	Yes
Cluster level	Municipality
Pop. weighting	Yes

**Notes:** Columns (1) and (2) show the predicted difference in pollution exposure for disadvantaged localities before the policy (DAC=1) and after the policy (DAC=1  $\times$  After 2015=1). Localities exposure was calculated using catchment areas: 10km circle surrounding the locality sector. Disadvantaged localities were classified using the 2010 Marginalization Index calculated by CONAPO. Regression uses population weights using 2010 Census data.

These pollution redistribution impacts are heterogenous with respect to different levels of marginalization: the highest level of marginalization has a higher burden of pol-

lution exposure than localities with low or very low marginalization indices. Panel a) subpanel (a) of Figure 1.2 shows these results. Panel a) subpanel (b) shows a robustness check using another index of social vulnerability, the “Social Lag Index”, calculated by CONEVAL.<sup>39</sup> Figure 1.2 shows that the exposure from mills did not change differentially for communities with higher levels of vulnerability, except for the “Very High” category of the social lag index. However, it is smaller than the magnitudes from fires. The heterogeneity in pollution exposure after the policy could be explained by different reasons such as ex-ante vulnerability or because mills with fields closer to disadvantaged communities could strategically pollute more near these areas without facing opposition to pollute in these areas. [27] show that in the case of Mexico, disparities could be explained by community pressure and collective action responses. However, additional work can be done trying to analyze whether this is the case in the sugarcane sector. These results are relevant given that previous research shows that pollution damages are not linear with income [46]. Moreover, given that defensive investments are an important part of the willingness to pay for pollution reduction [52] and they could be correlated with income, poorer households might not be able to cope with changes in pollution exposure.

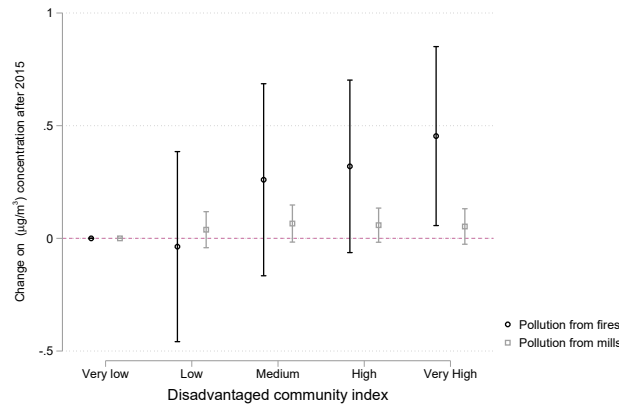
Table 1.5 shows the same specification in equation 1.9 for the mills ( $\text{SO}_2$  is not available for the small scale resolution). There is no significant difference between disadvantaged communities and other communities after the policy began. Similarly, panel b) of figure 1.2 show no significant difference for the different levels of marginalization.

Besides showing that the policy generated a relatively higher pollution exposure for the most vulnerable, I tested whether locations with higher poverty levels are the most affected by the fires. Table A.14 shows that the increase in fires is higher in localities

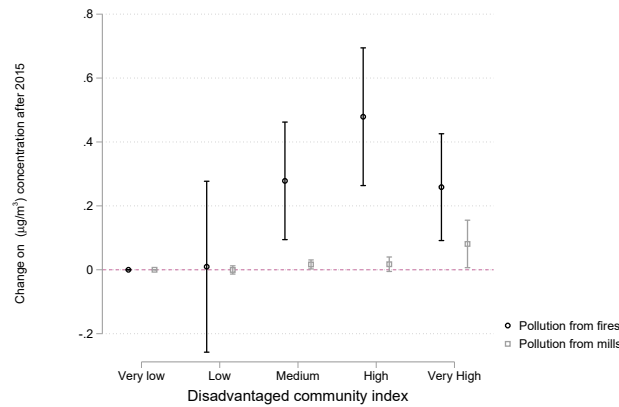
---

<sup>39</sup>This index considers data from the 2010 data based on different variables than the Marginalization Index calculated by CONAPO. The index considers indicators of infrastructure at the locality level and asset holding characteristics for the localities’ households.

Figure 1.2: Distribution of the effects of pollution  
 Panel a) exposure from fires



Panel b) exposure from mills



**Notes:** Panel a) shows the results of pollution associated to fires by level of marginalization according to the marginalization index and the social lag index.. Panel b) shows the results of pollution associated to mills by level of marginalization according to the marginalization index and the social lag index. Coefficients show the interaction between the marginalization level and an indicator after the policy. Regressions include mill fixed and year fixed effects. Confidence intervals calculated using clustered standard errors at the locality level. Confidence intervals calculated using two-way fixed effects at the municipality and year level.

that have poverty levels higher than each locality’s state median. This is consistent with [27] who found that pollution releases is higher in marginalized communities in the case of Mexico. This is another indicator that the most vulnerable communities were affected by incomplete regulation.

Table 1.5: Distribution of the effects of pollution coming from mills

	(1)
	Predicted PM <sub>2.5</sub> (mills)
DAC=1	-0.01557 (0.01044)
DAC=1 × After 2015=1	0.03893 (0.02610)
Obs.	17,075
R-squared	0.998
Year FE	Yes
Month FE	Yes
Mill FE	Yes
Cluster level	Municipality
Controls pop.	Yes

**Notes:** Columns (1) and (2) show the predicted difference in pollution exposure for disadvantaged localities before the policy (DAC=1) and after the policy (DAC=1 × After 2015=1). Localities exposure was calculated using catchment areas: 10km circle surrounding the locality sector. Disadvantaged localities were classified using the 2010 Marginalization Index calculated by CONAPO. Regression uses population weights using 2010 Census data.

### 1.6.5 The impacts of incomplete regulation on health outcomes

Do changes in pollution caused by incomplete regulation affect health outcomes? I examine this by analyzing whether the predicted pollution obtained in section 4.2 changes birth weight, gestational weight, very low birth weight incidence, and very preterm birth for populations located in the fires catchment area. Table 1.6 shows the main health results of pollution exposure in the last pregnancy trimester on birth outcomes. I find that pollution exposure in the last trimester of pregnancy significantly lowers birth weight and increases the incidence of very low birth, and very preterm birth. These effects are larger in the weeks 5 through 12 before giving birth.

Table 1.6: Effect of incomplete regulation on birth outcomes

	(1)	(2)	(3)	(4)
	Birth weight (grams)	Gestation length (weeks)	Very low birth weight (weight < 1,500g)	Very preterm birth (weeks < 32)
			Panel a)	
PM <sub>2.5</sub> ( $\mu\text{g}/\text{m}^3$ ) in w-4 weeks	-0.32690 [0.26571]	-0.00144 [0.00098]	0.00008** [0.00004]	0.00014*** [0.00005]
			Panel b)	
PM <sub>2.5</sub> ( $\mu\text{g}/\text{m}^3$ ) in w-8 weeks	-1.00148*** [0.33077]	-0.00221* [0.00116]	0.00012** [0.00005]	0.00014** [0.00006]
			Panel c)	
PM <sub>2.5</sub> ( $\mu\text{g}/\text{m}^3$ ) in w-12 weeks	-0.90981** [0.43649]	-0.00199 [0.00164]	0.00007 [0.00006]	0.00006 [0.00008]
Observations	62,129	63,803	64,026	64,026
Mean Dep. Variable	3,217.232	38.952	0.004	0.007
R-squared	0.193	0.185	0.174	0.179
Year FE	Yes	Yes	Yes	Yes
Locality FE	Yes	Yes	Yes	Yes
Cluster level	Locality	Locality	Locality	Locality

**Notes:** Columns (1)-(4) show changes in birth outcomes associated with pollution exposure within 4 (Panel a), 8 (Panel b) or 12 weeks (Panel c) from birthdate. Each estimate is obtained from separate regressions. All regressions control for average mothers' age and total of doctor visits during pregnancy and year and locality fixed effects. Standard errors clustered at the locality level in parenthesis.

The results in Table 1.6 imply that an additional  $\mu\text{g}/\text{m}^3$  of  $\text{PM}_{2.5}$  in the weeks 1-8 of the last trimester of pregnancy associate with a birth weight decrease of 1 gram on average for all mothers. [7] estimate that a unit increase of  $\text{PM}_{10}$  (in  $\mu\text{g}/\text{m}^3$ ) caused by sugarcane fires decreases birth weight by 5.2 grams. Other estimates on the impacts of pollution on birth weight find that a unit increase in  $\text{PM}_{10}$  exposure during the last trimester is associated with a 0.4 gram decrease in birth weight [42, 7]. My estimates are smaller in magnitude than [7] which could be due to existing differences in fire activity intensity in Brazil, as well as differences in the studied pollutants and identification strategies.<sup>40</sup>

For the other variables analyzed, I find that a unit increase of  $\text{PM}_{2.5}$  is associated with a 3% increase in the probability of very low birth weight ( $< 1,500\text{g}$ ) and a 2% increase in the probability of very preterm birth ( $< 32$  weeks). These results are consistent with other studies finding increases in very low birth weight and very preterm birth associated with an increase in fires [7].<sup>41</sup> These results suggest that increases in pollution due to input substitution are associated with worse health outcomes for the populations located in the fires catchment area. These estimates will be used in Section 6 to calculate a tax that would internalize the health costs of sugarcane burning originated by the incomplete regulation.

## 1.7 Internalizing the costs of burning

The previous sections showed that incomplete regulation increases the emissions of the unregulated input which impacts populations located nearby. One alternative to alleviate these damages is to regulate the associated harvest burning driven by incomplete

---

<sup>40</sup>[7] estimate this by comparing upwind and downwind fires which likely provide a more precise estimate of the impacts of pollution exposure. This approach is outside the scope of the paper but will be a priority for future work.

<sup>41</sup>[7] find that an additional z-score of fire activity per week in the last trimester of pregnancy increases the incidence of very low birth weight by 22 per 1000 and an increase in the incidence of preterm birth of 23 per 1000, although the later results are not significant.



regulation via a tax and compensate the damages to affected populations. The objective of this section is to calculate a tax that internalizes the existing health costs associated with agricultural burning. To do so, I obtain the difference between the social cost per unit of harvested sugarcane and the private cost of production paid by consumers and find the tax that would compensate communities affected by sugarcane burning. I then calculate this tax in the context of the sugarcane sector in Mexico using the estimated responses to the incomplete regulation.

Assuming a regulator that tries to maximize consumer surplus net of private costs and environmental damages, The regulator's welfare maximization problem is given by:

$$W = \underbrace{\int_0^y f(y)dy}_{\text{Consumer surplus}} - \underbrace{c(l, k)}_{\text{Prod. Cost}} - \underbrace{D(\gamma_k) - D(\gamma_l)}_{\text{Pollution damages}}$$

Where  $f(y)$  is the demand for sugarcane,  $c(l, k)$  is the producer cost,  $D(\gamma_k)$  is the health damages from pollution emissions of the capital intensive input  $\gamma_k$ , and  $D(\gamma_l)$  is the health damages from pollution emissions of the labor intensive input.

The firms' profit function is given by:

$$\pi = py - rk - wl - \gamma_l t$$

Where  $p$  is the price of the final output  $y$ , sugar,  $l$  is labor,  $k$  is capital,  $r$  and  $w$  are the prices of capital and labor, and  $t$  is the tax for each unit of processed sugar. The tax that would equate the social cost per unit of sugar and the private cost of production is be given by:

$$t = \frac{w \frac{\partial L}{\partial t} + \frac{\partial D(\gamma_k)}{\partial \gamma_k} \frac{\partial \gamma_k}{\partial k} \frac{\partial k}{\partial t} + \frac{\partial D(\gamma_l)}{\partial \gamma_l} \frac{\partial \gamma_l}{\partial l} \frac{\partial l}{\partial t} + r \frac{\partial k}{\partial t} - P \frac{\partial y}{\partial t}}{\frac{\partial \gamma_l}{\partial l} \frac{\partial l}{\partial t}}$$

Table 1.7: Parameters for tax calculation

$w$	Average ag. wage	\$109 MXN
$\frac{\partial L}{\partial t}$	Own estimate	9.42%
$\frac{\partial D(\sigma_k)}{\partial \sigma_k}$	[46]	0.40%
$\frac{\partial \sigma_k}{\partial k} \frac{\partial k}{\partial t}$	Own estimate	-3.05%
$\frac{\partial D(\sigma_l)}{\partial \sigma_l}$	Own estimate	2%
$\frac{\partial \sigma_l}{\partial l} \frac{\partial l}{\partial t}$	Own estimate	13.20%
$r$	EPA risk free rate	0.04
$\frac{\partial k}{\partial t}$	Own estimate	49%
$P$	Sugar price per ton	\$13,100 MXN
$\frac{\partial y}{\partial t}$	Own estimate	.19%

Using the parameters obtained in the previous sections and in existing studies summarized in Table 1.7, I calculate that the wedge between the social cost per unit of sugarcane harvested and the private cost of production paid by consumers is given by \$39 USD (\$789 MXN) per ton of sugarcane, which average price in 2017 was \$650 USD, meaning is a 6% tax per ton of sugarcane.

## 1.8 Conclusion

This paper showed the environmental justice consequences of incomplete regulation when facilities are able to shift where production occurs. I investigated the distributional consequences of incomplete regulation in the context of the sugarcane production in Mexico. By leveraging data on fires, pollution, and detailed production information on mills, this paper is able to identify the responses of producers to incomplete regulation. I found that following the introduction of regulation, regulated facilities increased the sugarcane harvest fires in their associated fields. I also found adjusting margins in the inputs used by mills. Consistent with an increase in fires, I showed that regulated facilities increased the manual workers and the sugarcane harvested using manual cut. I find that

the increase in fires is accompanied by an increase in pollution near fields and a decrease of pollution near mills. Finally, I find that the increase in pollution caused by the policy is associated with worse birth outcomes for exposed populations.

The responses to incomplete regulation regarding pollution are concerning due to the differences of poverty levels of the populations close to the mills and the fields. I analyzed whether the burden of pollution caused by the policy is higher for disadvantaged populations. This paper found that the pollution increase was higher for disadvantaged communities. This result contributes to the current discussions on the determinants of environmental justice. I contribute to this literature by looking a previously overlooked mechanism: incomplete regulation.

The results of the paper are relevant for current policy debates in Mexico on whether to regulate agricultural burning from sugarcane. Moreover, in 2017 the Mexican environmental agency proposed ammendments to the existing regulation to include facilities that use biofuels as main fuel (PROY-NOM-170-SEMARNAT-2017). The results of this paper show that if facilities are able to substitute production processes with fires, incomplete regulation might backfire. Therefore, considering these possible adjustment margins is important.

There are several limitations to this study. First, the pollution level estimates should be interpreted with caution given the geographic extent of pollution measures. However, I present consistent evidence that manual cut increased together with fires, which suggest that populations located near fields were exposed to pollution. To the extent that burning biomass increases pollution levels, which has been shown by other studies, populations are likely to experience higher pollution. Second, despite the efforts to link mills to their respective fields, the possibility of misassignment of this link remains. However, given the evidence using actual distribution areas for one of the states in Mexico, it is likely that this measurement error downward bias my results, which means that the

effects found in the paper could be a lower bound of the real effect. In fact, I showed how when restricting fires to the recorded distribution areas, the estimates are higher. Finally, there is still need to characterize other mechanisms driving distributional concerns of environmental policy and other environmental justice implications. However, by documenting a previously overlooked mechanism, this paper contributes to the literature on disparities in environmental impacts and its implications for environmental justice.

## Chapter 2

# Do Environmental Markets Cause Environmental Injustice? Evidence from California's Carbon Market

### 2.1 Introduction

Over the last three decades, policy makers have increasingly relied on market-based environmental policies - such as pollution trading and taxes - to address environmental problems. Expanded use of market-based policies followed each major amendment to the U.S. Clean Air Act since the 1970s [53]. Widespread adoption has occurred in other environmental domains: today, market-based policies cover 30% of global fisheries [54], account for over \$36 billion in global ecosystem service payments [55], and govern 20% of global greenhouse gas (GHG) emissions [56].

The central appeal of market-based environmental policies is allocative efficiency. In theory, such policies reduce the total abatement cost of meeting an environmental objective by inducing less abatement from polluters with higher abatement costs [57, 58,

59]. This contrasts with traditional command-and-control regulations, which typically require heterogeneous polluters to adopt uniform abatement actions.

At the same time, the particular reallocation of emissions induced by market-based policies also spatially alters who is harmed by pollution. This is of particular concern as a growing “environmental justice” (EJ) literature has documented that communities with lower income, higher minority share, and/or otherwise disadvantaged, systematically experience higher pollution concentrations than other communities, a statistic we refer to as the environmental justice gap (or EJ gap).<sup>1</sup> Could the adoption of environmental markets be compounding existing EJ gaps?

Whether a market-based environmental policy widens or narrows the EJ gap depends on the joint spatial distribution of polluting facilities, their abatement costs, and disadvantaged communities. Market-based policies induce relatively less abatement from facilities with steeper marginal abatement cost curves. If these facilities are upwind of disadvantaged communities, such policies will widen an existing EJ gap. Conversely, if these facilities are upwind of non-disadvantaged communities, a market-based policy will narrow the EJ gap [68].<sup>2</sup> Unfortunately, facility-level marginal abatement cost curves are usually unobserved, making it hard to anticipate the direction of EJ gap effects ex-ante. This difficulty underscores the need for ex-post empirical approaches, for which prior studies have largely found inconclusive EJ gap effects [69, 70, 71].

This paper estimates the EJ gap consequences of California’s greenhouse gas (GHG) cap-and-trade (C&T) program, which since 2013 has created the world’s second largest carbon market. This program has also been a focal point of EJ concerns, as local air pollution emissions are typically co-produced with GHG emissions.<sup>3</sup> The possibility that

---

<sup>1</sup>EJ gaps across many settings have been shown through case [60, 61, 62, 63, 64] and population-level [65, 66, 67] studies.

<sup>2</sup>Additionally, for a policy regulating global pollutants like greenhouse gases, the EJ gap effect depends on the extent in which GHG and local pollutants are co-produced.

<sup>3</sup>Similar EJ concerns have arisen elsewhere. Recent efforts to introduce state-level U.S. climate policies

the program could widen California's existing EJ gaps in local air pollution has, among other critiques, led to political opposition that temporarily paused the program's initial development in 2011 and nearly halted renewal efforts in 2017. However, to date, there has been limited causal evidence on whether the program has indeed widened EJ gaps.

We make two contributions, one empirical and another methodological, in order to establish the EJ gap consequences of California's C&T program. First, we find that the C&T program has lowered GHG and criteria air pollution (i.e., PM<sub>2.5</sub>, PM<sub>10</sub>, NO<sub>x</sub>, and SO<sub>x</sub>) emissions for sample facilities. Specifically, we exploit the program's facility-level eligibility rule based on historical emissions and its timing to estimate a break in differential emission trends between regulated and unregulated facilities after 2013. This research design is possible because we observe facility GHG and criteria air pollution emissions for both regulated and unregulated facilities, and for periods before and after the program's introduction, data availability that is not common across cap-and-trade programs. For example, facility-level pre-program emissions are not directly observed for the European Union Emissions Trading System (EU-ETS), the world largest carbon market [75, 76, 66]. Even in settings where emissions data is available, emissions-based eligibility thresholds can sometimes be too low for there to be sufficient control units within the same jurisdiction, as in the case of Southern California's RECLAIM NO<sub>x</sub> C&T program [69]. We compare regulated and unregulated units within the same jurisdiction. Our identifying assumption requires that any existing differential emission pre-trends between regulated and unregulated facilities would have continued after 2013 if not for the C&T program.

We estimate that C&T reduced emissions annually at a rate of 3-9% across GHG and criteria air pollutants during 2012-2017. To isolate the C&T effect from that of other concurrent climate programs in California, such as renewable portfolio and low carbon

---

and renew the European Union Emissions Trading System were opposed on EJ grounds [72, 73, 74].

fuel standards, we restrict attention to facilities that were only directly regulated by C&T. Emissions abatement induced by these complementary climate programs have in general made it difficult to discern whether C&T contributed to the recent 27.1 million ton CO<sub>2</sub>e decline in total California GHG emissions between 2012-2017 [77, 78]. Our estimates imply that GHG emissions across sample facilities declined by 3.2 million tons of CO<sub>2</sub>e during this period. The exclusion of C&T-regulated facilities subject to complementary program from our analysis suggests that this figure is a weak lower bound on the effect of C&T on total California GHG emissions.

We demonstrate that C&T emissions effects are robust to various model specification and sample restriction choices; to concerns about spillover effects between regulated and unregulated facilities; and to heterogeneity in emission effects as a function of a facility's average emissions. In a placebo test that systematically imposes trend breaks across sample years, we detect the largest trend break in 2013, the year when the program was actually introduced.

Our second contribution is to develop an empirical approach for determining how policy-driven changes in pollution *emissions* alter the spatial distribution of pollution *concentrations*. The canonical economics framework for evaluating environmental policies requires knowing the link between pollution “source” and “receptors” [79]. In practice, however, this mapping is rarely characterized and is instead assumed to follow simple spatial patterns such as assigning pollution concentrations to areas within the same geographic unit of a facility or within a distance circle centered at a facility [64]. In reality, the spatial and temporal patterns of pollution dispersal are far more complex and depend on topography and time-varying atmospheric conditions. Failure to accurately account for actual dispersal patterns can lead to bias estimates even in otherwise valid quasi-experimental settings [80].

To address this challenge, our estimation framework explicitly embeds an atmospheric



dispersal model, a computationally-intensive procedure that involves running over two million pollution trajectories. Specifically, our approach combines estimates of C&T emissions effects (and its uncertainty) at the facility level with an analysis of resulting EJ gap changes at the location level, as determined by the atmospheric dispersal model. In doing so, we build on prior studies using dispersal models which typically only conduct analysis at the location-level (e.g., [81]) or facility-level (e.g., [70]). Location-only studies insert observed (not policy-driven) emissions into a dispersal model and thus do not consider changes in pollution concentration arising from specific policies. Facility-only studies typically examine whether a policy's effect on emissions varies with demographic characteristics of downwind locations from a facility. We formally demonstrate that estimates from such facility-level regressions do not in general equal the EJ gap effect and need not even be of the same sign. We further show that for the EJ gap effect to be recovered from facility-level estimates, one must assume a highly simplistic spatial pattern of pollution dispersal, an assumption which we can reject for our setting.

Employing a definition of a “disadvantaged” zip code that serves as a basis for California's EJ policies, we detect three EJ gap findings. First, consistent with EJ concerns in the lead up to the C&T program's introduction, we find not only were there baseline EJ gaps across criteria air pollutants in 2008, but that gaps were widening in the 2008-2012 period before the program. Second, the C&T program has narrowed EJ gaps since 2013. Third, while EJ gaps have narrowed, they have not been eliminated: by 2017, the C&T program returned EJ gaps roughly to 2008 levels. These EJ gap effects are robust across a variety of checks. In particular, we find that allowing for heterogeneous emissions effects as a function of a facility's average emissions leads to slightly larger declines in EJ gaps. We further demonstrate similar EJ gap effects when employing an alternative atmospheric dispersal model that generates secondary  $PM_{2.5}$  concentrations. An analysis of spatial heterogeneity reveals that EJ gaps narrowed most for disadvantaged zip codes

in California's Central Valley, while a few disadvantaged zip codes in Los Angeles County experienced widening gaps.

We demonstrate the importance of modeling pollution dispersal for our results. Our EJ gap effects become unstable if instead of modeling pollution dispersal, we were to employ more conventional approaches for assigning pollution emissions to concentrations. We posit that our empirical approach may have broader applicability. In particular, there is a common need across many environmental policy settings to track how policy-driven changes in pollution emissions alter the spatial distribution of pollution concentration [82, 83, 80].

The paper is structured as follows: Section 2.2 considers a conceptual framework for how a C&T program could widen or narrow an existing EJ gap and offers background on California's GHG C&T program. Section 2.3 summarizes our data. Section 2.4 details our empirical approach. Section 2.5 presents our results. Section 2.6 provides a discussion.

## 2.2 Background

We begin by discussing how the introduction of a cap-and-trade (C&T) program can either widen or narrow existing pollution concentration gaps between disadvantaged and other communities. We then review California's greenhouse gas (GHG) cap-and-trade program.

### 2.2.1 Cap-and-trade and the environmental justice gap

In a textbook C&T program, the regulator establishes a limit (or cap) on total emissions within a jurisdiction by issuing a fixed supply of emission permits. Regulated facilities are then either given, or must purchase, permits to cover their emissions. Permit

trading allows the marginal abatement cost (MAC) of emissions to be equalized amongst regulated facilities to the permit price.<sup>4</sup>

Two key consequences of C&T are often emphasized. First, by placing a price on pollution, a C&T program induces polluting facilities to internalize (some of) the social costs of their emissions.<sup>5</sup> Second, by equalizing MACs across facilities, a C&T program allocates emissions by inducing relatively less abatement from facilities with steeper MAC curves and more abatement from facilities with flatter MAC curves. In theory, the resulting allocation of abatement achieves the aggregate emissions cap at the lowest total abatement cost across regulated facilities [59].

What is less clear is how the allocative efficiency achieved by C&T alters the spatial distribution of pollution concentration. In particular, there is growing concern that the same market forces resulting in allocative efficiency may also be altering the difference in pollution concentrations experienced between disadvantaged and other communities. This difference, which we call the “environmental justice gap” (or EJ gap) has been shown to be positive in the many settings [60, 61, 62, 63, 64, 65, 66, 67].

The introduction of C&T can either widen or narrow an existing EJ gap. Figure 2.1 illustrates this ambiguous effect for a stylized two-facility setting with emissions ( $e$ ) on the horizontal axis and permit prices ( $\tau$ ) on the vertical axis. The first facility is upwind of a disadvantaged community (DAC) with a marginal abatement curve labeled “DAC” (in orange). The second facility is upwind of a non-disadvantaged community and has a marginal abatement curve labeled “non-DAC” (in gray).<sup>6</sup> To establish an existing positive EJ gap prior to the introduction of C&T, we allow the DAC facility to have larger emissions in the absence of C&T, or when  $\tau = 0$ . When C&T is introduced, each

<sup>4</sup>The modern C&T framework was initially developed by [57] and [84].

<sup>5</sup>Whether social costs are fully internalized depends on if the cap is set at the socially optimal level.

<sup>6</sup>The horizontal axes in Figure 2.1 indicates emissions rather than abatement in order to illustrate emissions levels prior to C&T when  $\tau = 0$ .

facility's MAC is equated to the equilibrium permit price  $\tau = \tau^*$ . What happens to the EJ gap?

In the left panel of Figure 2.1, the DAC facility has a steeper MAC curve than the non-DAC facility, causing the DAC facility to abate less than the non-DAC facility under C&T. In this case, C&T widens the EJ gap. The right panel of Figure 2.1 shows an alternative case whereby the DAC facility has a flatter MAC curve than the non-DAC facility. Following C&T, the DAC facility abates more than the non-DAC facility, narrowing the EJ gap.

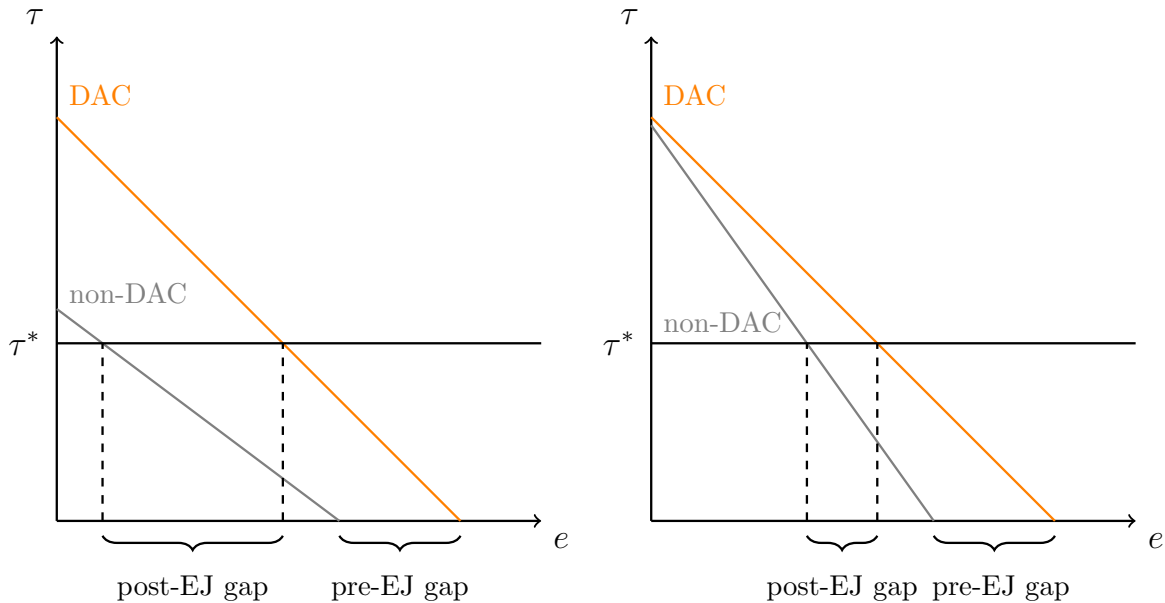
Thus, in settings with an existing positive EJ gap, whether C&T widens or narrows the EJ gap depends on whether facilities upwind of DAC communities have relatively steeper or flatter MAC curves. Furthermore, for a cap-and-trade system regulating a global pollutant such as greenhouse gases, the EJ gap effect depends on the extent in which GHG and local air pollutants are co-produced.

Unfortunately, facility-level MAC curves are rarely observed, which limits the ability to anticipate EJ gap effects of proposed C&T programs. Ex-post studies also face several empirical challenges. First, isolating the effect of reallocation from cap-and-trade requires restricting attention to facilities that are only regulated by cap-and-trade and not additionally by complementary climate programs.<sup>7</sup> Second, to remove the influence of macroeconomic conditions, one needs to estimate the effect of cap-and-trade for regulated facilities relative to unregulated facilities. Third, estimated C&T-driven facility emissions must be mapped onto location-level pollution concentrations in order to examine resulting EJ gap changes. Section 2.4 details how we overcome these challenges.

---

<sup>7</sup>Returning to Figure 2.1, suppose a complementary climate program binds for one facility such that its emissions are unchanged following the introduction of cap-and-trade. Any subsequent change in the EJ gap following cap-and-trade now depends on the complementary program, and in particular whether it binds for the DAC or non-DAC facility and at what emissions level.

Figure 2.1: EJ gap under cap-and-trade



NOTES: Panels illustrate how the introduction of a C&T program can widen or narrow an existing EJ gap in a two facility setting. Horizontal axes indicate emissions. Vertical axes indicate marginal abatement costs, and equivalently the permit price under C&T. The marginal abatement cost curve for facility upwind of a disadvantaged community (labeled DAC) is shown in orange. The marginal abatement cost curve for facility upwind of a non-disadvantaged community (labeled non-DAC) is shown in gray.  $\tau^*$  indicates the permit price under C&T. In the left panel, the DAC-upwind facility has a relatively steeper MAC curve. In the right panel, the DAC-upwind facility has a relatively flatter MAC curve.

### 2.2.2 California's GHG cap-and-trade program

California's has one of the world's most sophisticated and ambitious climate policies. In 2006, California passed Assembly Bill 32 (AB 32), requiring total GHG emissions across the state to reach 1990 emissions level by 2020. AB 32 remains the only economy-wide climate policy in the U.S.: all other state or national climate policies regulate specific sectors, whereas AB 32 covers all GHG emission sources.

To meet this GHG target, AB 32 established a suite of climate programs. One key program was cap-and-trade, introduced in 2013 and administered by the California Air Resources Board (CARB).<sup>8</sup> The program requires participation by all stationary

<sup>8</sup>Prominent complementary programs to C&T under AB 32 include a Renewable Portfolio Standard for electricity generation and a Low Carbon Fuel Standard for refineries.

GHG-emitting facilities producing at least 25,000 metric tons of annual carbon dioxide equivalent emissions, or CO<sub>2</sub>e, during any year between 2009-2012.<sup>9</sup> This eligibility criteria covers all sectors that directly emit GHGs from stationary sources and is unique amongst other AB 32 climate programs.<sup>10,11</sup> California's C&T program has since created the world's second largest carbon market by permit value, following the European Union Emissions Trading System (EU-ETS).

In 2016, California met AB 32's 2020 GHG target four years early. That same year, the state extended its GHG target to 40% below 1990 levels by 2030. This was shortly followed by a 2030 extension of the C&T program. However, critical questions remain regarding the performance and consequences of the C&T program.

First, it remains unclear whether C&T has lower GHG emissions. In particular, when C&T coexists with complementary climate programs, an overall GHG emissions cap can be met with little or no abatement induced by C&T if these complementary programs bind. Indeed, an ex-ante analysis of California's GHG C&T program demonstrated a potentially large role played by such complementary programs on overall GHG abatement [78].<sup>12</sup> Second, even if C&T lowered GHG and local air pollution emissions, it remains unclear whether the resulting change in the spatial distribution of air pollution concentrations widens or narrows California's EJ gap.

---

<sup>9</sup>Greenhouse gases covered by the program were CO<sub>2</sub>, CH<sub>4</sub>, N<sub>2</sub>O, HFCs, PFCs, SF<sub>6</sub>, NF<sub>3</sub> and other fluorinated GHGs. The 25,000 metric ton eligibility criteria is re-evaluated

<sup>10</sup>The 2013 timing of the C&T program is also unique. Most other AB 32 climate programs were introduced earlier.

<sup>11</sup>The GHG C&T program does not directly regulate local criteria air pollution emissions. Any changes in the spatial distribution of local air pollution concentration due to the program is driven by the program's reallocation of local air pollution emissions that is co-produced with GHG emissions.

<sup>12</sup>Furthermore, even a positive GHG permit price does not ensure that the C&T program caused GHG emissions to fall. Suppose, for example that there was some form of restriction on GHG emissions prior to the C&T program leading to a pre-program positive shadow price on GHG abatement. A C&T program with an overall cap set equal to total emissions under the prior restriction would generate a positive permit price despite no change in overall GHG emissions.

## 2.3 Data

Our analysis involves two primary datasets: 1) GHG and criteria air pollution emissions at the facility-by-year level and 2) an indicator of whether a zip code is considered to be “disadvantaged” according to California legislation.

**Facility emissions** We obtain 2008-2017 facility-level annual emissions of GHG (or CO<sub>2</sub>e), PM<sub>2.5</sub>, PM<sub>10</sub>, NO<sub>x</sub>, and SO<sub>x</sub>, all in metric tons, from CARB’s Pollution Mapping Tool.<sup>13</sup> We observe GHG as well as criteria air pollutions emissions for both C&T-regulated and non-regulated stationary facilities, before and after the introduction of the C&T program.<sup>14</sup>

Several additional facility-level variables serve as inputs for the atmospheric dispersal model. CARB provides facility latitude and longitude as well as pollution-specific stack heights for a subset of facilities. For other facilities, we impute missing pollution-specific stack heights using sector averages constructed from non-missing observations.

**Definition of a disadvantaged community** There is no established definition of a “disadvantaged” community. Previous papers in other settings use a location’s median income or minority share of population as proxy measures [69, 70, 85]. For our setting, we select a policy-relevant definition of a “disadvantaged” community. Senate Bill 535 (SB 535), passed in 2012, requires a portion of the revenue from the auction of C&T

<sup>13</sup>Available here: [https://ww3.arb.ca.gov/ei/tools/pollution\\_map/](https://ww3.arb.ca.gov/ei/tools/pollution_map/)

<sup>14</sup>Stationary facilities with annual emissions past a certain threshold must report emissions. For GHGs, the data reporting threshold is 10,000 metric tons of CO<sub>2</sub>e, set by CARB. For criteria air pollutants, CARB sets a reporting threshold of 10 metric tons per year, but each air district can set lower data reporting thresholds. As a consequence, we observe criteria air pollution emissions below 10 metric tons, with no evidence of bunching at 10 tons (see histograms of sample facility-year emissions in Figure B.1). We confirmed that emissions data in CARB’s Pollution Mapping Tool matches values found in source datasets: CARB’s Mandatory Reporting Regulation (MRR) dataset for GHG emissions and the California Emissions Inventory Development and Reporting System (CEIDARS) for criteria air pollution emissions. Details on California’s emissions reporting requirements can be found: [https://ww3.arb.ca.gov/ei/tools/pollution\\_map/doc/caveats%20document12\\_22\\_2017.pdf](https://ww3.arb.ca.gov/ei/tools/pollution_map/doc/caveats%20document12_22_2017.pdf)

permits to be directed towards benefiting disadvantaged communities. SB 535 formally defines a “disadvantaged community” using CalEnviroScreen, a scoring system based on multiple indicators developed by the California Environmental Protection Agency. Specifically, a zip code is considered disadvantaged if it contains all or part of a census tract with a CalEnviroScreen score above the top 25th percentile. Zip codes designated as disadvantaged are shaded in dark blue in Figure 2.2a. Importantly, pre-2013 data was used in constructing CalEnviroScreen, which mitigates the concern that cap-and-trade may have affected zip code designation. We further augment our zip code level data with average 2008-2012 population obtained from the U.S. Census Bureau.

## 2.4 Empirical Approach

Our analysis proceeds along three steps. First, we use facility-by-year-level data to estimate how the GHG C&T program altered GHG,  $PM_{2.5}$ ,  $PM_{10}$ ,  $NO_x$ , and  $SO_x$  emissions. Second, we feed C&T-driven  $PM_{2.5}$ ,  $PM_{10}$ ,  $NO_x$ , and  $SO_x$  emissions predicted from the first step into an atmospheric dispersal model to generate zip code-by-year-level concentrations of these pollutants due to the program. Finally, we examine whether the C&T program changed the concentration gap for these pollutants between disadvantaged and other communities following its 2013 introduction.

**Step 1: Estimating C&T effects on emissions** We exploit the facility-level eligibility criteria based on pre-program GHG emissions and the 2013 timing of the C&T program to identify its effects on GHG,  $PM_{2.5}$ ,  $PM_{10}$ ,  $NO_x$ , and  $SO_x$  facility-level emissions during 2008-2017. Because the program’s eligibility criteria is based on pre-C&T GHG emissions, we expect regulated and unregulated facilities to differ in pre-program emissions levels and perhaps also in pre-program emission trends. Our empirical test



therefore examines whether differential emission trends exhibit a break after 2013. For this test to have a causal interpretation, our identifying assumption requires that any existing differential emission pre-trends to have continued if not for the introduction of the C&T program.<sup>15</sup>

Specifically, let  $j$  index facilities.  $C_j \in \{0, 1\}$  is GHG C&T regulatory status with  $C_j = 1$  indicating facility  $j$  is regulated.<sup>16</sup> For facility  $j$  in year  $t$ ,  $Y_{jt}^p$  is annual emissions of pollutant  $p \in \{GHG, PM_{2.5}, PM_{10}, NO_x, SO_x\}$ . Because emissions exhibit a skewed distribution and contain zero values, we apply an inverse hyperbolic sine transformation, which like a log transformation lends a percentage effect interpretation, but with the added advantage of retaining zero-valued observations [86]. To examine differential emission trends driven by the C&T program, we estimate the following specification:

$$\text{asinh}(Y_{jt}^p) = \kappa_1^p[C_j \times t] + \kappa_2^p[C_j \times \mathbf{1}(t \geq 2013) \times t] + \phi_j^p + \gamma_t^p + \nu_{jt}^p \quad (2.1)$$

Facility-specific dummy variables  $\phi_j^p$  removes time-invariant determinants of pollution  $p$  for facility  $j$ . Year-specific dummy variables  $\gamma_t^p$  remove common determinants of emissions affecting all sample facilities in year  $t$ , such as California-wide economic conditions.

$\kappa_1^p$  captures the differential emission pre-trend for pollutant  $p$  between facilities that would and would not eventually be regulated by the C&T program during 2008-2012,

---

<sup>15</sup>Because there is no overlap in pre-program GHG emissions for regulated and unregulated facilities, we are unable to implement a matching estimator that matches on pre-program emissions, as is done in [69] and [76]. Implementing such a matching approach would require emissions data from facilities outside of California. That comparison, however, may be confounded by systematic unobserved differences between California and non-California facilities.

<sup>16</sup>All but 39 facilities that emit local air pollution found in CARB's Pollution Mapping Tool have time-invariant GHG C&T regulatory status between 2008-2017. These 39 facilities all switched status in 2017. Under the C&T program, a regulated (unregulated) facility can become unregulated (regulated) if annual GHG emissions fall below (above) the 25,000 metric tons threshold in any year during a prior compliance period. Of the 39 facilities that switched status in 2017, 8 switched even though annual GHG emissions during the previous 2015-2016 compliance period should not have permitted a regulatory status change. Because we do not know if these switches are due to actual changes in regulatory status or coding errors, we retain these 39 facilities in our sample and re-assign them their previous (time-invariant) regulatory status for 2017. In a robustness check, we drop observations from these 39 facilities in our estimation.

reported in annual percentage point changes.  $\kappa_2^p$  is the change, or break, in the differential emission trend after the program's introduction during 2013-2017.  $\nu_{jt}^p$  is clustered at the county-level to allow for arbitrary forms of heteroskedasticity and serial correlation within a county.

We employ two sample restrictions to strengthen identification of trend break effects in equation (2.1). First, despite the C&T program's unique eligibility criteria and timing, the presence of other major climate programs under AB 32, such as the Renewable Portfolio Standard for electricity generators and the Low Carbon Fuel Standard for refineries, may confound C&T effects for these facilities. We remove electricity generators and refineries from our sample to avoid this possibility.<sup>17</sup> Second, to ensure better comparability between treated and control facilities, we restrict our sample to facilities with sample average annual GHG emissions below the 75th percentile.<sup>18</sup> As a robustness check, we consider smaller and larger cutoff percentiles.

Our benchmark sample contains 106 regulated and 226 unregulated facilities. Each regulated facility is shown as a black dot in Figure 2.2a. Table B.1 shows average 2008-2012 annual GHG and criteria emissions and sectoral distribution for sample regulated and unregulated facilities. Since C&T regulatory status is defined by historical GHG emissions, it is unsurprising that regulated and unregulated facilities exhibit different average pre-program emissions, nor does this invalidate our differential emissions trend break design, *per se*. Table B.1 also shows a slight sectoral imbalance between regulated and unregulated facilities, with more regulated facilities in extraction and more unregulated facilities in services. In a robustness check, we replace year fixed effects in equation (2.1) with sector-by-year fixed effects to address concerns that this sectoral imbalance may confound our estimates.

---

<sup>17</sup>This restriction also addresses concerns about the the 2013 closure of the San Onofre Nuclear Generating Station, a power plant in southern California [87].

<sup>18</sup>The 75th percentile corresponds to average annual emissions of 62,770 metric tons of CO<sub>2</sub>e.

To construct facility-by-year emissions driven by the C&T program (relative to California-wide determinants of pollution), we apply a hyperbolic sine transformation to the first two terms of equation (2.1) and the estimated facility-level fixed effect.<sup>19</sup> Because facilities differ by average emission levels, the inclusion of facility-level fixed effects allows us to generate heterogeneous C&T-driven pollution abatement across regulated facilities despite estimating a common percentage effect.<sup>20</sup> This implicitly assumes that larger emitting facilities abate more under C&T. To examine this assumption, in a robustness check, we estimate variants of equation (2.1) that allow the post-C&T trend break to vary as linear and quadratic functions of facility-level average annual emissions.

**Step 2: Modeling pollution dispersal** Our second step determines how C&T-driven criteria air pollution disperses spatially across California. The standard approach is for the researcher to prescribe the set of locations affected by emissions from a particular source, either by assuming emissions only disperses within areas in the same administrative unit of the source or within a radially uniform distance from the source. For example, one may assume emissions from a facility in Los Angeles County only affect Los Angeles County or areas within a certain radial distance of that facility. Actual affected areas, however, may not conform to these assumptions and instead may vary depending on topography or time-varying meteorological conditions. To fully capture the complexity of pollution dispersal, we turn to an atmospheric dispersal model.

We feed predicted facility-by-year PM<sub>2.5</sub>, PM<sub>10</sub>, NO<sub>x</sub>, and SO<sub>x</sub> emissions from step 1,

<sup>19</sup> Specifically, C&T-driven emissions is:

$$\hat{Y}_{jt}^p = \sinh \left( \hat{\kappa}_1^p [C_j \times t] + \hat{\kappa}_2^p [C_j \times \mathbf{1}(t \geq 2013) \times t] + \hat{\phi}_j^p \right) * e^{(RMSE)^2/2}$$

where hat notation indicates estimated parameters and RMSE is the root mean squared error from equation (2.1). In theory, the hyperbolic sine transformation can generate negative emission values. In practice, our benchmark model predicts negative emissions for 1%, 1%, 0.2%, and 0.3% of sample observations for PM<sub>2.5</sub>, PM<sub>10</sub>, NO<sub>x</sub>, and SO<sub>x</sub>, respectively. We replace these negative values with zeros.

<sup>20</sup>For example, a 10% abatement effect implies 10 tons of abatement for a facility with 100 tons of average annual emissions and 5 tons of abatement for a facility with 50 tons of average annual emissions.

together with the location and stack height of each facility, into the Hybrid Single Particle Lagrangian Integrated Trajectory Model (HYSPLIT), an atmospheric dispersal model developed by the U.S. National Oceanographic and Atmospheric Administration (NOAA) with meteorological conditions from NOAA's 40-km resolution North American Model Data Assimilation System (NAMDAS) [88]. An emerging literature uses HYSPLIT to convert pollution emissions to concentrations [70, 89, 90].

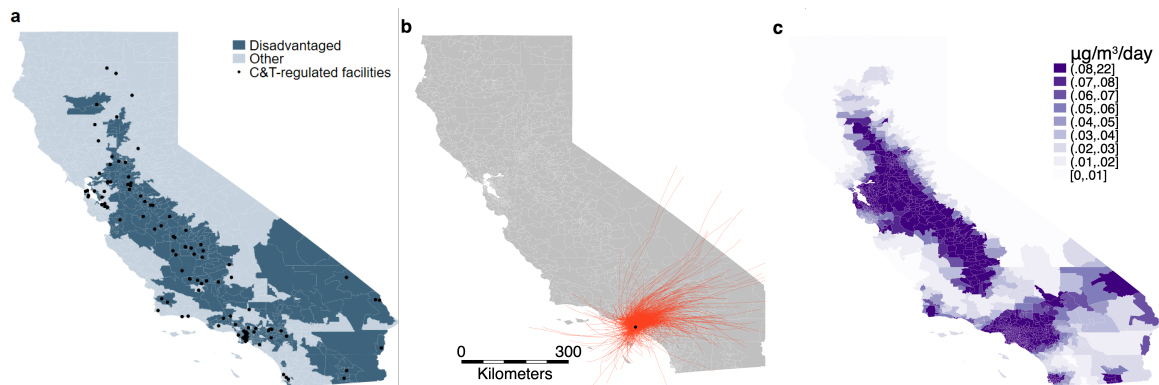
We choose HYSPLIT because it provides a middle-of-the-road approach for our application, balancing atmospheric realism with computational tractability. HYSPLIT is less computationally intensive than chemical dispersal models such as WRF-Chem, but at the cost of not incorporating atmospheric chemistry which is important for modeling secondary pollutant formation. At the same time, HYSPLIT is more reliable for modeling pollution dispersal beyond distances of 50 kilometers, which less computationally-intensive Gaussian-plume models like AERMOD or APEEP do poorly [91].

We note several features of our HYSPLIT implementation. First, to account for high-frequency variation in meteorological conditions, we run forward particle trajectories at four hour intervals, implicitly assuming that annual emissions are distributed uniformly within the year. Each trajectory runs for 24 hours, a duration long enough to ensure most emitted particles leave California.<sup>21</sup> Second, because HYSPLIT does not explicitly account for particle decay, we apply half-life parameters from the atmospheric chemistry literature set at 24 hours for  $\text{PM}_{2.5}$  and  $\text{PM}_{10}$ [93], 3.8 hours for  $\text{NO}_x$  [94], and 13 hours for  $\text{SO}_x$  [95]. Third, we assume that a particle no longer contributes to surface pollution concentrations once it exits the planetary boundary layer, beyond which there is far less turbulent mixing. We conservatively set the boundary layer height at 1 km above the surface, which is about double the typical height for California [96]. As a robustness

---

<sup>21</sup>Unlike [92], we do not discard the first hour of each particle trajectory because doing so may omit highly localized pollution concentrations that may be important for our distributional analysis.

check, we also consider boundary layer heights of 0.5 and 2 km. As an illustration of pollution dispersal modeled by HYSPLIT, Figure 2.2b shows the trajectories of pollution emitted by a regulated facility in Los Angeles during 2016. In total, we compute over 2 million particle trajectories from the roughly one hundred regulated facilities in our sample during the 2008-2017 period. This procedure takes about 24 hours to complete using over one thousand facility-by-year parallelized nodes on a high-performance computing cluster.



NOTES: Panels illustrates how facility-level emissions is converted to zip code-level pollution concentrations using an atmospheric dispersal model. Shading in panel (a) shows California zip codes that are designated as disadvantaged (dark blue) and zip codes that are not (light blue) according to California policy. Black dots show sample facilities regulated by California's GHG C&T program. Panel (b) shows HYSPLIT-generated particle trajectories every 4-hours from a regulated facility during 2016. Panel (c) shows zip code-level average daily  $PM_{2.5}$  concentrations (in  $\mu g/m^3/day$ ) during 2008-2017 driven by facilities regulated by the C&T program as modeled by HYSPLIT.

HYSPLIT generates particle-level trajectories. To convert this into concentration units, we sum HYSPLIT trajectories for each zip code and year and divide by the volume of the atmosphere between a zip code's surface and the boundary layer. We further divide by 365 days. This gives us a zip code-by-year measure of average daily C&T-driven pollution concentration for the 1 km-high air column above each zip code in units of  $\mu g/m^3/day$ .<sup>22</sup> Figure 2.2c shows our benchmark HYSPLIT-generated daily concentration

<sup>22</sup>Other HYSPLIT applications convert HYSPLIT particles into concentration units by regressing HYSPLIT output onto concentration output from a different atmospheric dispersal model using the same emissions sources (see for example: [97]) to obtain predicted concentrations using that fitted relationship.

(in  $\mu\text{g}/\text{m}^3/\text{day}$ ) for each zip code, averaged across 2008-2017 for  $\text{PM}_{2.5}$ . Figure B.4 similarly shows average 2008-2017 zip-code concentrations for  $\text{PM}_{10}$ ,  $\text{NO}_x$ , and  $\text{SO}_x$ .<sup>23</sup> Note that pollution concentration levels in Figure B.4 are generally below those recorded in ambient monitors because we are only considering pollution concentrations driven by C&T-driven emissions from sample regulated facilities.

Lastly, as noted, a major limitation with HYSPLIT is that it does not model secondary pollution formation. To see if secondary  $\text{PM}_{2.5}$  concentrations exhibits a different spatial pattern than primary  $\text{PM}_{2.5}$  concentrations, in a robustness check, we replace HYSPLIT with InMAP, a reduced-complexity dispersal model based on the WRF-Chem model which generates secondary pollutants [98].

**Step 3: Estimating C&T-driven change in EJ gap trends** In our third step, we examine whether the C&T program altered the difference in pollution concentrations between disadvantaged and other communities, or the EJ gap. Let  $D_i \in \{0, 1\}$  denote disadvantaged status, with  $D_i = 1$  indicating that zip code  $i$  contains all or part of a “Disadvantaged Community Census Tract,” as defined by Senate Bill 535. For zip code  $i$  in year  $t$ , we take C&T-driven pollution concentration from HYSPLIT,  $E_{it}^p$ , for criteria air pollutant  $p \in \{\text{PM}_{2.5}, \text{PM}_{10}, \text{NO}_x, \text{SO}_x\}$ , and estimate the following specification:

$$E_{it}^p = \beta_1^p [D_i \times t] + \beta_2^p [D_i \times \mathbf{1}(t \geq 2013) \times t] + \psi_i^p + \delta_t^p + \epsilon_{it}^p \quad (2.2)$$

where  $\psi_i^p$  are zip code-specific dummies and  $\delta_t^p$  are year-specific dummies.  $\beta_1^p$ , or the pre-C&T EJ gap trend, captures the linear trend in the EJ gap (from facilities that would eventually be regulated by the C&T program) during 2008-2012, before the program was

---

We are unable to perform that adjustment as there are no alternative measures of C&T-driven pollution concentrations in the literature.

<sup>23</sup>Figure 2.2, Figure B.4, and Table B.6 show that criteria air pollution from GHG C&T-regulated facilities disperses across all of California and not just zip codes designated as disadvantaged.

introduced. A positive trend (i.e.,  $\beta_1^p > 0$ ) would indicate that the EJ gap was widening prior to the C&T program. Our main parameter of interest is  $\beta_2^p$ , which captures the change in the EJ gap trend after the program's introduction, or the post-C&T EJ gap trend break. Conditional on  $\beta_1^p > 0$ ,  $\beta_2^p < 0$  implies that the introduction of the C&T program slowed the previous positive EJ gap trend. We consider two additional trend break statistics. The first statistic asks whether the post C&T EJ gap trend break is sufficiently large such that the EJ gap has actually narrowed in level terms after the C&T program. This would be captured by  $\beta_1^p + \beta_2^p$ , or the post-C&T EJ gap trend, with  $\beta_1^p + \beta_2^p < 0$  indicating that the EJ gap is narrowing.<sup>24</sup> A second statistic examines the relative degree in which C&T program has slowed the prior EJ gap trend. Specifically,  $\frac{\beta_2^p}{\beta_1^p} * 100 = \left( \frac{(\beta_1^p + \beta_2^p) - \beta_1^p}{\beta_1^p} \right) * 100$  captures the percentage change in the EJ gap trend following the introduction of the C&T program.

C&T-driven pollution concentration,  $E_{it}^p$ , the outcome variable in equation (2.2), is predicted C&T-driven emissions from equation (2.1) via HYSPLIT. As a consequence,  $\epsilon_{it}^p$ , the error term in equation (2.2), does not account for statistical uncertainty in C&T emission effects from equation (2.1). Instead,  $\epsilon_{it}^p$  may capture residuals that arise when estimating an average EJ effect in the presence of heterogeneous EJ effects. To address inference concerns, we conduct two standard error adjustments. First, we cluster  $\epsilon_{it}$  at the county level to allow for arbitrary forms of heteroskedasticity and serial correlation when heterogeneous treatment effects are not independent and identically distributed. Second, to incorporate statistical uncertainty in predicted C&T-driven emissions from equation (2.1), we conduct a bootstrap procedure drawing multiple vectors of C&T-driven emissions from the estimated empirical distributions of  $\kappa_1^p$  and  $\kappa_2^p$ , which are then

<sup>24</sup>Observe that while  $\beta_2^p < 0$  alone implies that the C&T program resulted in EJ gap benefits by slowing the growth in the EJ gap, it does not necessarily imply that this post-trend break effect is strong enough to offset the magnitude of the pre-trend such that EJ gap is narrowing in absolute terms following the program. For that to occur, one needs  $\beta_2^p < -\beta_1^p$ , or  $\beta_1^p + \beta_2^p < 0$ .

fed into steps 2 and 3. In practice, we implement 250 bootstrap draws to generate a component of the standard error for  $\beta_1^p$  and  $\beta_2^p$  that accounts for statistical uncertainty in equation (2.1). We add this component to the standard error from directly estimating equation (2.2) when reporting uncertainty for  $\beta_1^p$  and  $\beta_2^p$ . Figure B.5 plots the empirical distribution of  $\beta_1^p$  and  $\beta_2^p$  across bootstrapped draws.<sup>25</sup> Appendix B.1.1 provides more details on this bootstrap procedure.

Finally, to estimate an average EJ gap effect across individuals in California, we weight each zip code-by-year observation in equation (2.2) by average zip code population during 2008-2012, the period prior to the program.

**Comparison with prior uses of pollution dispersal models** Our empirical approach is part of a broader effort across natural and social sciences to use atmospheric dispersal models to map pollution emissions to concentrations. Prior studies can be broadly classified into two groups: whether the analysis is done at the location-level or at the facility-level.

Location-level analyses typically feed observed emissions into a dispersal model, but without first estimating the emissions effects of environmental policies [99, 100, 81, 101, 92, 97, 102]. Because these studies omit estimation of policy-driven emissions (i.e., our Step 1), they cannot attribute changes in pollution concentrations to specific policies.<sup>26</sup>

Facility-level studies examine whether a policy's effect on emissions varies with the demographic characteristics of households downwind of facilities, as determined by the atmospheric dispersal model [70, 85]. This approach augments the facility-level in equation

---

<sup>25</sup>As with prior literature, we omit uncertainty associated with atmospheric dispersal, or the mapping between facility-level emissions and zip code-level concentration. One possibility involves resampling meteorological conditions in HYSPLIT via a bootstrapping algorithm. Given that our use of HYSPLIT takes 24 hours, overlaying such an approach to the existing 3-step procedure is currently unrealistic under available computational resources.

<sup>26</sup>For example, [92] and [97] insert observed air pollution emissions from coal-fired power plants into a version of HYSPLIT to examine how much U.S.  $PM_{2.5}$  concentrations are due emissions from these plants, but cannot speak to the policies that are affecting coal-fired power plant emissions.



(2.1) by adding a term that interacts the policy treatment with demographic characteristics of downwind locations. However, given the complex spatial nature of pollution dispersal whereby concentrations in multiple locations may be affected by emissions from multiple facilities, it is not obvious whether one can recover EJ gap changes, the estimand of interest, from such an approach.

In Appendix B.1.2, we formally demonstrate that the coefficient on the interaction term from such dispersal-augmented facility-level regressions does not in general equal the EJ gap effect, nor does it necessarily have the same sign, making it hard to draw EJ gap conclusions from such regressions. We then show one special case where equality does hold but which requires - among other assumptions - a particularly strong assumption on the spatial pattern of pollution dispersal: emissions from each regulated facility must affect either *only* disadvantaged communities or *only* non-disadvantaged communities. That is, facilities cannot alter pollution concentrations in both types of locations. This assumption can be rejected in our setting: panels a and b of Figure 2.2 show how emissions from one regulated sample facility alters pollution concentrations in both disadvantaged and other communities.

Our approach combines both facility- and location-level analyses. As such, we are able to attribute changes in emissions due to the C&T program and quantify the resulting change in the EJ gap as a consequence of these emissions.

## 2.5 Results

This section presents our results. Section 2.5.1 shows the effect of C&T on differential emission trends between regulated and unregulated facilities. Section 2.5.2 examines how these C&T-driven emissions altered trends in the pollution concentration gap between disadvantaged and other communities across California.

### 2.5.1 Cap-and-trade effects on emissions

**Main results** Table 2.1 reports the pre-C&T differential emissions trend (i.e.,  $\kappa_1^p$  from equation (2.1)) and the post-C&T differential emissions trend break (i.e.,  $\kappa_2^p$  from equation (2.1)) for GHG and criteria air pollutants. Column 1 shows a statistically significant trend break in GHG emissions, indicating that the C&T program led to a reduction in GHG emissions. Prior to the program, the gap in GHG emissions between regulated and unregulated facilities increased at an annual rate of 19 percentage points. Following the introduction of the program, this trend slowed by 30 percentage points leading the gap in GHG emissions to fall at an annual rate of 11 percentage points between 2012-2017. For criteria air pollutants, columns 2-4 show a statistically significant, negative emissions trend break following the program's introduction for PM<sub>2.5</sub>, PM<sub>10</sub>, NO<sub>x</sub>. For SO<sub>x</sub>, the trend break is negative but not statistically significant, suggesting that all subsequent SO<sub>x</sub> results should be interpreted with caution.

We predict C&T-driven emissions using estimates in Table 2.1 together with facility-level fixed effects. This generates heterogeneous facility-level C&T-driven abatement between 2012-2017, or  $\hat{Y}_{j,2017}^p - \hat{Y}_{j,2012}^p$  as defined in footnote 19, and shown in Figure B.3 for GHG, PM<sub>2.5</sub>, PM<sub>10</sub>, NO<sub>x</sub>, and SO<sub>x</sub>. Averaged across sample regulated facilities, between 2012 and 2017, the C&T program reduced emissions annually at a rate of 9%, 5%, 4%, 3%, and 9% for GHG, PM<sub>2.5</sub>, PM<sub>10</sub>, NO<sub>x</sub>, and SO<sub>x</sub>, respectively.<sup>27</sup> GHG permit prices for the California C&T program have largely hovered above the program's price floor since 2013. Detecting emissions abatement from sectors directly regulated by only C&T, however, is consistent with permit prices at the price floor when complementary climate programs bind for other C&T-covered sectors. When such programs bind, aggregate demand for GHG permits fall, causing permit prices to hit the price floor.

<sup>27</sup>This is calculated by averaging  $(\frac{\hat{Y}_{j,2017}^p - \hat{Y}_{j,2012}^p}{\hat{Y}_{j,2012}^p})/5$ , as defined in footnote 19, across regulated sample facilities for each pollutant  $p$ .

Table 2.1: Trend break in emissions

	Outcome is (asinh) emissions				
	(1)	(2)	(3)	(4)	(5)
	GHG	PM <sub>2.5</sub>	PM <sub>10</sub>	NO <sub>x</sub>	SO <sub>x</sub>
$\kappa_1^p$	0.187 (0.052) [0.001]	0.058 (0.043) [0.183]	0.083 (0.033) [0.016]	0.075 (0.039) [0.061]	0.006 (0.035) [0.875]
$\kappa_2^p$	-0.297 (0.077) [0.000]	-0.097 (0.048) [0.053]	-0.117 (0.039) [0.005]	-0.104 (0.050) [0.042]	-0.037 (0.043) [0.393]
$\kappa_1^p + \kappa_2^p$	-0.111 (0.036) [0.004]	-0.039 (0.018) [0.039]	-0.034 (0.018) [0.068]	-0.029 (0.019) [0.138]	-0.031 (0.019) [0.108]
Facilities	316	302	302	303	303
Counties	41	40	40	40	40
Observations	2,054	1,968	1,968	1,970	1,965

NOTES: Estimates of pre-C&T differential emissions trend (i.e.,  $\kappa_1^p$  from equation (2.1)) and post-C&T differential emissions trend break (i.e.,  $\kappa_2^p$  from equation (2.1)) for GHG, PM<sub>2.5</sub>, PM<sub>10</sub>, NO<sub>x</sub>, and SO<sub>x</sub> across columns. All models include facility-specific and year-specific dummy variables. Standard errors clustered at the county-level in parentheses, p-value in brackets.

However, provided that total abatement driven by complementary programs is insufficient for meeting the total GHG cap, C&T will still induce abatement from sectors that are only regulated by C&T.

In total, sample regulated facilities reduced 3.2 million tons of CO<sub>2</sub>e between 2012-2017. This figure is likely a weak lower bound on the effect of C&T on total California GHG emissions as C&T is likely to have weakly negative emissions effects on regulated facilities subject to complementary climate programs but are excluded from our analysis, As a point of reference, California's statewide GHG emissions fell by 27.1 million tons of CO<sub>2</sub>e [103] between 2012-2017.

**Robustness checks** We subject these emission effects to several robustness checks. First, Figure B.2 considers placebo program start years, plotting  $\kappa_2^p$  for GHG, PM<sub>2.5</sub>, PM<sub>10</sub>, NO<sub>x</sub>, and SO<sub>x</sub> emissions from variants of equation (2.1) that impose alternative C&T start years across 2009-2016. With the exception of the SO<sub>x</sub> results, we detect the strongest trend break coefficient when we assign the treatment year to its actual occurrence in 2013.

Table B.2 considers several alternative specification and sample restriction choices. Table B.1 shows that regulated and unregulated facilities are not perfectly balanced across sectors. To address concerns that differential trends across sectors may confound our estimates, column 1 of Table B.2 replaces year fixed effects with sector-by-year fixed effects. Column 2 drops the handful of facilities whose treatment status switched only in 2017. Columns 3 and 4 change the 75th percentile average GHG emissions cutoff to the 70th and 80th percentiles.<sup>28</sup> None of these robustness checks produces estimates that differ meaningfully from our benchmark estimates in Table 2.1.

Our C&T-driven emissions which includes facility fixed effects, implicitly assumes more pollution abatement from facilities that emit more on average. To examine whether this assumption is reasonable, column 2 of Table B.3 reports a variant of equation (2.1) that further includes an interaction between the trend break term and a linear function of facility-level average emissions. A positive interaction coefficient would imply that larger emitting facilities are abating less, contradicting our assumption. With the exception of GHG emissions for which the linear interaction term is positive but of very small magnitude, the coefficient on this interaction term for every criteria air pollution is negative. This suggests that our benchmark model, which estimates an average trend break coefficient across facilities (regardless of size) is understating the degree in which

---

<sup>28</sup>The 70th and 80th percentiles for sample average annual GHG emissions corresponds to 48,834 and 82,173 tons of CO<sub>2</sub>e, respectively.

large-emitting facilities are also abating more under C&T. Column 3 of Table B.3 shows that heterogeneity by average emissions does not exhibit nonlinearity, as indicated by statistically imprecise quadratic interaction terms.

Finally, there may be a Stable Unit Treatment Value Assumption (SUTVA) as pollution may shift from a regulated to unregulated facilities following the introduction of C&T. If so, the resulting increase in unregulated facility emissions may lead to more negative estimates of the trend break parameter  $\kappa_2^p$ . Following [69], we consider two robustness checks in Table B.4 to examine this possibility. In the first test, we observe that a facility located in a county under U.S. Clean Air Act nonattainment for a particular pollutant is largely unable to increase pollution levels. This idea is implemented in column 2, which restricts the sample of unregulated facilities to those located in nonattainment counties for that pollutant under the Clean Air Act.<sup>29</sup> Our second test notes that firms with multiple facilities can more readily reallocate pollution across their facilities. In column 3, we restrict the control group of unregulated facilities to those whose parent company only operates a single plant.<sup>30</sup> If treatment spillovers were present, the trend break coefficient  $\kappa_2^p$  should be of smaller magnitude in columns 2 and 3 than in our benchmark estimate, shown in column 1. This is not the case.

## 2.5.2 Cap-and-trade effects on EJ gaps

**Validating pollution dispersal modeling** We consider two sensibility checks for our measure of C&T-driven pollution concentrations via HYSPLIT before turning to our main EJ gap results. First, we examine whether HYSPLIT-generated criteria air

---

<sup>29</sup>In Table B.4, column 2 does not apply to GHG emissions because it is not a criteria pollutant regulated under the Clean Air Act. For  $\text{SO}_x$ , there are no counties in nonattainment during our sample period. For  $\text{NO}_x$ , because there were not enough counties under  $\text{NO}_2$  nonattainment to construct a control group, we follow [69] by looking at nonattainment under Clean Air Act's one-hour ozone standard as  $\text{NO}_x$  is a precursor pollutant to ozone.

<sup>30</sup>We link each facility from CARB with its parent company as indicated by the EPA. We employ a fuzzy string matching algorithm as facility names are not standardized across the two datasets.

pollution concentrations correlate with monitored ambient air pollution concentrations. Specifically, we match zip code-level HYSPLIT-generated pollution concentration averaged over 2008-2017 to the average ambient pollution concentration of that zip code as recorded by pollution monitors averaged over the same period, obtained from the U.S. Environmental Protection Agency.<sup>31</sup> we do not expect a perfect fit between these two variables as ambient pollution at any location is composed of emissions originating from many more sources (i.e., stationary and non-stationary, within and beyond California) than our subset of stationary sources regulated by California's GHG C&T program. However, a positive correlation between the two pollution concentration measures would provide reassurance that HYSPLIT-generated pollution concentration from C&T regulated facilities is detected by ambient pollution monitors. The positive correlations shown in Table B.5 indicate that is indeed the case.<sup>32</sup>

Next, we examine the EJ gap in 2008 driven by facilities that would eventually be regulated by the C&T program. Prior work documented strong baseline EJ gaps in California [104]. Indeed, this baseline EJ gap informed initial EJ concerns regarding California's C&T program. Table B.6 shows that steps 1 and 2 of our approach reproduces EJ gaps in 2008. Disadvantaged communities experienced higher levels of  $PM_{2.5}$ ,  $PM_{10}$ ,  $NO_x$ , and  $SO_x$  concentrations in 2008 than other communities on average due to emissions from facilities that would eventually be regulated by the C&T program.

**Main results** We now turn to our main results examining the time evolution of EJ gaps between 2008-2017, shown in Table 2.2 and Figure 2.3. Across  $PM_{2.5}$ ,  $PM_{10}$ ,  $NO_x$ , and  $SO_x$ , the EJ gap widens during 2008-2012, the period prior to the C&T program, as

<sup>31</sup>Available here: [https://aqs.epa.gov/aqsweb/airdata/download\\_files.html](https://aqs.epa.gov/aqsweb/airdata/download_files.html)

<sup>32</sup>We are interested in modeling where C&T-driven pollution is dispersed. As such, we do not directly use ambient pollution data (either from ground-based monitoring stations or remotely-sensed satellites) in our analysis as it is often difficult to determine which component of any location's ambient pollution originates from C&T-regulated facilities. Such "backwards" atmospheric modeling often yield indeterminate results.

Table 2.2: Trend break in the environmental justice gap

	(1)	(2)	(3)	(4)
	PM <sub>2.5</sub>	PM <sub>10</sub>	NO <sub>x</sub>	SO <sub>x</sub>
$\beta_1^p$	0.042 (0.015) [0.006]	0.065 (0.017) [0.000]	0.085 (0.037) [0.026]	0.037 (0.025) [0.151]
$\beta_2^p$	-0.063 (0.022) [0.006]	-0.090 (0.029) [0.003]	-0.143 (0.074) [0.060]	-0.101 (0.051) [0.053]
$\beta_1^p + \beta_2^p$	-0.021 (0.015) [0.159]	-0.026 (0.020) [0.203]	-0.058 (0.050) [0.252]	-0.064 (0.027) [0.024]
$(\beta_2^p / \beta_1^p) * 100$	-149.699 (36.368) [0.000]	-139.739 (29.971) [0.000]	-168.282 (53.375) [0.002]	-272.291 (66.043) [0.000]
Zip codes	1649	1649	1649	1649
Counties	58	58	58	58
Observations	16,416	16,416	16,416	16,416

NOTES: Estimates of the pre-C&T EJ gap trend (i.e.,  $\beta_1^p$  from equation (2.2)), the post-C&T EJ gap trend break (i.e.,  $\beta_2^p$  from equation (2.2)), the post-C&T EJ gap trend (i.e.,  $\beta_1^p + \beta_2^p$ ), and the percentage change in the EJ gap trend following the introduction of the C&T program (i.e.,  $\frac{\beta_2^p}{\beta_1^p} * 100$ ) for PM<sub>2.5</sub>, PM<sub>10</sub>, NO<sub>x</sub>, and SO<sub>x</sub>, across columns. All models include zip code-specific and year-specific dummy variables. Observations weighted by zip code-level average population during 2008-2012. Parentheses indicate standard errors that account for statistical uncertainty in C&T predicted emissions ( $\nu_{it}^p$  from equation (2.1) via the bootstrap procedure in Appendix B.1.1) and county-level heterogeneity in EJ gap effects of arbitrary form ( $\epsilon_{it}^p$  from equation (2.2)). P-value in brackets.

indicated by the positive pre-C&T EJ gap trend (i.e.,  $\beta_1^p$  from equation (2.2)). Following 2013, the EJ gap trend falls: the post-C&T EJ gap trend break (i.e.,  $\beta_2^p$  from equation (2.2)) is negative and statistically significant. This drop in the EJ gap trend is sufficiently

large such that the EJ gap is actually narrowing following C&T, as indicated by the negative post-C&T EJ gap trend across pollutants (i.e.,  $\beta_1^p + \beta_2^p$ ). In percentage terms (i.e.,  $\frac{\beta_2^p}{\beta_1^p} * 100$ ), the EJ gap trend fell between 140-270% across pollutants after the program's introduction. Figure 2.3 plots this trend break as well as annual EJ gap coefficients from a more flexible version of equation (2.1) using year-specific EJ gap coefficients.<sup>33</sup> Figure 2.3 also highlights that while the C&T program has led EJ gaps to narrow since 2012, it has not eliminated them. By 2017, EJ gaps are roughly at 2008 levels across pollutants.

**Spatial heterogeneity** Estimates from equation (2.2) shown in Table 2.2 and Figure 2.3 examine the time evolution of EJ gaps averaged across disadvantaged and other zip codes. Additionally, one may be interested in how EJ gap effects vary spatially, particularly given the localized nature of EJ concerns. To examine spatial heterogeneity in trend break effects across disadvantaged zip codes, we estimate a variant of equation (2.2) allowing zip code-specific post-C&T EJ gap trend break coefficients.<sup>34</sup> Figure 2.4 shows the percentage change in the EJ gap trend following the introduction of C&T for each disadvantaged zip code for PM<sub>2.5</sub>, PM<sub>10</sub>, NO<sub>x</sub>, and SO<sub>x</sub>. Across pollutants, post-C&T EJ gaps narrowed the most for disadvantaged zip codes in California's Central Valley. For PM<sub>2.5</sub>, PM<sub>10</sub>, and NO<sub>x</sub>, Figure 2.4 also shows a cluster of zip codes in Los Angeles County that experienced widening post-C&T EJ gaps. Figure B.6 shows histograms for

---

<sup>33</sup>Specifically, the annual coefficients in Figure 2.3 are  $\beta_\tau^p$  from

$$E_{it}^p = \sum_{\substack{2008 \leq \tau \leq 2017 \\ \tau \neq 2012}} \beta_\tau^p [D_i \times \mathbf{1}(t = \tau)] + \psi_i^p + \delta_t^p + \epsilon_{it}^p$$

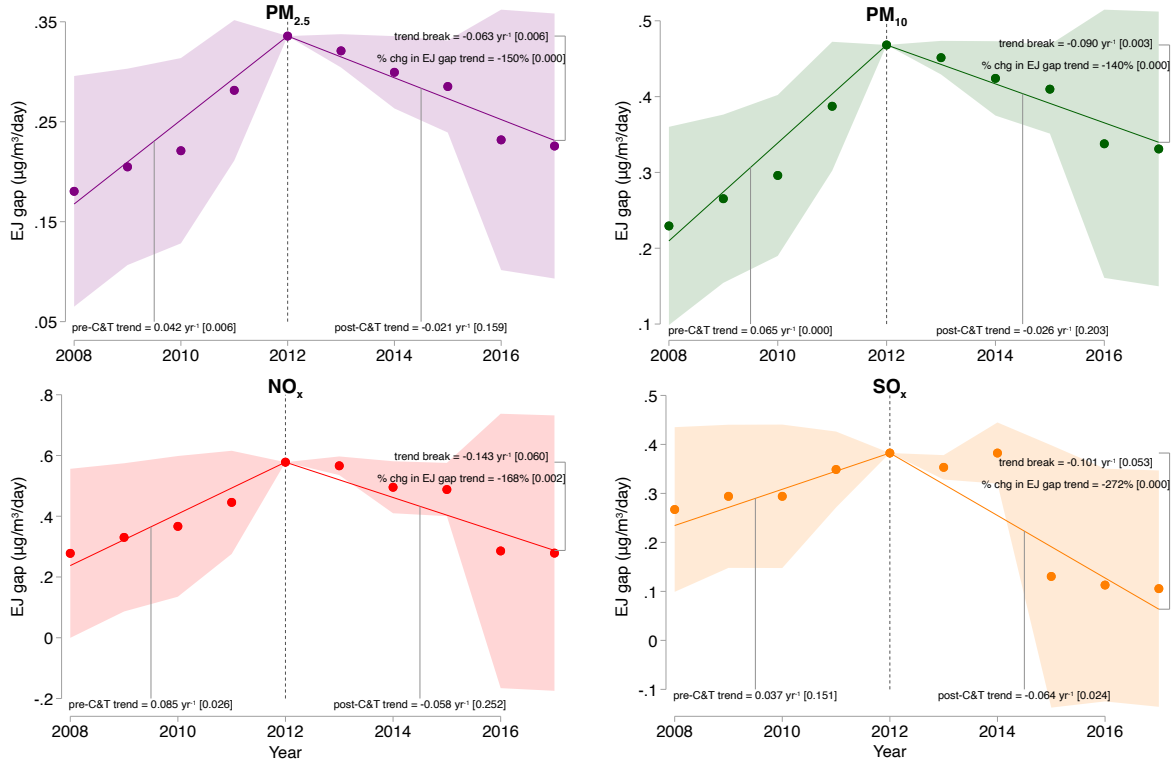
<sup>34</sup>Specifically, we estimate the following variant of equation (2.2)

$$E_{it}^p = \beta_1^p [D_i \times t] + \sum_i \beta_{2i}^p [D_i \times \mathbf{1}(t \geq 2013) \times t] + \psi_i^p + \delta_t^p + \epsilon_{it}^p$$

where  $\beta_{2i}^p$  is the post-C&T trend break for zip code  $i$ . Figures 2.4 and B.6 plot  $\frac{\beta_{2i}^p}{\beta_1^p} * 100$ , the percentage change in the EJ gap trend following the introduction of the C&T program for zip code  $i$  relative to the average pre-C&T EJ gap trend across disadvantaged zip codes.



Figure 2.3: Environmental justice gap before and after the cap-and-trade program

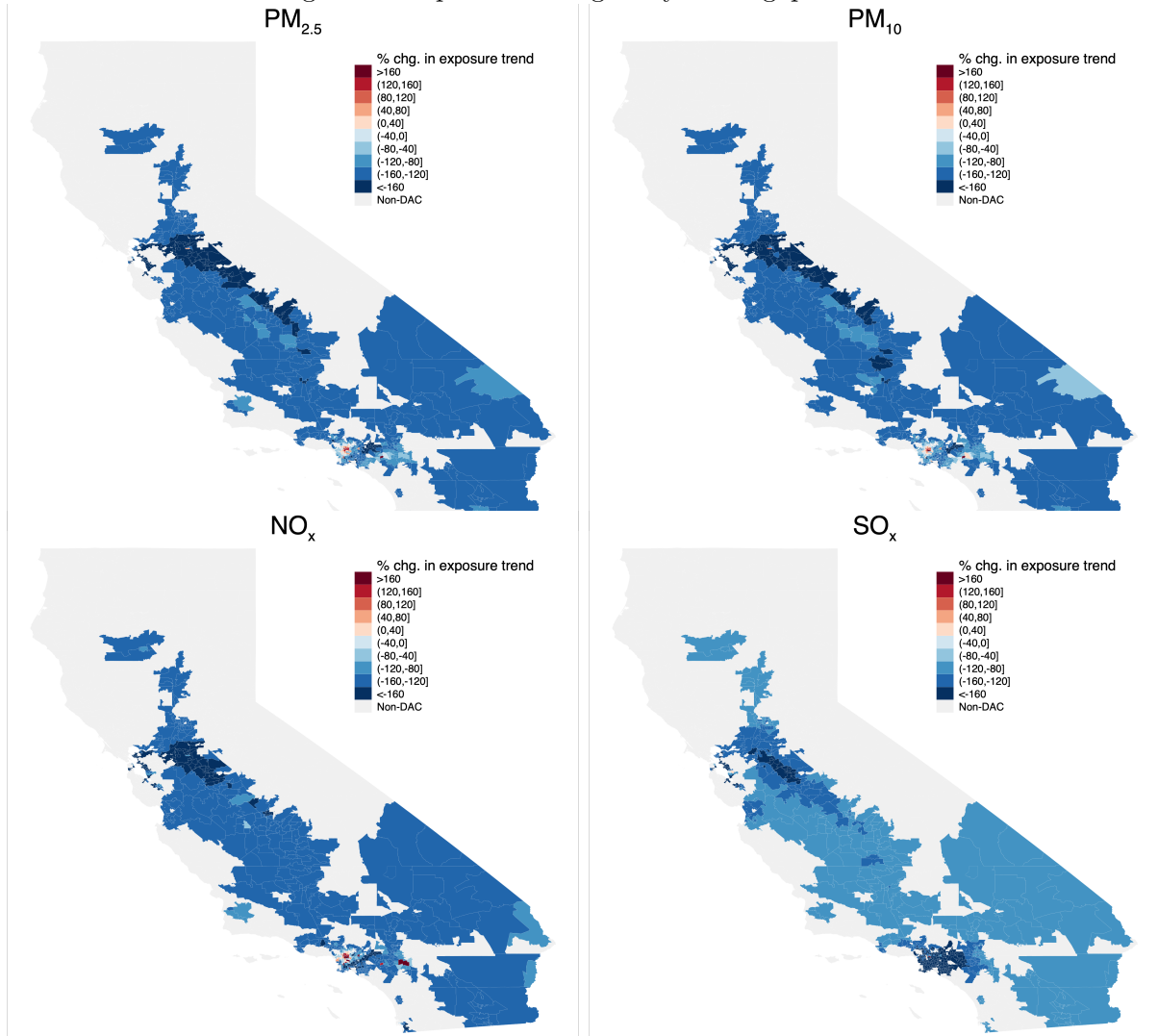


NOTES: Panels show the estimated average daily pollution concentration gap (in  $\mu\text{g}/\text{m}^3/\text{day}$ ) between disadvantaged and other zip codes (i.e., “EJ gap”) during 2008-2017 for PM<sub>2.5</sub>, PM<sub>10</sub>, NO<sub>x</sub>, and SO<sub>x</sub>, respectively. Dots show year-specific EJ gap. Solid lines show linear fit for EJ gap trend before (2008-2012) and after (2013-2017) the C&T program. Associated text indicates point estimates and standard errors for the pre-C&T linear trend, post-C&T trend break, post-C&T linear trend, and the percentage change in the EJ gap trend (i.e.,  $\beta_1^p, \beta_2^p, \beta_1^p + \beta_2^p, \frac{\beta_2^p}{\beta_1^p} * 100$ ). 95% confidence interval and p-values (in brackets) account for statistical uncertainty in C&T predicted emissions ( $\nu_{it}^p$  from equation (2.1) via the bootstrap procedure in Appendix B.1.1) and county-level heterogeneity in EJ gap effects of arbitrary form ( $\epsilon_{it}^p$  from equation (2.2)). Trend break estimates also reported in Table 2.2.

the distribution of percentage changes in EJ gap trends across disadvantaged zip codes.

**Robustness checks** We subject our EJ gap trend effects to several robustness checks. Most robustness checks forgo the bootstrap procedure across steps 1-3 (detailed in Appendix B.1.1) given the computational demands of that procedure. Instead, Figure 2.5 presents only point estimates of the percentage change in the EJ gap trend following C&T (i.e.,  $\frac{\beta_2^p}{\beta_1^p} * 100$ ) for each robustness check and compares that with the point estimate

Figure 2.4: Spatial heterogeneity in EJ gap effects



NOTES: Panels maps the zip code-specific percentage change in the EJ gap trend following the introduction of the C&T program for disadvantaged zip codes across  $PM_{2.5}$ ,  $PM_{10}$ ,  $NO_x$ , and  $SO_x$ . Blue (red) shading indicates reduced (increased) EJ gap trends following C&T for disadvantaged zip codes. Gray shading shows non-disadvantaged zip codes.

and 95% confidence interval of our benchmark result for which inference does account for statistical uncertainty from equation (2.1) via our bootstrap procedure.<sup>35</sup>

Within step 1, we conduct eight EJ gap robustness checks, drawing on C&T emis-

<sup>35</sup>Coefficients  $\beta_1^p$  and  $\beta_2^p$  in accompanying Tables B.7 and B.8 cluster standard errors  $\epsilon_{it}^p$  from equation (2.2) at the county-level but are not adjusted for statistical uncertainty in equation (2.1).

sions effects shown in Tables B.2-B.4. Equation (2.1) models changes in the emissions difference between C&T regulated and non-regulated facility as linear trends. We find a similar result when we estimate a more flexible version of equation (2.1) with year-specific emission differences (M2 of Figure 2.5 and column 1 of Table B.7); when we replace year fixed effects with sector-by-year fixed effects in equation (2.1) (M3 of Figure 2.5 and column 2 of Table B.7); and when we drop facilities that switched regulatory status in 2017 (M4 of Figure 2.5 and column 3 of Table B.7). Next, we consider restricting facilities to those with sample average annual GHG emissions below the 70th and 80th percentiles, respectively (M5-6 of Figure 2.5 and columns 4-5 of Table B.7). These alternative facility sample restrictions do not alter EJ gap trend effects.

We further allow the post C&T emissions trend break to vary as a linear function of sample average emissions. Recall from the heterogeneous emissions effects shown in column 2 of Table B.3 that large-emitting facilities are abating more than is assumed in our baseline model which assumes a common percentage emissions change. For  $PM_{2.5}$ ,  $PM_{10}$ , and  $NO_x$ , allowing for heterogeneity in emissions effects results in a slightly larger, though not statistically different, percentage change in the EJ gap trend (M7 of Figure 2.5 and column 6 of Table B.7). That is, our baseline model without heterogeneous emissions effects is slightly understating the EJ gap fall as a consequence of C&T. For  $SO_x$ , this dimension of heterogeneity implies much larger drops in the post-C&T EJ gap trend. Lastly, we examine EJ gap effects after restricting the set of unregulated C&T facilities to those in counties under Clear Air Act nonattainment and those whose parent company only operates a single facility (M8-9 of Figure 2.5 and columns 7 and 8 of Table B.7). SUTVA concerns do not alter EJ gap trend effects.

We conduct four robustness checks within step 2. We use pollution half-life parameters taken from the atmospheric chemistry literature because HYSPLIT does not model pollution decay over time. Our results are relatively stable to whether we allow for a

10% larger half-life parameter which implies a slower decay rate (M10 of Figure 2.5 and column 1 Table B.8) or a 10% smaller half-life parameter which implies a faster decay rate (M11 of Figure 2.5 and column 2 of Table B.8). Likewise our results are little affected when we lower the height of the planetary boundary layer to 0.5 km (M12 of Figure 2.5 and column 3 Table B.8) or raise it to 2 km (M13 of Figure 2.5 and column 4 Table B.8).

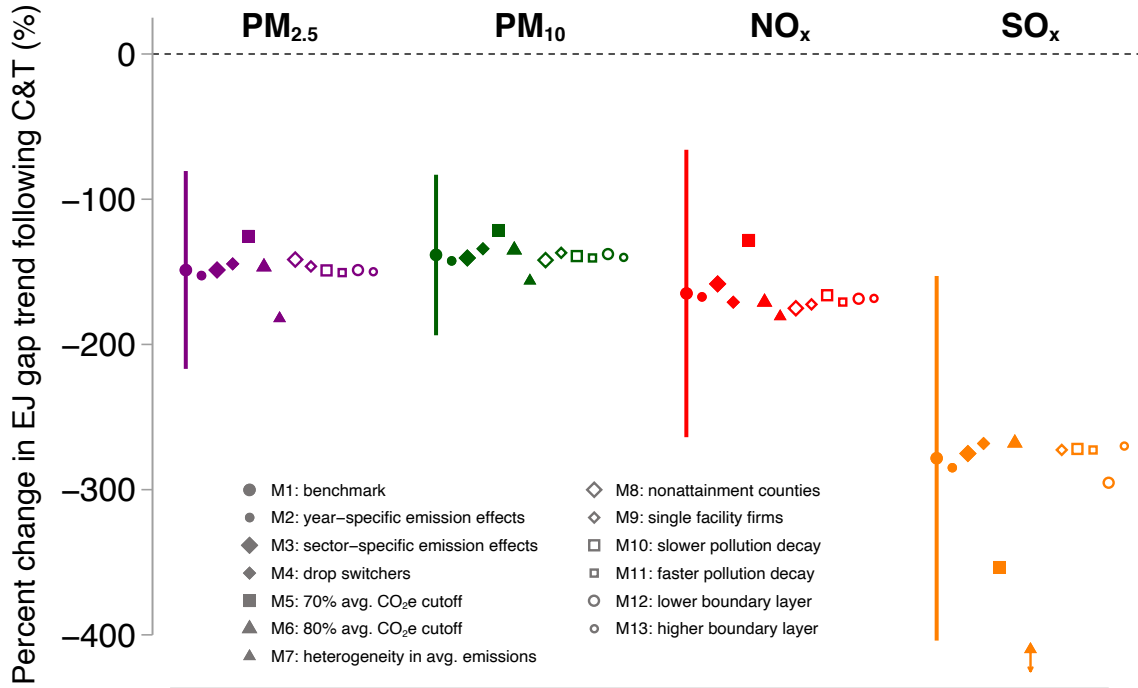
We conduct three robustness checks within step 3. The first set of checks consider alternative error structures for  $\epsilon_{it}^p$ . We find that precision increases when we allow  $\epsilon_{it}^p$  to be spatially correlated within a uniform kernel across a distance of 500 km distance [105], roughly the longitudinal width of California, and serially correlated across 5 years [106] (column 5 of Table B.8). Likewise, precision increases when we allow for error terms to be correlated across the four local pollutants using a Seemingly Unrelated Regression (SUR) procedure (column 6 of Table B.8). Equation (2.2) examines the EJ gap in daily pollution levels of  $\mu\text{g}/\text{m}^3/\text{day}$ , the concentration unit typically used for air pollution policy and by the public health literature. In Table B.9, we detect a post-C&T EJ gap trend break after applying an inverse hyperbolic sine transformation to our outcome variable, showing C&T-driven concentrations in disadvantaged communities decreased as a percentage of concentration in other communities after 2013. Standard errors reported in Table B.9 are adjusted for statistical uncertainty from equation (2.1) using our bootstrap procedure.

Finally, to examine the potential role of secondary  $\text{PM}_{2.5}$ , we replace HYSPLIT in step 2 of our procedure with InMAP, a reduced-complexity dispersal model based on output from WRF-Chem, which incorporates atmospheric chemistry in order to model total (i.e., primary and secondary)  $\text{PM}_{2.5}$  concentrations from C&T-driven facility-level  $\text{PM}_{2.5}$ ,  $\text{NO}_x$ , and  $\text{SO}_x$ , emissions [98].<sup>36</sup> InMAP, however, has one major limitation: it uses dispersal

---

<sup>36</sup>In addition to the inputs used in HYSPLIT, InMap requires the diameter, temperature, and emissions velocity for each smokestack. We obtain these inputs from CARB. In the case of facilities with more than one stack, we use the mean value across stacks. In the case of facilities with missing observations, we use the industry-level average.

Figure 2.5: Robustness checks for EJ gap effects



NOTES: Percentage change in the EJ gap trend following the introduction of the C&T program (i.e.,  $\frac{\beta_3^C}{\beta_1^C} * 100$ ) for PM<sub>2.5</sub>, PM<sub>10</sub>, NO<sub>x</sub>, and SO<sub>x</sub> across robustness checks. M1: benchmark model point estimate and 95% confidence interval accounting for uncertainty in equations (2.1) and (2.2). Point estimate shown for all other models. M2: using year-specific effects to estimate C&T-driven emissions. M3: C&T-driven emissions effects estimated using sector-by-year fixed effects. M4: C&T-driven emissions effects estimated without facilities that switched status in 2017. M5: restricting sample to facilities with average annual GHG emissions below the 70th percentile. M6: restricting sample to facilities with average annual GHG emissions below the 80th percentile. M7: allowing heterogeneous emissions effects by average annual emissions. M8: restricting unregulated facilities to those in counties under Clear Air Act nonattainment. M9: restricting unregulated facilities to those whose parent company only operates a single plant. M10: applying a slower pollution decay (i.e., 10% larger half-life parameter). M11: applying a faster pollution decay (i.e., 10% smaller half-life parameter). M12: applying a planetary boundary layer set at 0.5 km. M13: applying planetary boundary layer set at 2 km. Point estimates also reported in Tables B.7-B.8.

patterns in 2005, whereas our sample period is 2008-2017. Because InMAP does not model dispersal patterns during our sample period, we are unable to directly compare estimates using InMAP-generated concentrations with that using HYSPLIT-generated

concentrations.<sup>37</sup> Instead, we examine the role of secondary PM<sub>2.5</sub> by comparing how EJ gap trend estimates differ between InMAP-generated primary PM<sub>2.5</sub> concentration and InMAP-generated total PM<sub>2.5</sub> concentrations. If these two InMap estimates are similar, it is plausible that the true EJ gap effect for secondary PM<sub>2.5</sub> is similar to effects using HYSPLIT-generated primary PM<sub>2.5</sub> concentrations. Table B.10 replicates the structure of Table 2.2. Column 1 examines InMAP-generated primary PM<sub>2.5</sub> concentrations while column 2 examines InMAP-generated total PM<sub>2.5</sub> concentrations. Both show similar EJ gap effects.

**The importance of modeling pollution dispersal** Our empirical approach explicitly embeds an atmospheric dispersal model within a causal inference framework. Compared with conventional methods for assigning pollution concentration from emission sources, this approach lends two benefits. It accounts for actual pollution dispersal patterns as dictated by topography and time-varying meteorological conditions. It also determines resulting pollution concentrations across all locations in California, rather than a subset of locations assumed to be exposed to policy-driven emissions. To demonstrate the importance of accounting for pollution dispersal for our results, we compare estimates from using our approach with that of more conventional methods of assigning pollution concentrations from emission sources.

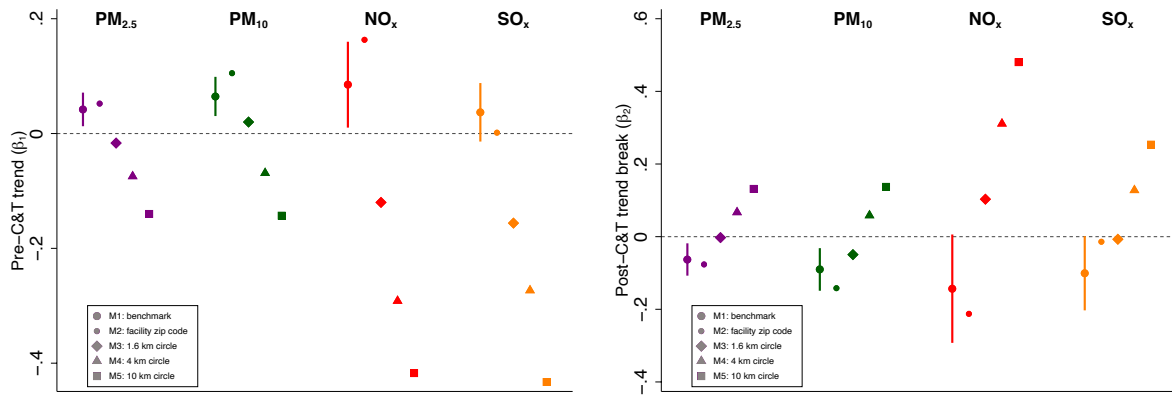
Figure 2.6 plots estimates of the pre-C&T trend, or  $\beta_p^1$  (left panel), and the post-C&T trend break, or  $\beta_p^2$  (right panel), across criteria pollutants under different assumptions about how facility-level emissions alter location-specific concentrations.<sup>38</sup> In M1, we show our benchmark estimate where pollution dispersal is modeled by HYSPLIT every 4

---

<sup>37</sup>Furthermore, there is a difference in units between HYSPLIT and InMap. For any given location, HYSPLIT produces the stock of pollution concentration during a given period, whereas InMAP produces that period's average flow of pollution concentration.

<sup>38</sup>Unlike Figure 2.5, Figure 2.6 does not plot  $\frac{\beta_p^2}{\beta_p^1} * 100$  because  $\beta_p^1$  and  $\beta_p^2$  do not have consistent sign across the different methods for assigning emissions to concentrations.

Figure 2.6: Importance of modeling pollution dispersal



NOTES: Left panel shows estimates of pre-C&T trend (i.e.,  $\beta_1^p$ ) and right panel shows estimates of post-C&T trend break (i.e.,  $\beta_2^p$ ) for PM<sub>2.5</sub>, PM<sub>10</sub>, NO<sub>x</sub>, and SO<sub>x</sub> across different methods for assigning pollution concentrations from emissions. M1: benchmark model with point estimate and 95% confidence interval accounting for uncertainty in equations (2.1) and (2.2). Point estimate shown for all other models. M2: pollution concentration assigned only to zip code of emitting facility. M3-5: pollution concentration assigned to zip codes with centroid within 1.6 km, 4 km and 10 km circle of emitting facility, respectively. Point estimates also reported in Table B.11.

hours throughout the 2008-2017 period. In M2 (and column 1 of Table B.11), we assume that the area affected by a facility's emissions is limited to the zip code of that facility, referred to in the literature as "unit-hazard coincidence" [64]. In M3-5 (and columns 2-4 of Table B.11), we employ a distance-based measure by assuming that the area affected by a facility's emissions is limited to zip codes with centroids that are within 1.6, 4, and 10 km circles around the facility. These radial distances appear in the literature but nonetheless are chosen largely arbitrarily. Point estimates of  $\beta_1^p$  and  $\beta_2^p$  vary greatly across these alternative methods for assigning pollution concentrations. Not only do some estimates fall well outside the 95% confidence intervals of our benchmark results, but they also have different signs.

## 2.6 Discussion

Many market settings are characterized by efficiency-equity tradeoffs. We find that California's carbon market led to an equity co-benefit by narrowing the criteria air pollution concentration gap between disadvantaged and other communities. This result brings causal evidence to a debate that continues to shape one of the world's most ambitious climate policies and climate policies elsewhere. Moreover, the integration of pollution dispersal modeling and causal inference employed in this paper may have broader applications across a variety of environmental valuation settings.

Equity concerns regarding California's cap-and-trade program remain. First, while we show that the program has led the pollution concentration gap between disadvantaged and other communities to fall, this gap has not been eliminated five years into the program. Second, pollution concentration constitutes only one component of the many distributional concerns regarding the program. Questions remain over how the program may have altered the distribution of health outcomes as well as the distribution of the program's cost burden. A comprehensive understanding of welfare inequality must also account for sorting as households move in response to changes in pollution concentrations [107, 64] and for entry decisions by polluters [108]. Third, a broader notion of equity must also consider the ability of disadvantaged communities to partake in decision-making around environmental policies. Such procedural justice issues remain in California though recent policies such as AB 617 are beginning to engage disadvantaged communities directly in the design of local pollution regulations [109].

More generally, despite these findings for California, market-based environmental policies should not be used explicitly to address environmental justice concerns. Market-based policies are intended for allocative efficiency and not distributional objectives, per se. The EJ gap consequences detected in California emerges from the state's spa-



tial distribution of polluting facilities and demographic characteristics. In other settings where facilities with steeper marginal abatement cost curves are upwind of disadvantaged communities, an environmental market could widen the environmental justice gap. Difficulties with observing facility-level marginal abatement cost curves make it hard to anticipate ex-ante how proposed market-based policies will alter existing EJ gaps. As a safeguard against potential widening EJ gaps, policies that specifically address environmental justice concerns should be considered in tandem with market-based policies. In short, environmental justice problems need environmental justice policies.

# Chapter 3

## Droughts and rural households' wellbeing: Evidence from Mexico

### 3.1 Introduction

Global temperature has increased during the last decades and it is likely that, compared to pre-industrial levels, global warming will reach 1.5°C at some point between 2030 and 2052 [110]. It is expected that the intensity of droughts will increase by the end of the 21st century as a result of rising temperatures [111, 112, 113]. The adverse impacts of these changes in climate will not be uniform across the planet. Developing countries are more vulnerable than their developed counterparts as they depend more on agriculture and, in many cases, are already overexposed to extreme weather events and to higher temperature levels [114, 115, 116]. Furthermore, changes in water availability will have major negative impacts on rural areas, disproportionately affecting those who are already vulnerable to weather fluctuations and with limited adaptation capacity, such as small and subsistence farmers, who tend to have low education levels and low access to technology, information, and financial resources [117, 118].

Understanding the impacts that extreme events have on rural households, as well as the factors that affect their capacity to adapt, is crucial for the design of policies and interventions that can improve such capacity [119]. Existing literature has found that rural households in the developing world are indeed particularly vulnerable to weather extremes [120, 121] and extreme rainfall [122]. Extreme rainfall and floods have been shown to increase children's labor force participation [123], have negative effects on children's height and cognitive tests [124], and reduce per-capita consumption while increasing poverty [122]. Droughts can decrease farm revenues and employment in agricultural activities [120, 125], increase risk of illness [126], and negatively affect schooling outcomes such as math and reading scores [127].

Mexico's location and geographic characteristics make it prone to hydrometeorological events [128] and its socioeconomic characteristics make it highly vulnerable to the negative effects of extreme weather events and climate change [129, 130]. Only 21% of Mexico's agricultural land has access to irrigation [131], which makes crop [132] and livestock production [133] highly dependent on rainfall. Most of the agricultural activities take place in rural areas [134], defined as communities with less than 2500 people, where 22% of the Mexican population lives [135]. According to the official poverty measurement, more than 55% of rural inhabitants in Mexico were poor in 2018 [136].

The current literature provides some evidence on the potential impacts that climate change and extreme weather events can have for human populations in Mexico. Climate change has the potential to reduce agricultural production [137, 138, 133] and land values [116]. It could also reduce local employment, increase migration from rural areas [139] and negatively affect human health [138]. Under some climate change scenarios, it is possible that almost 240,000 rural households could be pushed below the poverty line in rural Mexico [140]. Droughts and floods could increase poverty [141], while droughts could also increase the probability of rural-urban migration [142] and of migration to

the U.S. [143, 129]. These studies have shown that climate change and extreme weather events can have serious negative consequences for Mexico. However, to the best of our knowledge, the impact that droughts could have on rural households' wellbeing has not been studied in a comprehensive way using household level data. The present study aims to help in closing this gap.

Droughts are certainly not a new event in Mexico. Pre-Hispanic documents provide evidence on the occurrence of droughts going back as far as the eleventh century [144]. Furthermore, droughts were present during two of the most significant events in the history of the country. A drought preceded the Spanish conquest and persisted for several years affecting what is now central Mexico; arguably this could have interacted with epidemic disease and contributed to the collapse of the indigenous population [145]. Drought conditions over most of Mexico during 1909 and 1910 have long been mentioned as a contributing factor behind the Mexican Revolution [146, 147]. Some assert that the drought increased the sense of injustice among rural households that were therefore ready to take the arms when the Revolution started [148]. Finally, droughts during the 1960s were accompanied by increases in violent protests [149].

Notwithstanding this long history of droughts and the fact that Mexican agriculture has evolved in parallel to repeated periods of dryness, the country remains highly vulnerable to droughts, in particular households practicing subsistence agriculture [147]. More than evidence of a lack of willingness to adapt, this reflects the fact that in many cases farmers' possibilities to adapt have barriers and limits [150]. Households can use ex-ante and ex-post coping mechanisms but, in many cases, these will not be sufficient to fully protect them against weather shocks [151].

During 2011 Mexico was affected by one of the worst droughts in the past 70 years [133]. Agricultural production was severely reduced [147], cattle and goat stocks decreased [133], and dams located in the northern region of the country reached critical

levels [152]. The drought affected almost 70% of the territory [153] and the economic losses were equivalent to 10% of the GDP [154]; the federal government had to make use of Mexico's Natural Disasters Fund to implement national and local programs to mitigate the negative impacts of the drought [152, 153]. Unfortunately, this intense drought is not likely to be an isolated event; climate projections for Mexico suggest an increase in drought conditions during the 21st century [155, 156, 157, 158]. The possibility that the frequency and duration of droughts might increase in Mexico as a result of climate change [159, 160, 161] is particularly worrisome given Mexico's low levels of adaptive capacity [134] and high levels of poverty [162]. The burden of droughts tends to fall disproportionately on poor households who, in many cases, have to divert their scarce resources towards reducing the immediate negative impacts (e.g., reduction in consumption) at the cost of future productivity [163].

A better understanding of the way in which rural households might be affected by droughts is crucial for the adequate design of adaptation policies. Following this logic, the objective of this paper was to estimate the impact of droughts on rural households' wellbeing in Mexico, specifically on per-capita earnings, poverty, and children's school attendance. We were interested in estimating causal effects, to do so we used an empirical strategy that allowed us to isolate the drought effect from other confounding factors. Furthermore, we looked specifically at droughts, instead of looking at variations of temperature or rainfall as previous studies that use household level data for Mexico have done.

## 3.2 Data and methods

In order to analyze the effects of droughts on rural households in Mexico, we combined data from the Mexican Drought Monitor with data from Mexico's National Labor Survey.

We focused our analysis on the rural areas of the country as they are the more vulnerable to the negative productivity effects of droughts. Vulnerability of the urban areas in Mexico arises mostly from the energy sector [147] and from potential food price increases; looking at those effects was beyond the scope of our analysis.

### 3.2.1 Drought and precipitation datasets

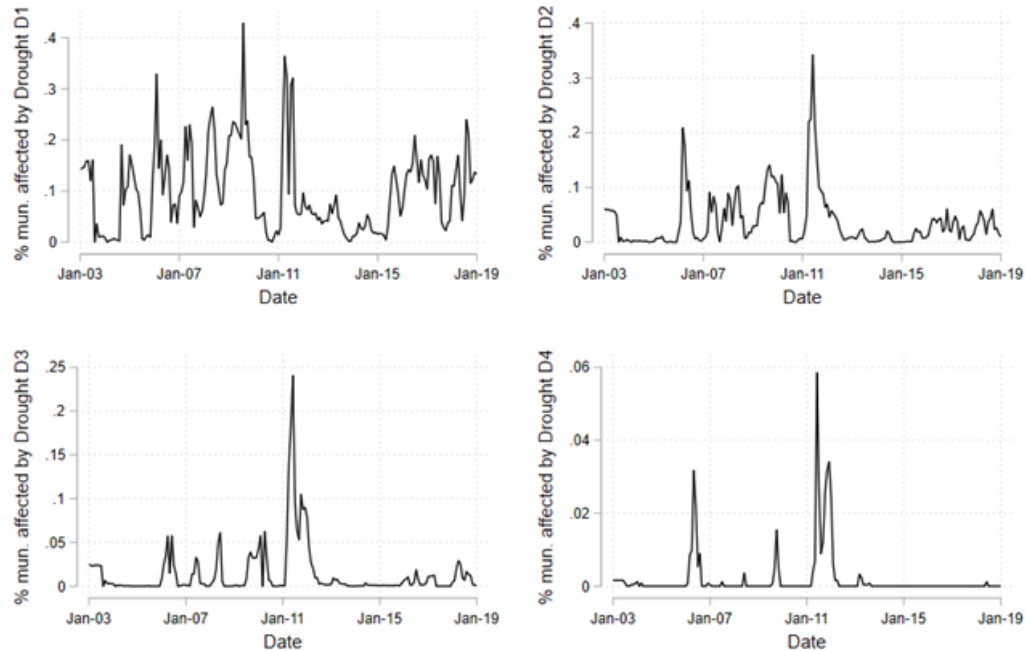
The data on droughts came from the Mexican Drought Monitor, which is part of the North American Drought Monitor (NADM). The NADM is a joint effort between Canada, Mexico and the United States, which began back in 2002 and has generated monthly data on droughts since then. Monitoring droughts is not an easy task because droughts are the result of a complex combination of various geophysical phenomena [164]. The monitor system uses data on precipitation (the Standardized Precipitation Index, and Percent of Average Precipitation); water availability, temperatures and evaporation (Palmer index, Palmer hydrological index, and Palmer Z index); a vegetation health index (VHI); and soil moisture. All these data layers are overlaid in a map, and a group of experts determines whether there is a drought and its intensity. Droughts are classified in four different levels according to their intensity: moderate drought (D1), severe drought (D2), extreme drought (D3), and exceptional drought (D4). The levels differ according to their likely impact on crops and grassland, the risk of wildfires that they entail, and the groundwater and surface water availability.

We used geographic information systems to associate each Mexican locality with the drought it experienced, at the monthly level, during the period January 2010 to December 2012. Localities represent the smallest administrative division in Mexico (municipalities being next). Figure 3.1 presents the percentage of Mexican municipalities affected by each type of drought during a given month in the period January 2003 to January 2019. The

panels for severe, extreme and exceptional droughts show that there were considerably more municipalities exposed to those drought-levels in 2011 than during the previous and subsequent years. This is consistent with other sources that consider 2011 to be one of the driest years in the history of Mexico [165, 133]. In order to better illustrate the intensity and the spatial distribution of the 2011 drought, Figure 3.2 compares the presence of droughts during the last month of each quarter of 2010 with the same month for 2011. The contrast between the drought conditions during 2010 and 2011 is clear. If, for example, we look at the month of June, we notice that a few parts of Mexico were experiencing drought conditions during 2010. Meanwhile, more than half of the country experienced moderate to exceptional droughts during 2011; almost 10% of the territory was under conditions of exceptional drought [152]. As Figure 3.2 shows, in addition to the temporal variation there is spatial variation in terms of the presence of droughts across different parts of Mexico. We used these two sources of variation as part of our strategy to identify the causal effects of droughts on the wellbeing of rural households.

We also used historical precipitation data at the municipality level from the European Centre for Medium-Range Weather Forecasts ERA Interim weather product. This weather product reports daily gridded rainfall data in a  $.125^\circ \times .125^\circ$  pixel, approximately 13 km x 13 km. We consider this resolution appropriate for Mexico, given that the average municipality area is 793 km<sup>2</sup>. We calculated the monthly total precipitation for the 1979-2010 period at the municipality level by overlaying the municipality polygons to the gridded data. We then created an indicator variable, “High precipitation”, which takes the value of one if the household is in a municipality with high historic levels of precipitation (900mm or more of annual precipitation according to the 1979-2010 normal) and zero otherwise.

Figure 3.1: Municipalities affected by drought



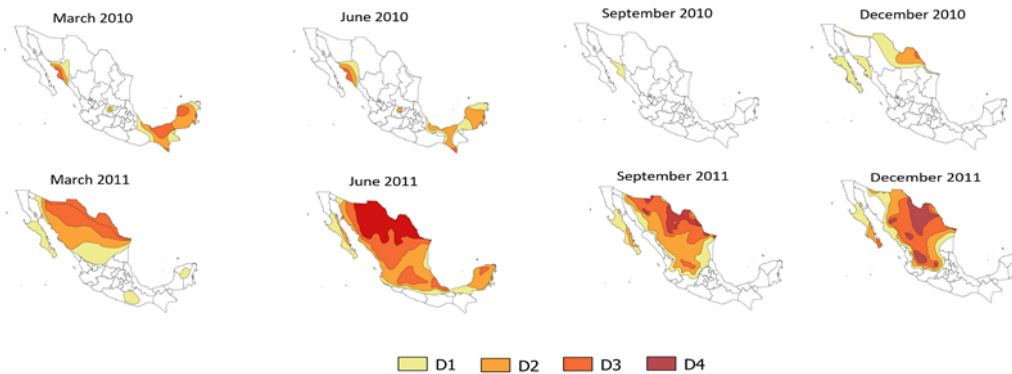
NOTES: Percent of municipalities affected by each drought classification (D1-D4). Authors' estimations using data from the Mexican Drought Monitor (MDM) between January, 2003 and January, 2019. The MDM uses the drought classification of the North American Drought Monitor, which defines four drought intensity levels: moderate drought (D1), severe drought (D2), extreme drought (D3), and exceptional drought (D4). The four figures present the percentage of municipalities affected by each of these four drought classifications during the period in the vertical axis, and the month-year in the horizontal axis. The drought we focus on in this paper happened during 2011.

### 3.2.2 Household level data

Household level data came from the National Labor Survey (Encuesta Nacional de Ocupación y Empleo, ENOE for its Spanish acronym) collected by Mexico's National Statistics Institute (INEGI for its Spanish acronym) from the first quarter of 2010 to the last quarter of 2011. ENOE's sample is representative of the urban and rural areas of the country and contains data about the household members' labor status in a quarterly basis. Given that rural households depend heavily on agriculture and are the more vulnerable to droughts, we restricted the sample to rural areas. In addition to labor information for all



Figure 3.2: Drought intensity per quarter



NOTES: Drought intensity during the last month of each quarter (2010-2011) over the Mexican territory. Authors' estimations using data from the Mexican Drought Monitor (MDM) between March, 2010 and December, 2011. The MDM uses the drought classification of the North American Drought Monitor, which defines four drought intensity levels: moderate drought (D1), severe drought (D2), extreme drought (D3), and exceptional drought (D4). As an example of the severity and extent of the drought, the heat maps present the drought level during the last month of each quarter of 2010 and 2011 at the locality level in Mexico (a locality is the smallest geographical disaggregation in Mexico, followed by a municipality). The drought we focus on in this paper happened during 2011.

household members 12 years of age and older, ENOE collects information on per-capita earnings, time allocated to unpaid domestic work, and children's school attendance, among other variables.

ENOE captures the exact month of the interview, which allowed us to match the household data to the monthly drought information available at the locality level. Households were surveyed for five consecutive quarters and 20% of the sample was replaced each quarter; attrition rate was 7.8%. We took advantage of the one-year span between the household's first and last interview (i.e. if a household first interview was in January 2010, the fifth interview took place in January 2011) to analyze households' responses to weather shocks in the short run. We created a short panel using households' information from their first and fifth interviews. This allowed us to control for seasonality and, equally important, for time-invariant unobserved heterogeneity at the household level.

The sample that resulted from combining the drought and ENOE datasets consists

of more than 13,000 rural households; 10,352 of such households did not experience a drought during their first ENOE interview, those are the households that we used in our analysis. Almost half of the households (5,186) that did not experience a drought in 2010 experienced one in 2011. The most common type of drought that rural households experienced during 2011 was a severe drought (2,106), and the least common was an exceptional drought (113). Panel A in Table 3.1 shows descriptive statistics for our dependent variables as well as for the occurrence of a drought. Per-capita earnings were slightly below 1,000 pesos per month during both 2010 and 2011; as a result, more than 50% of the households in our sample are poor. We defined poverty following the labor poverty trend index generated by Mexico's National Council of Poverty Evaluation (CONEVAL). The index calculates the share of people that are not able to acquire the National Basic Food Basket (also defined by CONEVAL). Although this index does not consider all income sources, it provides a proxy measure for poverty in terms of labor income. Panel B in Table 3.1 focused on the sample of adults who were 18 years old or more in the first interview. There is a notorious gender gap in employment: in 2010, 82% of the men and 32% of the women were employed, while 60% of the women and less than 1% of the men were doing household work. Finally, Panel C in Table 3.1 turned to children (aged between 12 and 17 in the first interview). Except for an increase in school attendance and a decrease in children's employment, all the variables are very stable over time.

### 3.2.3 Data analyses

In order to estimate the causal impacts of droughts on rural household's wellbeing, we restricted our estimating sample to those households that were not affected by a drought during their first ENOE interview (10,352 households), in this way we part with

Table 3.1: Descriptive Statistics

	All		Men		Women	
	2010	2011	2010	2011	2010	2011
	Panel A: Households					
Per-capita earnings	938.21 [1667.93]	962.05 [1667.82]				
Poor (=1)	0.57 [.50]	0.55 [.50]				
Drought (=1)	-	0.499 [.500]				
Observations	10352	10352				
	Panel B: Adults					
Employed (=1)	0.56 [.50]	0.57 [.50]	0.82 [.39]	0.83 [.37]	0.32 [.47]	0.32 [.47]
Housework (=1)	0.31 [.46]	0.31 [.46]	0.007 [.085]	0.009 [.092]	0.59 [.49]	0.59 [.49]
Drought (=1)	-	0.499 [.500]	-	0.502 [.500]	-	0.496 [.500]
Observations	23464	23464	11205	11205	12259	12259
	Panel C: Children					
School attendance (=1)	0.75 [.43]	0.81 [.39]	0.73 [.44]	0.8 [.40]	0.77 [.42]	0.82 [.38]
Employment (=1)	0.26 [.44]	0.21 [.41]	0.37 [.48]	0.32 [.47]	0.14 [.34]	0.1 [.30]
Housework (=1)	0.08 [.28]	0.07 [.25]	0.02 [.141]	0.015 [.120]	0.15 [.35]	0.13 [.33]
Drought (=1)	-	0.484 [.500]	-	0.494 [.500]	-	0.473 [.499]
Observations	4498	4498	2263	2263	2235	2235

NOTES: Descriptive statistics of the variables in the statistical analyses. Authors' estimations using the Mexican labor survey (ENOE) data from 2010 (pre-drought) and 2011 (post-drought) and from the Mexican Drought Monitor. The sample is restricted to rural households, which are those with less than 2,500 inhabitants. The table shows the descriptive statistics for both men and women (All), and for men and women separately. The table shows the mean and below the mean is the standard deviation in brackets. Panel A presents household level outcome and treatment (an indicator variable of the presence of any drought) variables. Panel B presents descriptive statistics for adults, who are those 18 years of age or older in the first interview. Panel C shows the characteristics of the subsample of children, who are between 12 and 17 years old (inclusive) in the first interview. Per-capita earnings are measured in Mexican pesos per month. Variables with (=1) are indicator variables equal to one if the condition described by the variable name is met and zero otherwise.

a subset of households that started off from the same initial weather conditions. We then followed these households to their fifth ENOE interview to estimate the effects that droughts had on those households that had been affected by then (5,166 households in the treatment group) as compared to households that were neither affected during the first nor the fifth interview (5,186 households in the control group). We only exploited data from the first and fifth interviews since these were collected in the same quarter for the corresponding year. In this way, we ensure that our results were not due to seasonality in agricultural production. Our estimations were based on the following equation, which uses a difference in differences approach with fixed effects at the household (or household member, depending on the dependent variable) level:

$$y_{it} = \alpha + \beta D_i \times Post_t + \delta Post_t + \mu_i + \varepsilon_{it}$$

where  $i$  denotes the household (household member) and  $t$  denotes time (of the first or last interview);  $y_{it}$  is an outcome variable (e.g., poverty measured at the household level or employment measured at the individual level);  $D_i$  is a dummy variable equal to 1 if the locality where the household resides experienced a drought (i.e., any of the four drought levels mentioned before, we do not have enough observations in each one of the drought levels to adequately identify heterogeneous effects by drought level);  $Post_t$  is a time index equal to zero for the first interview and equal to one for the fifth;  $\beta$  is the difference-in-differences estimator (our parameter of interest);  $\alpha$  is the constant of the regression, which absorbs the overall mean of those households (or household member) who were not treated (experienced no drought by the 5th interview) during the pre-drought period;  $\delta$  estimates the time trend;  $\mu_i$  are household (or household member, according to the dependent variable) fixed effects; and  $\varepsilon_{it}$  is an error term.

A difference-in-differences estimator would identify the causal effect of the drought

if the following two assumptions are met. First, there is no other event contemporaneous to the drought confounding the effect of the drought. And second, the pre-drought trend followed by our variables of interest for households (or household members) that experienced a drought in the fifth interview was parallel to the pre-drought trend for households that did not experience the drought in either interview (Angrist and Pischke, 2008). Our estimator, thus, identifies the discontinuous change post-drought and the change in trend post-drought between the treatment and the control group. Any differences in pre-drought characteristics does not threaten our identification as long as both treatment and control groups followed the same trend pre-drought. Since we limited our estimation sample to households that were not experiencing a drought during the first interview, all the households in our sample start from the same initial conditions; this provided us with greater confidence that the parallel trend assumption is in fact being satisfied.

Moreover, given that our estimation controlled for all time invariant observed and unobserved heterogeneity at the household or individual level through  $\mu_i$  [166, 167], our estimating equation did not include any time invariant variables. As such, in order to estimate  $\beta$  we did not need to include the time invariant indicator variable for the treated households,  $D_i$ , but only the interaction term ( $D_i \times Post_t$ ) and the indicator variable for the fifth interview ( $Post_t$ ). Likewise, since all the household and individual information available in the ENOE dataset (age, education, marital status, etc.) was time invariant, we could not explicitly estimate the effects of these variables. Nevertheless, we controlled for the heterogeneity that they capture by including the fixed effects in our regressions. Thus, our estimation used only within-household or within-individual variation to estimate the causal effect of droughts on the outcomes of interest. We could not control for any time-variant characteristics at the regional level, since we could not find a causal theory that could explain simultaneous monthly changes among the control

(treatment) households that was not affecting the treatment (control) households at the same time. There were no federal changes in policy, no simultaneous local changes in policy, and violent crime affected a widespread area in Mexico not limited to those that experienced the drought.

Our first approach to estimating the impact of droughts on rural wellbeing is to look at households' per-capita earnings and poverty status. For poverty we use a dichotomous variable that takes the value of one if the household is below the income poverty line established by CONEVAL to calculate the "trend of labor poverty" [168]. Next, we look at the effects that droughts have on the probability that adults are employed, as well as on the probability that they are fully dedicated to domestic work. By looking at the probability of being employed, we explore a potential transmission mechanism between droughts and reduced earnings. We also estimate the effect of droughts on the probability that children (between 12 and 18 years old) attend school since a reduction in schooling can have negative wellbeing implications in the long run. In addition to estimating the effects for all children and adults, we split our sample by gender. This allows us to estimate heterogeneous effects by gender, as well as to indirectly test for the presence of added worker effects (i.e., an increase in labor supply of women when their husbands become unemployed).

There is evidence in the literature showing that rural households adapt their production practices to local conditions so that they can cope with climate change (e.g., by planting drought tolerant local varieties or by using water harvesting) [114]. Therefore, in order to test if the effects of a drought are smaller for households (individuals) that are more accustomed to relative water scarcity, for our final estimations we split our sample using localities in municipalities with historically high precipitation levels.

### 3.3 Results and discussion

The results of our econometric estimations are shown in Table 2; each cell in the table represents an estimation of  $\beta$  from a different regression. Panel A shows results for the effects of droughts on per-capita earnings as well as on the probability that the household is considered poor. Following the literature on the negative impacts that droughts have in the Mexican agricultural sector (see for example, [137, 133, 147]), our main hypothesis was that rural households that experience a drought would be negatively affected in terms of their earnings and, in many cases, this would be reflected as an increase in the likelihood of being below the poverty line. According to our findings, households that experienced a drought had indeed lower per-capita earnings; the reduction in earnings is of almost 6% when compared to the average in 2010. This reduction in earnings translates into an increase of 5 percentage points in the probability that a household affected by a drought would be considered as poor compared to one not affected by it. These results are in line with those reported by [141] who found that, in Mexico, droughts increased poverty between 2.7 and 4.3 percent. Compared to [141] that used municipal-level data, by using panel data at the household-level we were able to provide direct evidence of the causal effects of droughts on earnings and poverty.

Ideally, we would have liked to explore all the mechanisms through which earnings decrease and the probability of being poor increases. With the data that we had we were able to look at one potential direct mechanism: employment. It has been reported that droughts can lead to reductions in on-farm employment [169] as well as reductions in employment at the national level [170], but they can also spur off-farm employment [171] and even migration [143]. Furthermore, in the absence of formal insurance and safety net mechanisms, households might decide to reallocate the time of family members across different activities as a response to external shocks [172]. Therefore, in addition to

Table 3.2: Main Results

	All	Men	Women
	Panel A: Households		
Per-capita earnings	-54.259**		
	[23.497]		
Poor (=1)	0.045***		
	[0.015]		
Observations	20704		
	Panel B: Adults		
Employed (=1)	-0.022**	-0.012	-0.031**
	[0.010]	[0.013]	[0.013]
Housework (=1)	0.014*	-0.001	0.028*
	[0.008]	[0.002]	[0.014]
Observations	46928	22410	24518
	Panel C: Children		
School attendance (=1)	-0.016	-0.028*	-0.004
	[0.010]	[0.015]	[0.016]
Observations	8996	4526	4470

NOTES: Econometric estimations of drought impacts in the locality by gender. Authors' estimations using the Mexican labor survey (ENOE) data from 2010 (pre-drought) and 2011 (post-drought) and the Mexican Drought Monitor. The sample is restricted to rural households, which are those with less than 2,500 inhabitants. The table shows the estimates for both men and women (All), and for men and women separately. Panel A presents the results for household level outcomes, Panel B for adults (18 years or more pre-drought) and Panel C for children (between 12- and 17-years old pre-drought). Per-capita earnings are measured in 2010 Mexican pesos per month. Variables with (=1) are indicator variables equal to one if the condition described by the variable name is met and zero otherwise. Each coefficient represents a difference-in-differences estimate from a separate regression (that is, a  $\beta$  from our estimating equation). Household level estimates control for household fixed effects, the estimates for adults and children control for individual fixed effects. All estimates control for an indicator variable of the 5th ENOE interview, thus controlling for time trends. Clustered robust standard errors at the state level are presented in brackets. \*\*\*  $p < 0.01$  \*\*  $p < 0.05$ , \*  $p < 0.1$

looking at employment, we also considered the effect that droughts have on time allocated to work exclusively in household chores. This allowed us to look, at least partially, at reallocation of time inside the household as a response to a drought. Panel B of Table 3.2 (first column) shows that the presence of a drought reduced in more than two percentage points the probability that an adult was employed, while it increased the probability that it would be fully dedicated to domestic work in almost one and a half percentage points. Our results on employment suggest that households affected by a drought were



not able to fully reassign labor to income generating activities and therefore participation in housework increased.

The previous analysis conceals differences in labor allocation by gender. It has been well documented that labor-supply responses after a shock can vary by gender [173, 174], therefore, this is an important issue to analyze. On one hand, it is possible that female labor supply would increase as a response to a decrease in their partners' level of employment, a phenomenon known as the added worker effect [175]. On the other hand, when there are gender differences in workforce participation, as is the case in rural Mexico [176], an increase in female participation might not be feasible. The second and third columns of Table 3.2, Panel B, show the effects of drought on employment and housework by gender. Although we could not directly test if women entered the labor market as a response to their spouse exiting the labor force, our analysis by gender shows that women are the driving force behind the decrease in probability of employment and the increase in domestic work. Therefore, instead of finding evidence supporting the added worker effect, our results suggest that droughts increased the gender gap in terms of participation in the labor market: male participation remained the same while female participation decreased. There is evidence suggesting that differences in employment participation by gender in rural Mexico can be attributed to gender roles within the family [176]. This and the possibility that physical strength is considered as an important endowment for many agricultural activities [176] can explain why females are the first ones to be left out of the labor market when a negative shock affects agricultural productivity.

In addition to its effects on per-capita earnings and poverty, droughts could have indirect negative effects on other aspects of households' wellbeing, like children's education. There is evidence showing that children leave school to enter the labor market when their parents become unemployed [175]. Negative shocks to commodity prices [177] as well as crop losses have also been shown to reduce school enrollment for rural children.

Therefore, children could be leaving school to work and partially compensate for the lost income resulting from the drought; they could also be leaving school to replace one member that was originally dedicated to household caring activities, and thus increase their domestic work. Panel C of Table 3.2 shows the effects of droughts on school attendance for children between 12 and 17 years old. The results show that droughts reduced the probability that boys will go to school in almost three percentage points; the effect for girls is very small and not statistically different from zero. We also tested for effects on employment or household work for children; the estimated  $\beta$  are not shown in the table since we did not find any statistically significant results for those variables. Therefore, although there is a decrease in boys' school attendance, we did not find direct evidence to support the hypotheses that they get out of school to get a formal employment or to do housework. It is possible that school attendance went down after the drought as a way to reduce the costs associated with attendance (e.g. transportation and school supplies). The cash transfers that parents received from the government program Oportunidades for the attendance of children to school was higher for girls than for boys attending middle school or high school [178]; this difference in the opportunity cost of attendance could explain why girls' school attendance did not decrease as a consequence of the drought. This result contrasts with the findings in [175], where teenage girls were more likely to drop out of school than teenage boys in response to the Mexican peso crisis; however, Oportunidades did not exist at the time.

Many rural communities in semi-arid regions of Mexico have developed ways to cope with droughts [179]. Arguably, households located in places where low levels of precipitation are the norm have already undertaken some ex-ante measures to deal with droughts, they might also be aware of ex-post measures to deal with lack of rainfall when it happens. If that is in fact the case, we should see that the effects of a drought differ by the level of historical precipitation that a given place has experienced; households in places with

precipitation levels that are usually high are less used to the lack of rainfall and would therefore be more exposed to its negative effects. To test this hypothesis, in the last part of our analysis we used an indicator variable to classify households according to the historical precipitation level of the municipality in which they are located. We estimated again the effects of droughts on per-capita earnings, poverty, employment and household work of adults, as well as on school attendance, but this time instead of splitting the sample according to gender we did it with respect to being in a high or low precipitation municipality.

The results, shown in Table 3.3 Panel A, show that per-capita earnings decreased after a drought for households located in places with high historical levels of precipitation but not for the rest of the households. Similarly, the likelihood that a household was poor after the drought increased 6 percentage points for households in high precipitation municipalities but not for their counterpart. The effects on employment and household work are shown in Panel B, the probability of being employed decreased for individuals living in households with high historical precipitation. Meanwhile, the probability that an adult will only do housework increased by one percentage point only for households in low precipitation municipalities. Results for school attendance, Panel C, show that children in municipalities with high precipitation are almost 3 percentage points less likely to go to school after a drought hits their household; there is no statistically significant effect for children in low precipitation municipalities. The results on employment and school attendance provide indirect evidence consistent with the hypothesis that households familiar with relative water scarcity might be less affected by a drought than those located in places where water availability is, in general, not an issue.

Table 3.3: Results by historical precipitation levels

	Historical precipitation	
	High	Low
	Panel A: Households	
Per-capita earnings	-80.158*	-1.993
	[38.875]	[38.951]
Poor=1	0.063***	0.023
	[0.014]	[0.028]
Observations	8432	12272
	Panel B: Adults	
Employed=1	-0.033*	-0.012
	[0.019]	[0.007]
Housework=1	0.016	0.011*
	[0.015]	[0.006]
Observations	18902	28026
	Panel C: Children	
School attendance=1	-0.029*	-0.012
	[0.014]	[0.017]
Observations	3732	5264

NOTES: Econometric estimations of drought impacts by historical precipitation in the municipality of residence. Authors' estimations using the Mexican labor survey (ENOE) data from 2010 (pre-drought) and 2011 (post-drought) and the Mexican Drought Monitor. We defined historical precipitation as high if the municipality experienced a mean precipitation level above 900mm between 1979 and 2010, and as low otherwise. The sample is restricted to rural households, which are those with less than 2,500 inhabitants. Panel A presents the results for household level outcomes, Panel B for adults (18 years or more pre-drought) and Panel C for children (between 12- and 17-years old pre-drought). Per-capita earnings are measured in Mexican pesos per month. Variables with (=1) are indicator variables equal to one if the condition described by the variable name is met and zero otherwise. Each coefficient represents a difference-in-differences estimate from a separate regression (that is, a  $\beta$  from our estimating equation). Household level estimates control for household fixed effects, the estimates for adults and children control for individual fixed effects. All estimates control for an indicator variable of the 5th ENOE interview, thus controlling for time trends. Clustered robust standard errors at the state level are presented in brackets. \*\*\*  $p < 0.01$  \*\*  $p < 0.05$ , \*  $p < 0.1$

### 3.4 Conclusions

Our results showed that there is a causal link between droughts and a decrease in rural households' wellbeing. Furthermore, we provide indirect evidence supporting the hypothesis that households in relatively dry areas have already taken some adaptation measures, and therefore can cope with a drought more easily than households in places

with higher precipitation levels. If that is in fact the case, public policies that inform and promote ex-ante adaptation measures in localities less experienced with droughts, but at risk of increased future exposure due to climate change, have the potential to ameliorate some of the negative welfare effects of droughts.

By no means we try to imply that our results are conclusive, they have many limitations given the data that we had at hand. We do not have panel data encompassing several years, which would have allowed us to look at drought effects over time and to have a cleaner empirical identification strategy. We cannot identify the role of specific coping mechanisms such as savings, access to credit markets, or cash transfers, which could potentially mitigate the impacts of a drought. Furthermore, we cannot verify that adaptation measures are in fact what explain the heterogeneous effects that we found for households located in relatively dry areas. Better data is needed in order to delve deeper into these crucial issues. Given the vulnerability of Mexican rural households to climate change, the federal administration should implement a data collection strategy that can properly capture rural households' adaptive capacity. Such data would provide valuable information for the design and successful implementation of public policies aimed towards promoting adaptation and reducing the vulnerability of rural households to climate change.

# Appendix A

## Appendix to Chapter 1

### A.1 Mathematical Appendix

Substituting  $x_L$ ,  $l_L^s$ , and  $M_L(\gamma_l)$  in the utility function of low-wealth households:

$$\begin{aligned} u(x_L, l_L^s, H_L) = & \log \left[ \frac{1}{c_x} \left[ \frac{w(2 - \beta) + \beta I_L + c_M(\mathcal{H} - D_L(\gamma_l))}{c_M + 2} \right] \right] \\ & + \log \left[ 1 - \left[ \frac{w(c_M + \beta) - \beta I_L + c_M(D_L(\gamma_l) - \mathcal{H})}{w(c_M + 2)} \right] \right] \\ & + \log \left[ \mathcal{H}_L + \beta \left[ \frac{\beta(I_L + w) + 2(w + D_L(\gamma_l) - \mathcal{H})}{\beta(c_M + 2)} \right] - D(\gamma_l) \right] \end{aligned}$$

Taking the derivative of  $u(\cdot)$  with respect to  $\gamma_l$ :

$$\frac{\partial u}{\partial \gamma_l} = - \frac{c_M D'(\gamma_l)}{\underbrace{w(2-\beta) + \beta I_L + c_M(\mathcal{H} - D(\gamma_l))}_{(*)}} - \frac{c_M D'(\gamma_l)}{\underbrace{w(c_M + 2) - w(c_M + \beta) + \beta I_L + c_M(\mathcal{H} - D(\gamma_l))}_{(**)}}$$

$$- \frac{c_M D'(\gamma_l)}{\underbrace{\mathcal{H}(c_M + 2) + \beta(I_L - w) + 2(w + D(\gamma_l) - \mathcal{H}) - D(\gamma_l)(c_M + 2)}_{(**)}}$$

Incomplete regulation causing an increase in  $\gamma_l$  will be regressive if  $\frac{\partial u}{\partial \gamma_l} < 0$

First, let's obtain conditions under which (\*) is negative:

(\*) can be rewritten as:

$$(*) = \frac{-[4c_M w - 2\beta c_M w + 2c_M \beta I_L + 2c_M^2(\mathcal{H} - D(\gamma_l))]}{w^2(4 - 3\beta^2) + 4\beta w I_L + \beta^2 I_L^2 + c_M(\mathcal{H} - D(\gamma_l))^2 + (\mathcal{H} - D(\gamma_l))(4w c_M - 2c_M w \beta + 2\beta I_L)}$$

Recall that  $0 < \beta \leq 1$ , which means that the denominator of (\*) will only be negative (implying the possibility of  $\frac{\partial u}{\partial \gamma_l} > 0$ ) if the denominator of (\*) is negative.

Working of the denominator of (\*\*):

$$(**) = w^2(4 - 3\beta^2) + 4\beta w I_L + \beta^2 I_L^2 + c_M(\mathcal{H} - D(\gamma_l))^2 + (-D(\gamma_l))(4w c_M + 2c_M w \beta - 2c_M w \beta + 2\beta I_L)$$

(\*\*) would only be negative if:

$$4w c_M + 2c_M w \beta - 2c_M w \beta + 2\beta I_L < 0 \implies \frac{c_M(2 - \beta)}{\beta} > \frac{I_L}{w}$$

Therefore,  $\frac{\partial u}{\partial \gamma_l} < 0$  unless  $\frac{c_M(2 - \beta)}{\beta} < \frac{I_L}{w}$ .

Substituting  $x_H$ ,  $l_H$ , and  $M_H(\gamma_k)$  in the utility function of high-wealth households:

$$u(x_H, l_H, H_H) = \log \left[ \frac{1}{c_x} (I_R + \phi Y) \right] + \log \left[ \mathcal{H} + \beta \left[ \frac{1}{2c_M} (I_R + \phi Y) - \frac{1}{\beta} (\mathcal{H} - D(\gamma_k)) \right] \right]$$

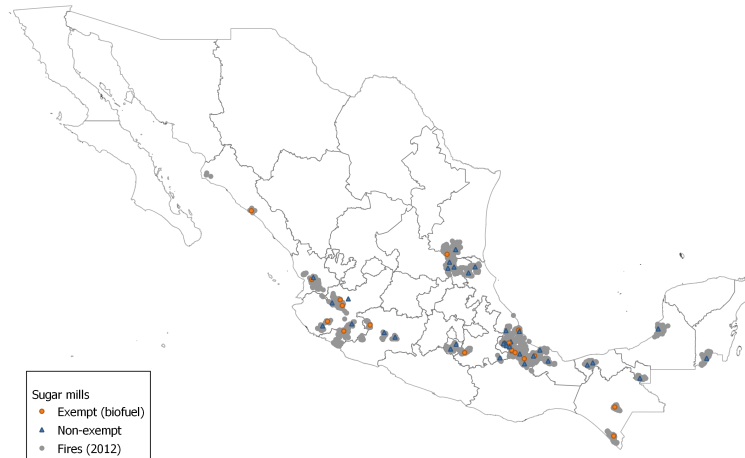
Obtaining the derivative with respect to  $\gamma_k$ :

$$\frac{\partial u}{\partial \gamma_k} = \frac{2c_M \frac{\partial D(\gamma_k)}{\partial \gamma_k}}{\beta(I_R + \phi Y) + 2D(\gamma_k)c_M}$$

The numerator of the previous expression is positive while the denominator will be positive unless  $\beta(I_R + \phi Y) < 2D(\gamma_k)$ .

## A.2 Appendix Figures

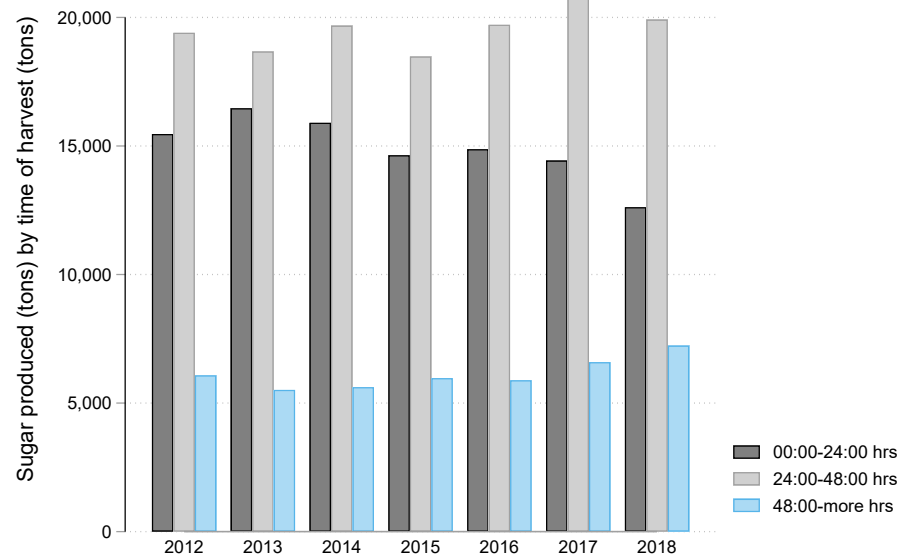
Figure A.1: Mills location



**Notes:** location of mills classified by exempt (biofuel use) and non-exempt or regulated by NOM-085-SEMARNAT-2011. Shadow areas are the centroid of the sugarcane fires in 2012.



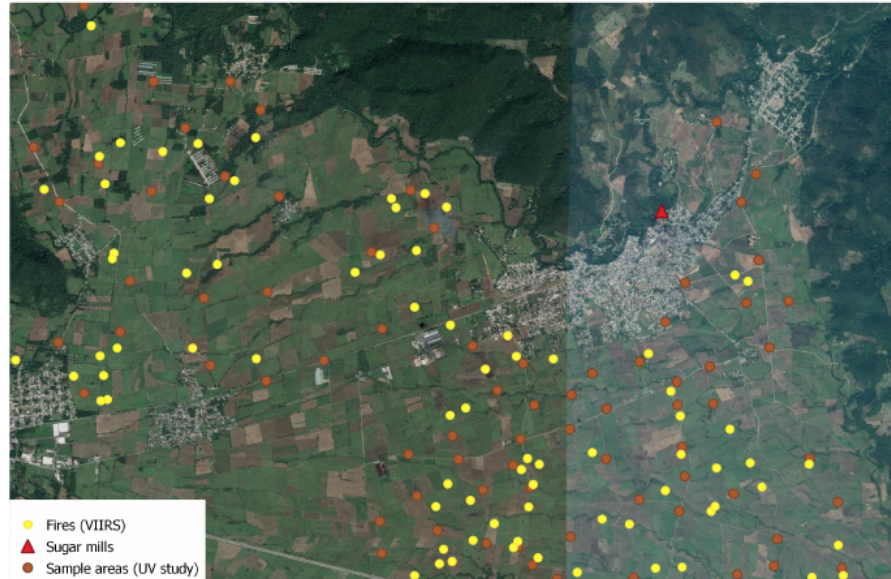
Figure A.2: Time to process harvested sugarcane



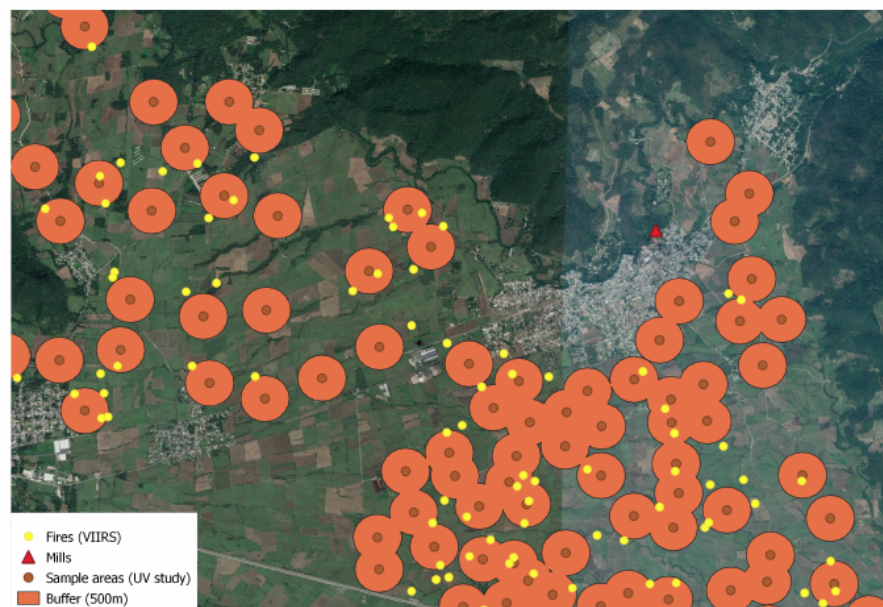
**Notes:** The figure shows the sugarcane processed (in tons) and its approximate time for processing in the mill after it was harvested by year.

### A.3 Appendix Tables

Figure A.3: Distribution areas  
Panel a)

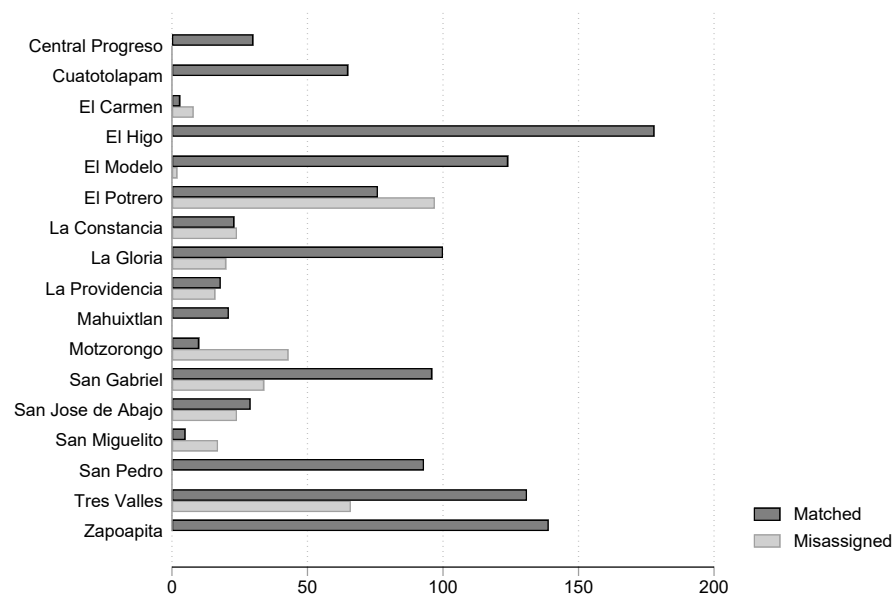


Panel b)



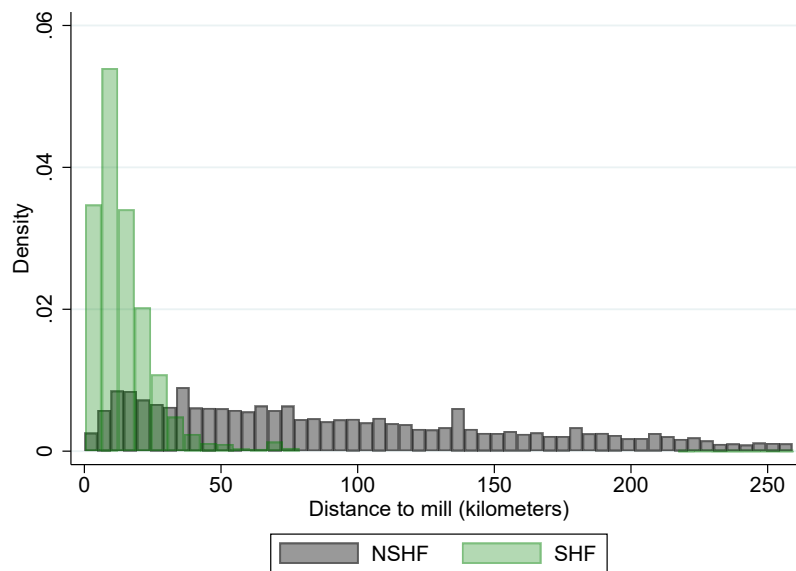
**Notes:** Panel a) shows the geographic extent of the sample areas (obtained by the Universidad Veracruzana study), sugarcane harvest fires (VIIRS), and a sugar mill. Panel b) shows the geographic extent of a 500m buffer surrounding the sample areas obtained by the Universidad Veracruzana study, along with the sugarcane harvest fires, and the sugar mill. The geographic area is in the city of Cordoba, Veracruz. The sugar mill is “El Potrero”.

Figure A.4: Distribution areas



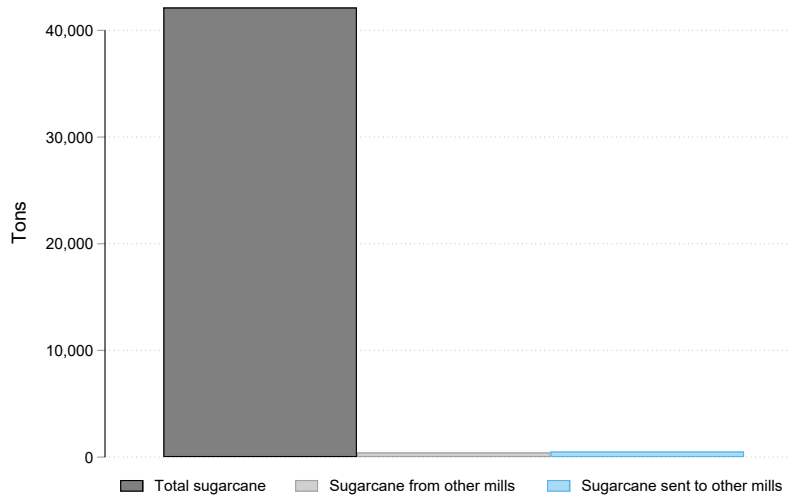
**Notes:** The figure shows the total number of fires for the sample area in the state of Veracruz by mill. Each bar shows the total of matched or misassigned fires comparing the distance algorithm classification and the actual sample areas for 2009.

Figure A.5: Calculated distance between sugarcane fires and other fires and mills



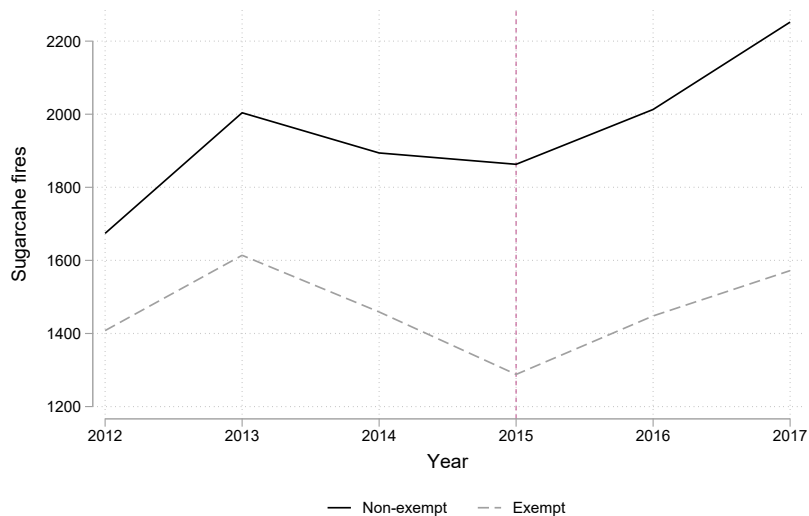
**Notes:** The figure shows the distribution of the distances between the fires and assigned mills. NSHF stands for “Non-sugarcane harvest fire” which are agricultural fires in cropland other than sugarcane. NSHF were classified using data from INEGI: *Cartas de Uso de Suelo y Vegetación, Serie V*. SHF stands for sugarcane harvest fire. SHF were classified by CONADESUCA and provided to the researcher.

Figure A.6: Sugarcane processed by ownership



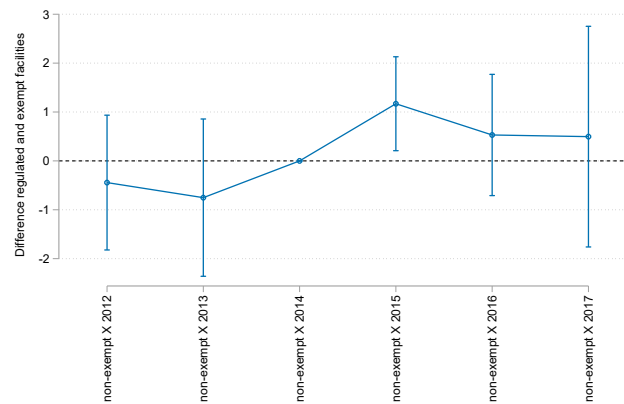
**Notes:** Total sugarcane processed (in tons) by type of land ownership. Total sugarcane is the sum of sugarcane from own/associated fields, sugarcane from other mills and sugarcane sent to other mills. Sugarcane from other mills is the total sugarcane sent from the fields owned/associated to other mills. Sugarcane sent to other mills is the average sugarcane that is sent to other mills due to capacity constraint associated with the own mills operations.

Figure A.7: Fires associated with exempt and non-exempt facilities

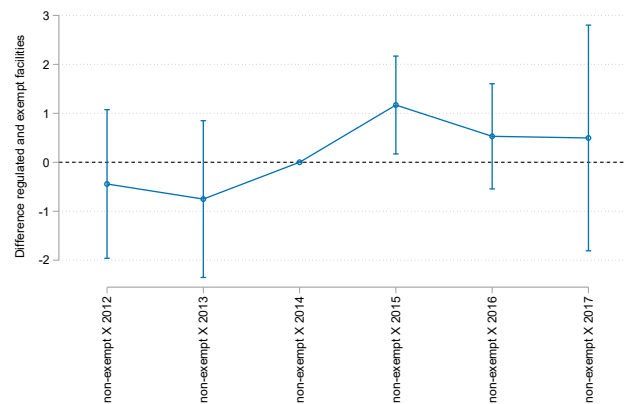


**Notes:** The figure show the mean sugarcane-harvest fires by type of facility. Non-exempt facilities are defined as facilities using oil as main fuel. Exempt facilities are defined as facilities using biofuels as main fuel. Vertical axis is the mean fires in sugarcane plots.

Figure A.8: Monthly fires-parallel trends controlling for sugar and oil prices  
 Panel a) Controls for international price of sugar

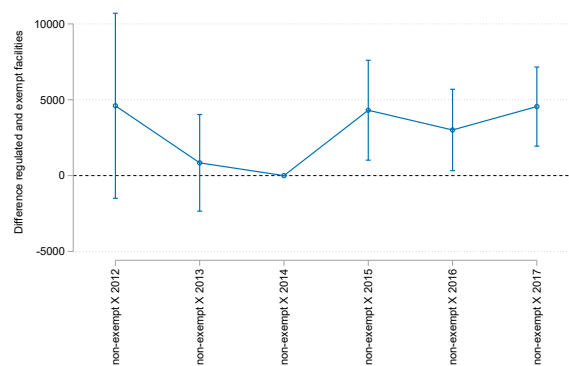


Panel b) Controls for the price of Mexican crude oil

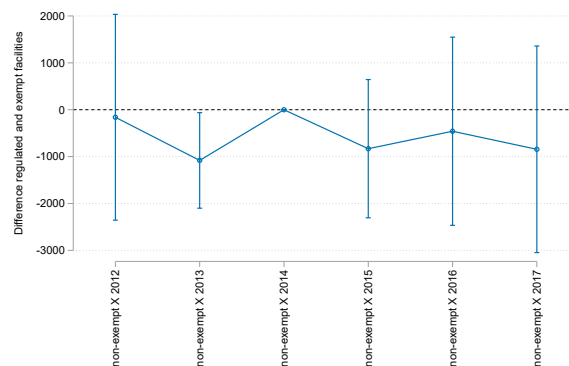


**Notes:** This figure shows the differences in differences-year specific coefficients for the total number of daily fires following equation 1.6 including controls of international sugar prices (Panel a)) and Mexican crude oil prices (Panel b)). The regulation started in 2015. 95% confidence intervals calculated using two-way fixed effects at the municipality and year level.

Figure A.9: Inputs-parallel trends  
 Panel a) Manual cut (tons)

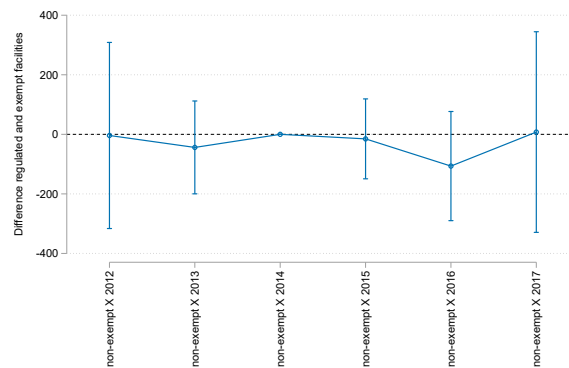


Panel b) Mechanical cut (tons)

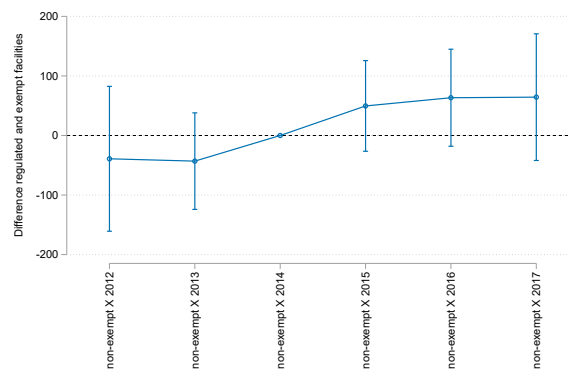


**Notes:** Panel a) shows the differences in differences-year specific coefficients for the total sugarcane in tons using manual cut following equation 1.7. Panel b) shows the differences in differences-year specific coefficients for the total sugarcane in tons using mechanical cut following equation 1.7. Confidence intervals calculated using two-way fixed effects at the municipality and year level.

Figure A.10: Inputs-parallel trends  
 Panel c) Hectares harvested



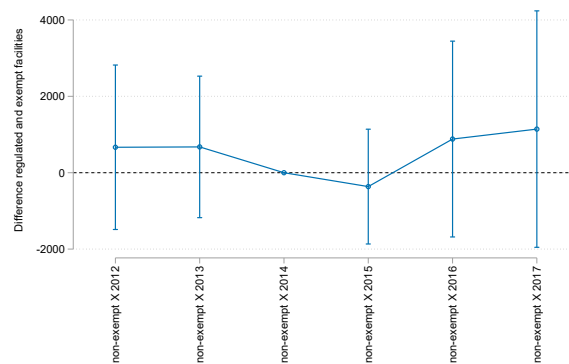
Panel d) Total workers



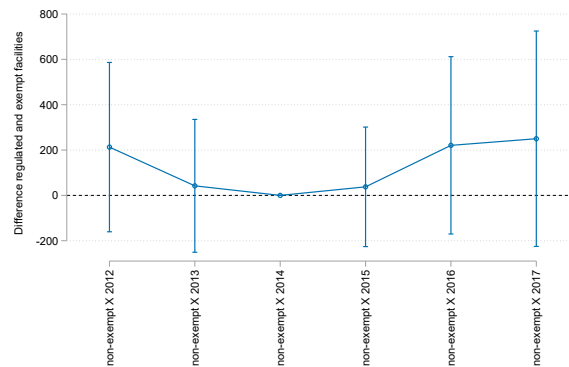
**Notes:** Panel c) shows the differences in differences-year specific coefficients for the harvested hectares following equation 1.7. Panel d) shows the differences in differences-year specific coefficients for the total number of manual workers following equation 1.7. Confidence intervals calculated using two-way fixed effects at the municipality and year level.



Figure A.11: Outputs-parallel trends  
 Panel a) Processed sugarcane

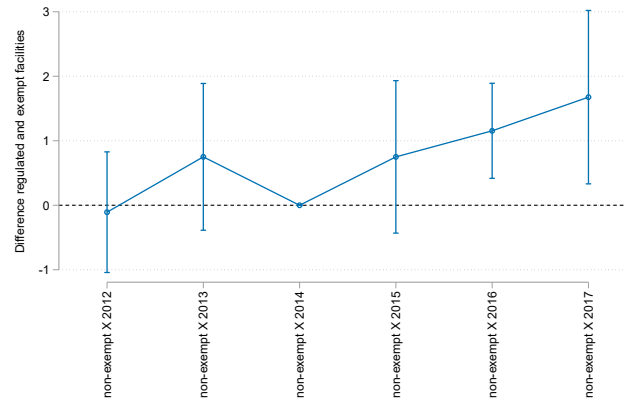


Panel b) Total sugar produced



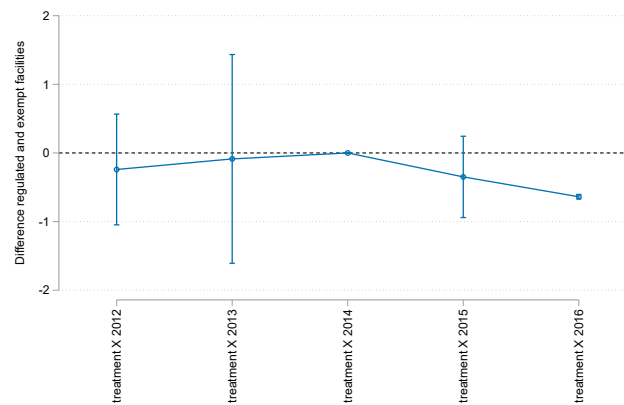
**Notes:** Panel a) shows the differences in differences-year specific coefficients for the total sugarcane processed at the mill (mills) following equation 1.7. Panel b) shows the differences in differences-year specific coefficients for the total produced sugar at the mill (tons) using mechanical cut following equation 1.7. Confidence intervals calculated using two-way fixed effects at the municipality and year level.

Figure A.12: Pollution in fields-parallel trends  
 Panel a) PM<sub>2.5</sub> pollution ( $\mu\text{g}/\text{m}^3$ )



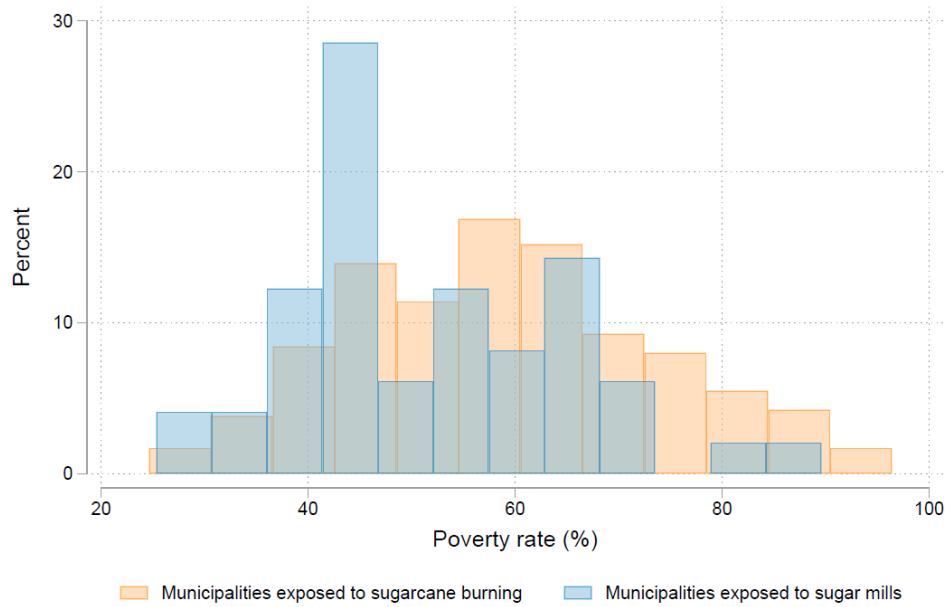
**Notes:** Panel a) shows the differences in differences-year specific coefficients for pollution from PM<sub>2.5</sub> in the fields following equation 1.8. Panel b) shows the differences in differences-year specific coefficients for pollution from SO<sub>2</sub> in the fields following equation 1.8. Confidence intervals calculated using two-way fixed effects at the municipality and year level. Confidence intervals calculated using two-way fixed effects at the municipality and year level.

Figure A.13: Pollution in mills-parallel trends  
 Panel a) PM<sub>2.5</sub> pollution ( $\mu\text{g}/\text{m}^3$ )



**Notes:** Panel a) shows the differences in differences-year specific coefficients for pollution from PM<sub>2.5</sub> in the mills following equation 1.8 using [40]. Confidence intervals calculated using two-way fixed effects at the municipality and year level. Confidence intervals calculated using two-way fixed effects at the municipality and year level.

Figure A.14: Poverty and location of fires and mills



**Notes:** The figure shows the percent of communities exposed to sugarcane burning and sugar production and their corresponding poverty rate. Poverty rate was obtained from INEGI using the 2010 Mexican Census data.

Table A.1: Descriptive statistics by type of facility before the policy

	(1)	(2)
	Exempt facilities	Non-exempt facilities
Panel a: Inputs data		
Manual cut (tons)	27769.69 (15268.95)	40982.75 (24692.98)
Mechanical cut (tons)	5796.26 (6671.87)	8880.16 (7900.13)
Total field workers (cutting)	1325.13 (650.75)	1811.07 (1116.84)
Total harvested sugarcane (hectares)	327.90 (357.74)	445.49 (618.76)
Total sugarcane (tons)	3041.26 (4286.52)	3015.94 (3887.12)
Sugar production efficiency	98.16 (44.40)	101.40 (40.16)
Sugarcane processing efficiency	111.59 (29.02)	111.83 (25.07)
Sugar extraction efficiency	20.34 (281.80)	13.12 (2.29)
Panel b: Outputs data		
Raw processed sugarcane (t)	36006.08 (15837.38)	51574.08 (23785.49)
Total sugar produced (t)	3945.55 (1898.63)	5901.07 (2857.84)
Total sugar produced per day (t)	555.64 (269.05)	828.56 (399.47)
Observations	3,006	1,517
Panel c: Fires and temperature data		
Total SHFs	0.25 (0.75)	0.37 (0.95)
Temperature (C)	21.85 (3.78)	21.60 (3.17)
Observations	47,690	23,845

**Notes:** Panel a) shows descriptive statistics for inputs and panel b) shows descriptive statistics for outputs at the sugar mill level at the weekly level. Panel c) shows descriptive statistics of sugarcane harvest fires and average temperature for daily observations at the sugar mill level. Column (1) shows the descriptive statistics for exempt facilities and Column (2) shows the descriptive statistics for non-exempt facilities. Standard deviation in parentheses.

Table A.2: Difference-in-differences estimates for monthly fires

	(1)	(2)	(3)
	Total SHFs	SHF=1	Log(SHF)
After 2015 × non-exempt	1.12952*** (0.38957)	0.00133 (0.01743)	0.11222*** (0.03168)
Pre 2015 mean	8.558	0.825	1.870
Obs.	2,394	2,394	1,975
R-squared	0.524	0.450	0.573
Year FE	Yes	Yes	Yes
Month FE	Yes	Yes	Yes
Mill FE	Yes	Yes	Yes
Linear trend	No	No	No
Weather Controls	Yes	Yes	Yes
Cluster level	Mun and year	Mun and year	Mun and year
Poisson	No	No	No

**Notes:** Column (1) shows the difference-in-differences estimator of the impact of being regulated by the emission limits after the policy started on the number of fires using equation 1.6. Column (2) shows the same specification but the dependent variable is an indicator variable on whether there is a fire or not in that field. Column (3) estimates the same specification in equation 1.6 with the log number of fires at the month level. Standard errors using two way clusters (municipality and year) in parenthesis.

Table A.3: Difference-in-differences estimates for monthly fires controlling for sugar and oil prices

	(1)	(2)
	Total SHFs	Total SHFs
After 2015 $\times$ non-exempt	1.13018** (0.38912)	1.12949** (0.39060)
Pre 2015 mean	8.558	8.558
Obs.	2,394	2,394
R-squared	0.525	0.524
Year FE	Yes	Yes
Month FE	Yes	Yes
Mill FE	Yes	Yes
Weather controls	Yes	Yes
Cluster level	Mun and year	Mun and year
Additional controls	Sugar price	Oil price

**Notes:** Column (1) shows the difference-in-differences estimator of the impact of being regulated by the emission limits after the policy started on the number of fires using equation 1.6 controlling for the international sugar prices. Column (2) shows the difference-in-differences estimator of the impact of being regulated by the emission limits after the policy started on the number of fires using equation 1.6 controlling for the Mexican mix crude oil prices. Standard errors using two way clusters (municipality and year) in parenthesis.

Table A.4: Effect on sugarcane fires using bootstrap standard errors

	(1)
	Total SHFs
After 2015 $\times$ non-exempt	0.04120** [0.00982,0.07258]
Pre 2015 mean	0.286
Obs.	71,535
R-squared	0.091
Year FE	Yes
Month FE	Yes
Mill FE	Yes
Weather controls	Yes
Cluster level	Bootstrap
Poisson	Yes

**Notes:** The table shows the results from equation (1.6) using bootstrap standard errors. Column (1) shows the resulting specification with dependent variable being total number of fires. Confidence intervals reported in brackets.

Table A.5: Effect on non-sugarcane fires

	(1)	(2)
	Total NSHFs	NSHF=1
After 2015 $\times$ non-exempt	0.24180 (0.25467)	-0.01129 (0.00806)
Pre 2015 mean	3.060	0.439
Obs.	71,535	71,535
R-squared	0.321	0.387
Year FE	Yes	Yes
Month FE	Yes	Yes
Mill FE	Yes	Yes
Weather controls	Yes	Yes
Cluster level	Mun and year	Mun and year

**Notes:** Column (1) shows the difference-in-differences estimator of the impact of being regulated by the emission limits after the policy started on the number of agricultural fires (non-sugarcane) using equation 1.6. Non-sugarcane fires were classified using land cover data from INEGI. Standard errors using two way clusters (municipality and year) in parenthesis.

Table A.6: Placebo test: sugarcane fires outside the harvest season

	(1)	(2)
	Total SHFs	SHF=1
After 2015 $\times$ non-exempt	0.00218 (0.00590)	0.00046 (0.00389)
Pre 2015 mean	0.034	0.024
Obs.	52,326	52,326
R-squared	0.054	0.059
Year FE	Yes	Yes
Month FE	Yes	Yes
Mill FE	Yes	Yes
Weather controls	Yes	Yes
Cluster level	Mun and year	Mun and year

**Notes:** Column (1) shows the difference-in-differences estimator of the impact of being regulated by the emission limits after the policy started on the number of fires using equation 1.6 for the months July-October, outside the sugarcane harvest window. Column (2) shows the same specification but the dependent variable is an indicator variable on whether there is a fire or not in that field. Column (3) estimates the same specification in equation 1.6 with the log number of fires at the month level. Standard errors using two way clusters (municipality and year) in parenthesis.

Table A.7: Effect on sugarcane fires - distribution areas

Panel a)			
	(1)	(2)	(3)
	Total SHFs	SHF=1	Total SHFs
After 2015 $\times$ non-exempt	0.02284* (0.01111)	0.01423** (0.00527)	0.32656*** (0.11845)
Pre 2015 mean	0.067	0.051	0.067
Obs.	25,000	25,000	25,000
R-squared	0.027	0.031	
Year FE	Yes	Yes	Yes
Month FE	Yes	Yes	Yes
Mill FE	Yes	Yes	Yes
Cluster level	Mun and year	Mun and year	Robust
Poisson	No	No	Yes
Buffer	300	300	300
Panel b)			
	(1)	(2)	(3)
	Total SHFs	SHF=1	Total SHFs
After 2015 $\times$ non-exempt	0.05044* (0.02502)	0.01985** (0.00710)	0.24923** (0.12634)
Pre 2015 mean	0.170	0.086	0.170
Obs.	25,080	25,080	25,080
R-squared	0.039	0.051	
Year FE	Yes	Yes	Yes
Month FE	Yes	Yes	Yes
Mill FE	Yes	Yes	Yes
Cluster level	Mun and year	Mun and year	Robust
Poisson	No	No	Yes
Buffer	500	500	500

**Notes:** Panel a) and b) show the results following the equation 1.6 considering the sugarcane distribution areas for the subset of sugar mills in Veracruz under the study “Digitalización del Campo Cañero en México para Alcanzar la Agricultura de Precisión de la Caña de Azúcar”. Panel a) shows the results using a buffer of 300m surrounding the sampling points and Panel b) shows the results using a buffer of 500m surrounding the sampling points. Column (1) shows the difference-in-differences estimator of the impact of being regulated by the emission limits after the policy started on the number of sugarcane fires. Column (2) shows the same specification but the dependent variable is an indicator variable on whether there is a fire or not in that field. Column (3) estimates the specification using a Poisson model using robust standard errors. Standard errors using two way clusters (municipality and year) in parenthesis for Columns (1) and (2).



Table A.8: Effect on sugarcane fires - compliant mills

	(1)	(2)
	Total SHFs	SHF=1
After 2015 $\times$ non-exempt	0.09283** (0.03238)	0.02223* (0.01011)
Pre 2015 mean	0.314	0.177
Obs.	13,805	13,805
R-squared	0.120	0.135
Year FE	Yes	Yes
Month FE	Yes	Yes
Mill FE	Yes	Yes
Cluster level	Mun and year	Mun and year
Compliant	Yes	Yes

**Notes:** The table shows the main results for daily fires with a restricted sample for facilities with known compliance by CONADESUCA. Column (1) shows the difference-in-differences estimator of the impact of being regulated by the emission limits after the policy started on the number of sugarcane harvest fires using equation 1.6. Column (2) shows the difference-in-differences estimator of the impact of being regulated by the emission limits after the policy started on the probability of sugarcane fire. Standard errors using two way clusters (municipality and year) in parenthesis.

Table A.9: Effect on sugarcane fires - compliant mills

	(1)	(2)
	Sample restriction 1	Sample restriction 2
After 2015 $\times$ non-exempt	0.03935** (0.01505)	0.04077** (0.01540)
Pre 2015 mean	0.285	0.289
Obs.	70,280	70,280
R-squared	0.092	0.091
Year FE	Yes	Yes
Month FE	Yes	Yes
Mill FE	Yes	Yes
Weather controls	Yes	Yes
Cluster level	Mun and year	Mun and year
Poisson	No	No

**Notes:** The table shows the main results for daily fires with two restricted sample of facilities. Column (1) shows the results with the sample restriction 1 that estimates the regressions dropping the mill “San Francisco Ameca” which is the only mill that acquired a biofuel powered boiler after the treatment started. Column (2) shows the results with the sample restriction 2 that estimates the regressions dropping the mill “Ingenio El Potrero”, which is the only mill that has the highest rate of mismatched fields according to Figure A4. Standard errors using two way clusters (municipality and year) in parenthesis.

Table A.10: Effects on wages

	(1)	(2)	(3)	(4)	(5)
			Wage		
After 2015 × non-exempt	-1.770 (6.57693)	-5.172 (8.05965)	-1.236 (8.66429)	1.722 (12.50082)	-0.308 (5.40046)
Mean	103.484	109.047	113.478	112.093	94.440
Obs.	9,769	1,978	2,005	2,001	1,969
R-squared	0.530	0.719	0.780	0.716	0.644
Year FE	Yes	Yes	Yes	Yes	Yes
Week FE	Yes	Yes	Yes	Yes	Yes
Mill FE	Yes	Yes	Yes	Yes	Yes
Cluster level	Mun-year	Mun-year	Mun-year	Mun-year	Mun-year
Age	All	15-30	30-45	45-60	60-more

**Notes:** Column (1) shows the difference-in-differences estimator of the impact of being regulated by the emission limits after the policy started on the daily wages following 1.7. Column (2)-(7) shows the difference-in-differences estimator of the impact of being regulated by the emission limits after the policy started on the wages for the workers different age categories. Data obtained from the social security information at the municipality level. The sample of mills was restricted to the municipalities that have either all mills with the same treatment status (all exempt or all non-exempt), therefore deleting 4 mills. Standard errors using two way clusters (municipality and year) in parenthesis.

Table A.11: Effects on outputs

	(1)	(2)
	Raw processed sugarcane (tons)	Total sugar produced (tons)
After 2015 × non-exempt	83.171 (904.27822)	78.483 (138.69765)
Mean	41,865.426	4,674.832
Obs.	8,568	8,568
R-squared	0.803	0.792
Year FE	Yes	Yes
Week FE	No	No
Mill FE	Yes	Yes
Cluster level	Mun and year	Mun and year

**Notes:** Column (1) shows the difference-in-differences estimator of the impact of being regulated by the emission limits after the policy started on the amount of sugarcane processed at the mill (tons) following specification 1.7. Column (2) shows the difference-in-differences estimator of the impact of being regulated by the emission limits after the policy started on the amount of sugar produced (tons) following specification 1.7. Standard errors using two way clusters (municipality and year) in parenthesis.

Table A.12: Effects on efficiency

	(1)	(2)	(3)
	Sugarcane processing efficiency	Sugar production efficiency	Sugar extraction efficiency
After 2015 $\times$ non-exempt	-0.857 (4.79311)	-4.678 (6.09324)	-7.528 (6.40081)
Mean	113.734	101.143	15.276
Obs.	5,707	5,707	5,707
R-squared	0.425	0.615	0.020
Year FE	Yes	Yes	Yes
Week FE	Yes	Yes	Yes
Mill FE	Yes	Yes	Yes
Cluster level	Mun and year	Mun and year	Mun and year

**Notes:** Column (1) shows the difference-in-differences estimator of the impact of being regulated by the emission limits after the policy started on the total kilograms of sugar obtained by ton of harvested sugarcane (measured by the KARBE indicator provided by CONADESUCA) at the mills following specification 1.7. Column (2) shows the difference-in-differences estimator of the impact of being regulated by the emission limits after the policy started on the total kilograms of sugar obtained by ton of processed sugarcane (measured by the KABE indicator provided by CONADESUCA) following specification 1.7. Column (3) shows the difference-in-differences estimator of the impact of being regulated by the emission limits after the policy started on the sugar extraction efficiency. Standard errors using two way clusters (municipality and year) in parenthesis.

Table A.13: Effect on pollution in mills location

	(1)	(2)	(3)	(4)
	PM2.5	Log(PM2.5)	SO2	Log(SO2)
After 2015 $\times$ non-exempt	0.09699 (0.26296)	-0.00254 (0.01911)	0.00975 (0.03289)	-0.00186 (0.01950)
Mean	15.610	2.495	1.388	0.036
Obs.	68,440	68,440	68,440	68,440
R-squared	0.444	0.532	0.385	0.485
Year FE	Yes	Yes	Yes	Yes
Month FE	Yes	Yes	Yes	Yes
Mill FE	Yes	Yes	Yes	Yes
Weather controls	Yes	Yes	Yes	Yes
Cluster level	Mun and year	Mun and year	Mun and year	Mun and year

**Notes:** Column (1) and (2) show the difference-in-differences estimator of the impact of being regulated by the emission limits after the policy started on the ambient pollution level of PM<sub>2.5</sub> and log(PM<sub>2.5</sub>), respectively following specification 1.8. Column (3) and (4) show the difference-in-differences estimator of the impact of being regulated by the emission limits after the policy started on the ambient pollution level of SO<sub>2</sub> and log(SO<sub>2</sub>), respectively following specification 1.8. Standard errors using two way clusters (municipality and year) in parenthesis.

Table A.14: Effect on sugarcane fires by poverty level

	(1)	(2)	(3)
	Total SHFs	Total SHFs	Total SHFs
After2015=1=1 × Treatment=1=1	0.03278*** (0.00653)	0.02212 (0.02501)	0.04010*** (0.00349)
Mean	0.289	0.266	0.312
Obs.	64,005	31,375	32,630
R-squared	0.087	0.074	0.096
Year FE	Yes	Yes	Yes
Month FE	Yes	Yes	Yes
Mill FE	Yes	Yes	Yes
Linear trend	No	No	No
Weather controls	No	No	No
Cluster level	Mun and year	Mun and year	Mun and year
Poverty level (wrt median)	All	Lower	Higher

**Notes:** The table shows the results from equation (1.6) with heterogeneity by poverty level in fields areas. Column (1) shows the resulting specification with dependent variable being total number of fires. Column (2) shows the results for fields located near localities with poverty level lower than the national median. Column (3) shows the results for fields located near localities with poverty level higher than the national median. Twoway-clustered standard errors

# Appendix B

## Appendix to Chapter 2

### B.1 Mathematical Appendix

#### B.1.1 Bootstrap procedure for incorporating uncertainty in C&T emission effects

This section details our bootstrap procedure over steps 1-3 to account for statistical uncertainty in C&T-driven emission effects from equation (2.1), reproduced here:

$$\text{asinh}(Y_{jt}^p) = \kappa_1^p[C_j \times t] + \kappa_2^p[C_j \times \mathbf{1}(t \geq 2013) \times t] + \phi_j^p + \gamma_t^p + \nu_{jt}^p$$

We obtain point estimates  $\hat{\kappa}_1^p$ ,  $\hat{\kappa}_2^p$  and standard errors  $\hat{\sigma}_{\kappa_1^p}$  and  $\hat{\sigma}_{\kappa_2^p}$  from equation (2.1).

We then iterate the following procedure for draws  $b = 1 \dots 250$ :

- Draw  $\hat{\kappa}_1^p(b) \sim N(\hat{\kappa}_1^p, \hat{\sigma}_{\kappa_1^p})$  and  $\hat{\kappa}_2^p(b) \sim N(\hat{\kappa}_2^p, \hat{\sigma}_{\kappa_2^p})$
- Construct  $\hat{Y}_{jt}^p(b) = \text{sinh} \left( \hat{\kappa}_1^p(b)[C_j \times t] + \hat{\kappa}_2^p(b)[C_j \times \mathbf{1}(t \geq 2013) \times t] + \hat{\phi}_j^p \right) * e^{(RMSE)^2/2}$ , where RMSE is the root mean squared error from equation (2.1)

- Feed  $\widehat{Y}_{jt}^p(b)$  into HYSPLIT to generate zip code-by-year pollution concentration,  $E_{it}^p(b)$
- Estimate equation (2.2) using  $E_{it}^p(b)$  as the outcome variable to obtain  $\widehat{\beta}_1^p(b)$  and  $\widehat{\beta}_2^p(b)$

Figure B.5 plots the empirical distributions for  $\widehat{\beta}_1^p(b)$  and  $\widehat{\beta}_2^p(b)$  for  $p \in \{PM_{2.5}, PM_{10}, NO_x, SO_x\}$ . Denote standard errors across 250 bootstrap runs as  $\widehat{\sigma}_{\beta_1^p}(\nu_{jt}^p)$  and  $\widehat{\sigma}_{\beta_2^p}(\nu_{jt}^p)$  where the  $\nu_{jt}^p$  argument indicates the dependence on statistical uncertainty from equation (2.1). Denote  $\widehat{\sigma}_{\beta_1^p}(\epsilon_{jt}^p)$  as the estimated standard error arising from heterogeneity in  $\beta_1^p$  obtained by directly estimating equation (2.2) with county-level clustered errors. Our reported standard error for  $\beta_1^p$  is  $\widehat{\sigma}_{\beta_1^p} = \widehat{\sigma}_{\beta_1^p}(\epsilon_{jt}^p) + \widehat{\sigma}_{\beta_1^p}(\nu_{jt}^p)$ . Likewise, for  $\beta_2^p$ .  $\widehat{\sigma}_{\beta_1^p}$  and  $\widehat{\sigma}_{\beta_2^p}$  are reported in Table 2.2 and used to construct the confidence intervals displayed in Figure 2.3.

### B.1.2 Can the EJ gap effect be recovered using dispersal-augmented facility-level regressions?

Facility-level analyses examine how a policy's emissions effects vary with characteristics of locations that are downwind of facilities, as determined by an atmospheric dispersal model [70, 85]. For example, one may estimate the following dispersal-augmented facility-level regression for the change in facility  $j$  emissions before and after the introduction of a policy:

$$\Delta Y_j = \phi_0 C_j + \phi_1 C_j s_j + \phi_2 s_j + \varepsilon_j \quad (\text{B.1})$$

where  $C_j \in \{0, 1\}$  is regulatory status and  $s_j \in [0, 1]$  is the share of affected downwind locations that is disadvantaged, as determined by the dispersal model. In these models, the coefficient of interest is  $\widehat{\phi}_1$ , the added emissions effect for facilities that disproportionately

affect disadvantaged communities.

How does  $\widehat{\phi}_1$  relate to the EJ gap effect, the estimand of interest? As in Section 2.4, let  $i$  index locations (e.g., California zip codes in our setting) and  $D_i \in \{0, 1\}$  denote disadvantaged status. For simplicity, assume there are the same number of disadvantaged and non-disadvantaged locations,  $N = \sum_{i:D_i=0}(1 - D_i) = \sum_{i:D_i=1} D_i$ . The EJ gap effect is the difference between the change in pollution concentration for disadvantaged communities and that of non-disadvantaged communities, due to C&T-driven emission changes from regulated facilities (relative to unregulated facilities), or  $\widehat{\Delta Y}_j$ . Formally, this estimand is

$$\begin{aligned}
 \theta &= \underbrace{\frac{1}{N} \sum_j \widehat{\Delta Y}_j s_j}_{\text{avg. DAC concentration from C\&T-driven emissions}} - \underbrace{\frac{1}{N} \sum_j \widehat{\Delta Y}_j (1 - s_j)}_{\text{avg. non-DAC concentration from C\&T-driven emissions}} \\
 &= \frac{1}{N} \sum_j \widehat{\Delta Y}_j (2s_j - 1) \\
 &= \frac{1}{N} \sum_j (\widehat{\phi}_0 + \widehat{\phi}_1 s_j) (2s_j - 1) \tag{B.2}
 \end{aligned}$$

The last line applies C&T-driven relative emissions change for regulated facilities as  $\widehat{\Delta Y}_j = \widehat{\phi}_0 + \widehat{\phi}_1 s_j$ , where  $\widehat{\phi}_0$  and  $\widehat{\phi}_1$  are estimated coefficients from equation (B.1).

It is clear from (B.2) that  $\widehat{\phi}_1$  does not generally equal  $\theta$ . But is the sign of  $\widehat{\phi}_1$  at least consistently the same as the sign of  $\theta$ ? The following example rejects this claim. For simplicity, let  $\widehat{\phi}_0 = 0$ . Next, suppose  $s_1 = 1$  for the first facility and  $s_{j>1} < 0.5$  for all

other facilities. The estimand is then:

$$\begin{aligned}\theta &= \frac{1}{N} \left( \hat{\phi}_1 + \sum_{j>1} \hat{\phi}_1 s_j (2s_j - 1) \right) \\ &= \frac{\hat{\phi}_1}{N} \left( \underbrace{1 + \sum_{j>1} \underbrace{s_j (2s_j - 1)}_{<0}}_{\geq 0} \right)\end{aligned}$$

indicating that  $\theta$  and  $\hat{\phi}_1$  can be of different signs. Thus, simply showing, for example, that emissions are relatively higher for facilities that disproportionately affect disadvantaged communities (i.e.,  $\hat{\phi}_1 > 0$ ) does not imply that the EJ gap has widened (i.e.,  $\theta > 0$ ).

Lastly, can  $\hat{\phi}_1$  ever equal  $\theta$ ? Returning to equation (B.1), we explore one such special case. Assume that exactly  $N$  facilities only affect disadvantaged communities (i.e.,  $s_j = 0$ ), and that another  $N$  facilities only affect non-disadvantaged communities (i.e.,  $s_j = 1$ ). Then the estimand becomes:

$$\begin{aligned}\theta &= \frac{1}{N} \left( \sum_{j:s_j=0} -\hat{\phi}_0 + \sum_{j:s_j=1} (\hat{\phi}_0 + \hat{\phi}_1) \right) \\ &= \frac{1}{N} (-N\hat{\phi}_0 + N\hat{\phi}_0 + N\hat{\phi}_1) \\ &= \hat{\phi}_1\end{aligned}$$

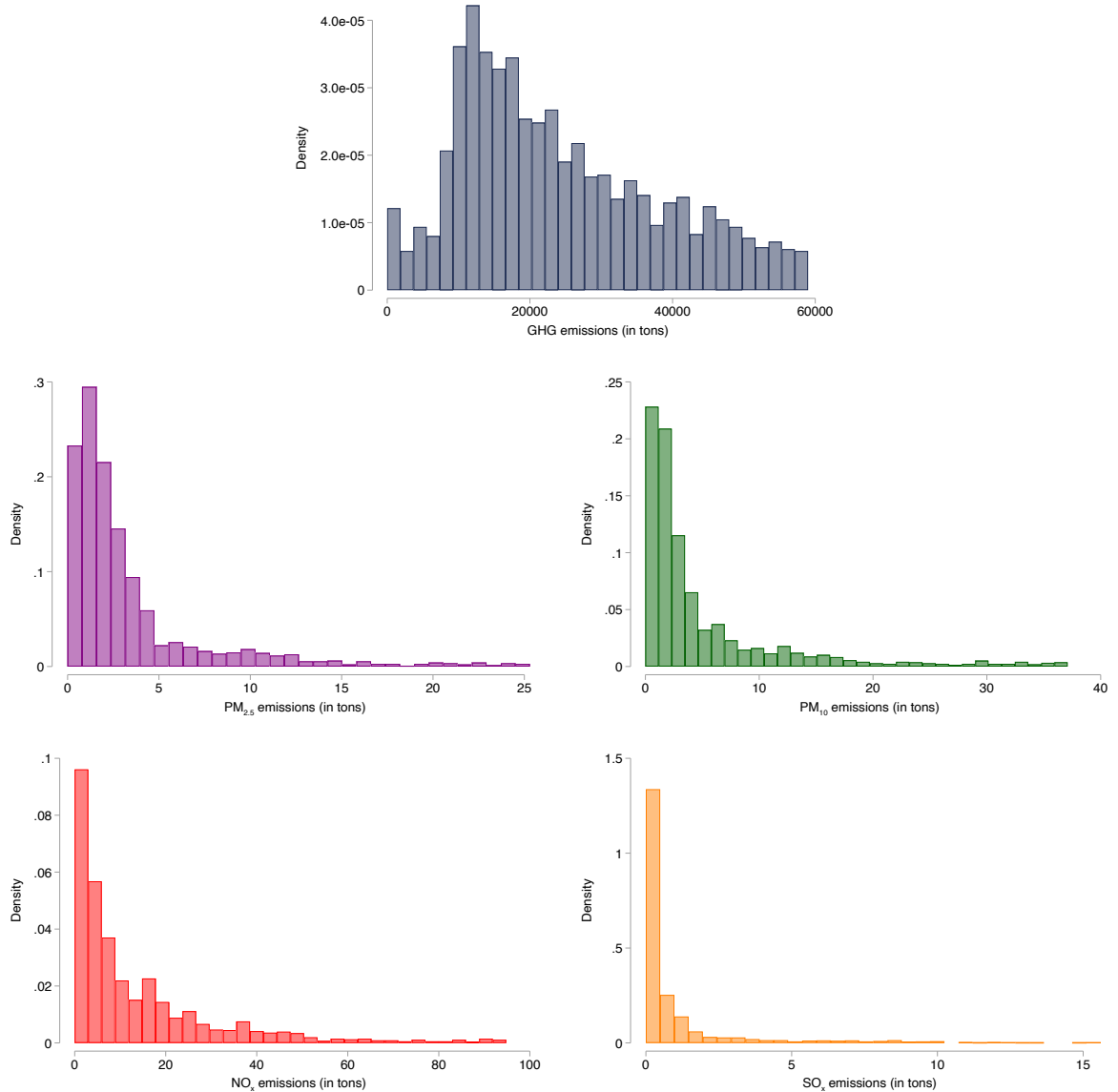
Observe how restrictive the assumptions are for this special case. It requires that facilities *only* affect disadvantaged communities or *only* affect non-disadvantaged communities, that is  $s_j \in \{0, 1\} \forall j$ . Facilities cannot alter pollution concentrations in both types of locations. Furthermore, this case requires that the number of facilities in both groups equal the number of disadvantaged communities, which must also equal the number of



non-disadvantaged communities.

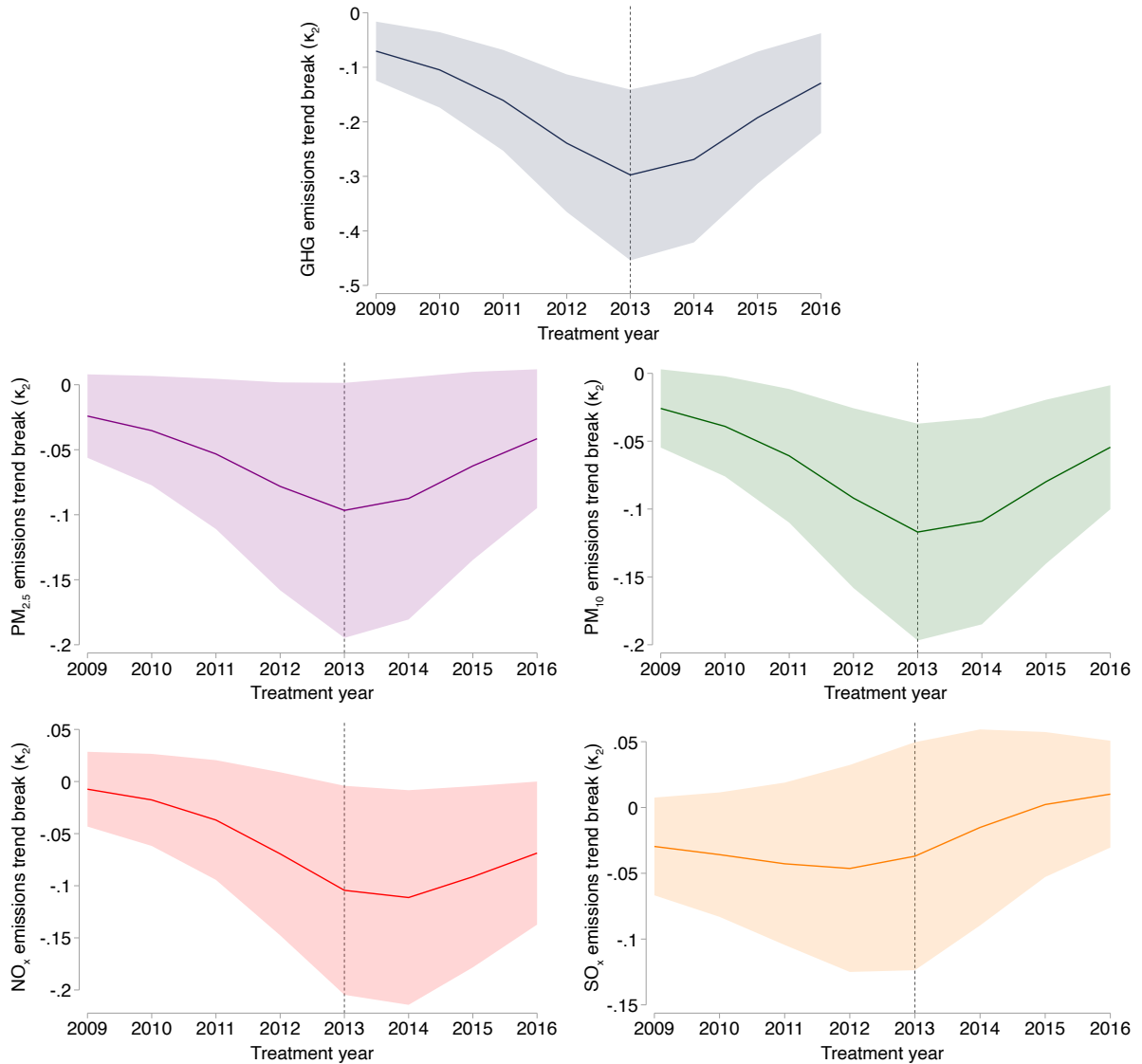
## B.2 Appendix Figures

Figure B.1: Distribution of sample facility-year emissions



NOTES: Panels show the distribution of facility-year GHG, PM<sub>2.5</sub>, PM<sub>10</sub>, NO<sub>x</sub>, and SO<sub>x</sub> emissions for sample observations. Observations above the 95th percentile are truncated.

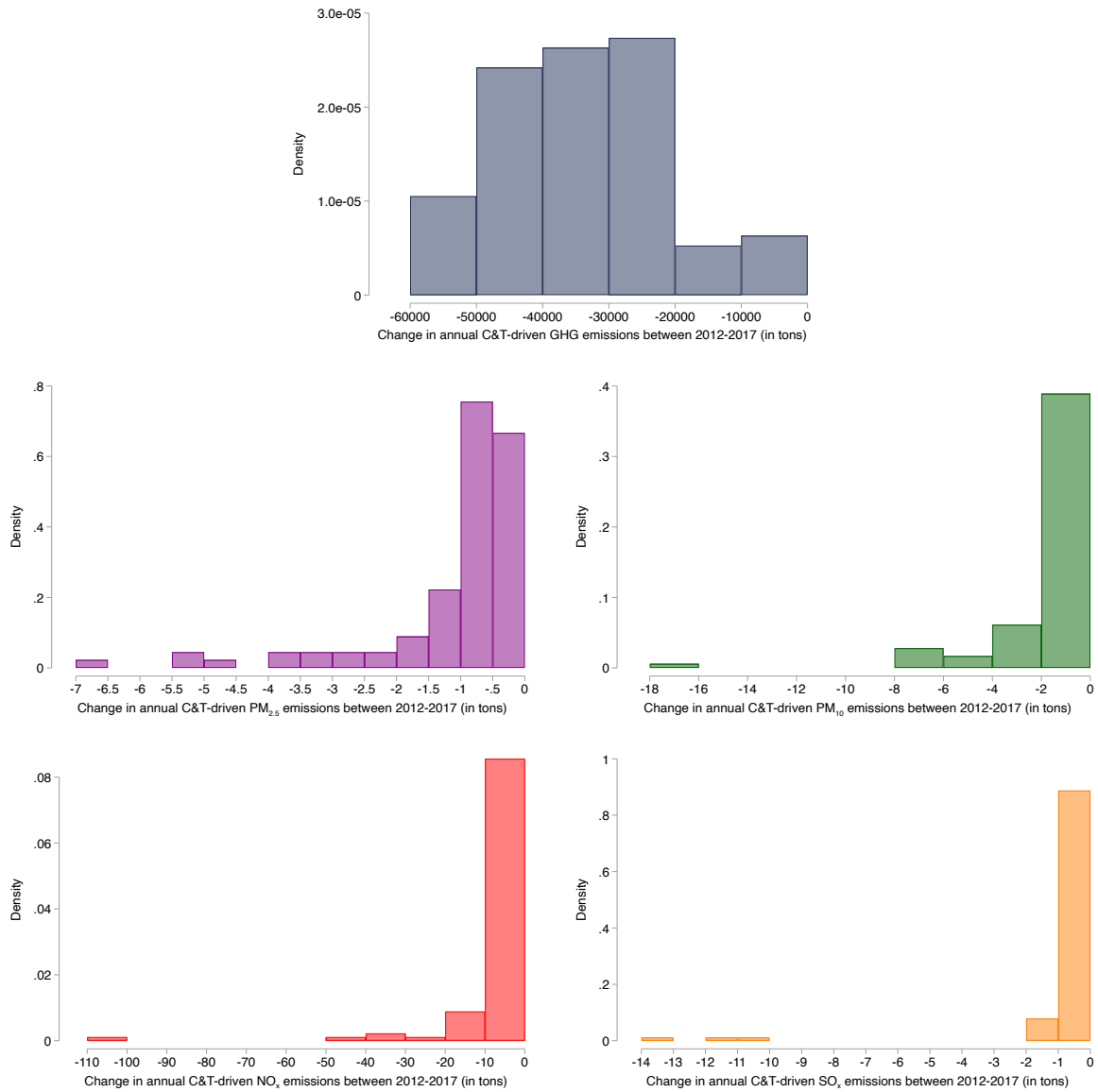
Figure B.2: Emissions robustness: placebo C&amp;T program timing



NOTES: Panels show estimated (true and placebo) emissions trend break coefficients (i.e.,  $\kappa_2$  from eq. (2.1)) for GHG, PM<sub>2.5</sub>, PM<sub>10</sub>, NO<sub>x</sub>, and SO<sub>x</sub> emissions from varying the start year of the C&T program. Vertical line at 2013 indicates actual introduction of the program. Shaded areas indicate 95% confidence intervals.

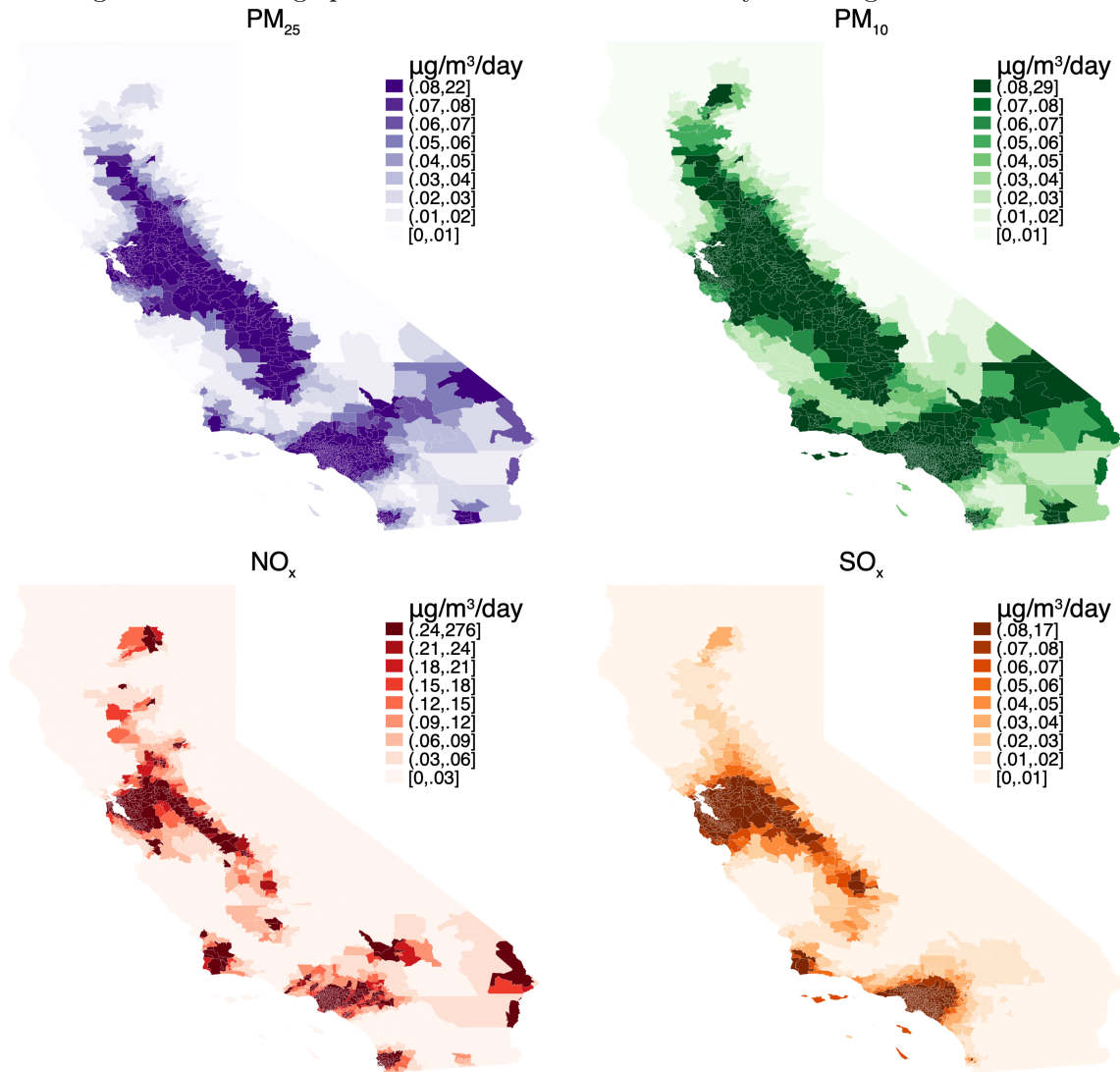
### B.3 Appendix Tables

Figure B.3: Facility-level C&T-driven abatement between 2012-2017



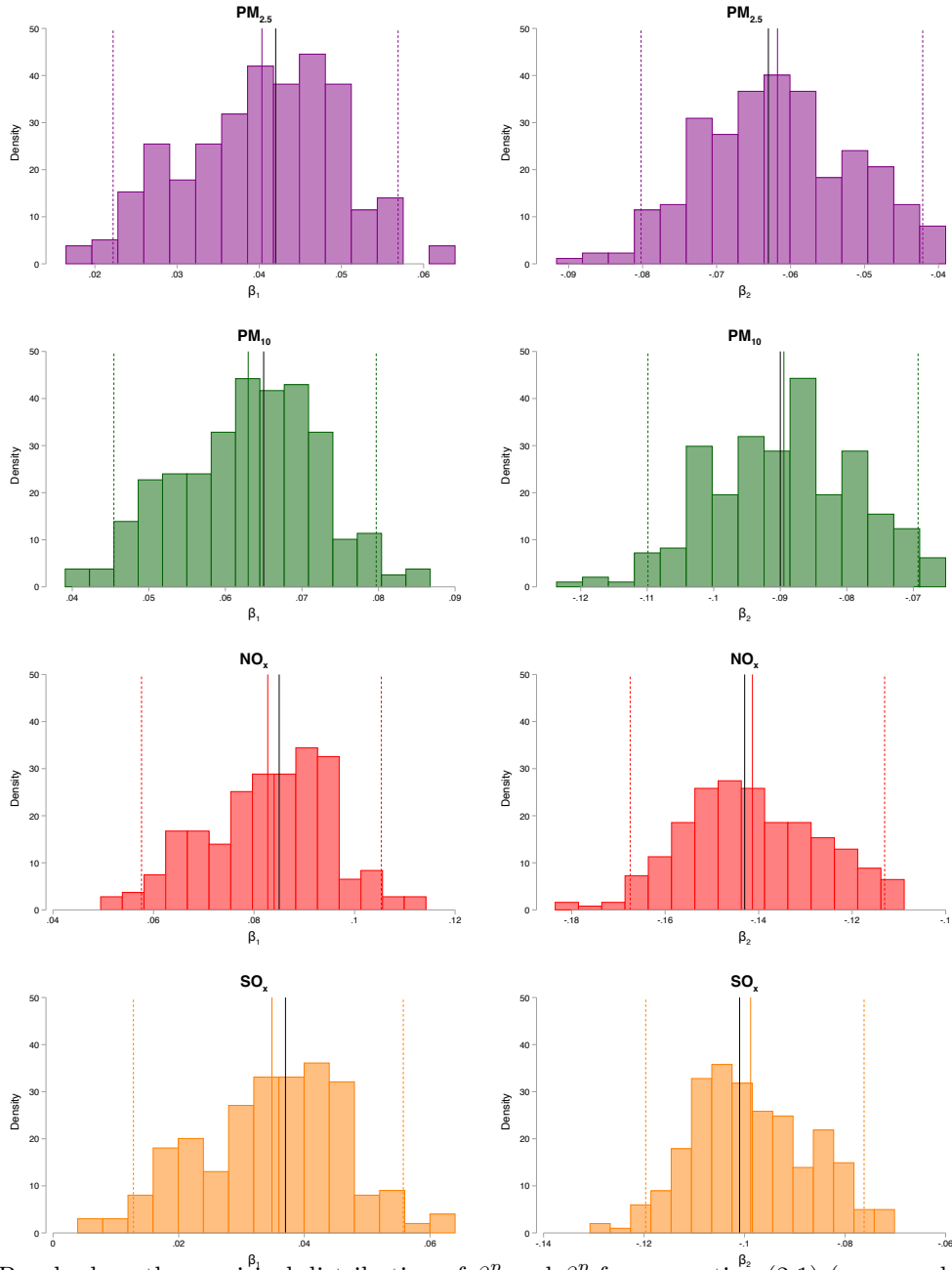
NOTES: Panels show the distribution of facility-level change in C&T-driven pollution between 2012-2017 (or abatement) predicted from step 1 for GHG, PM<sub>2.5</sub>, PM<sub>10</sub>, NO<sub>x</sub>, and SO<sub>x</sub> emissions, respectively.

Figure B.4: Average pollution concentrations driven by C&T regulated facilities



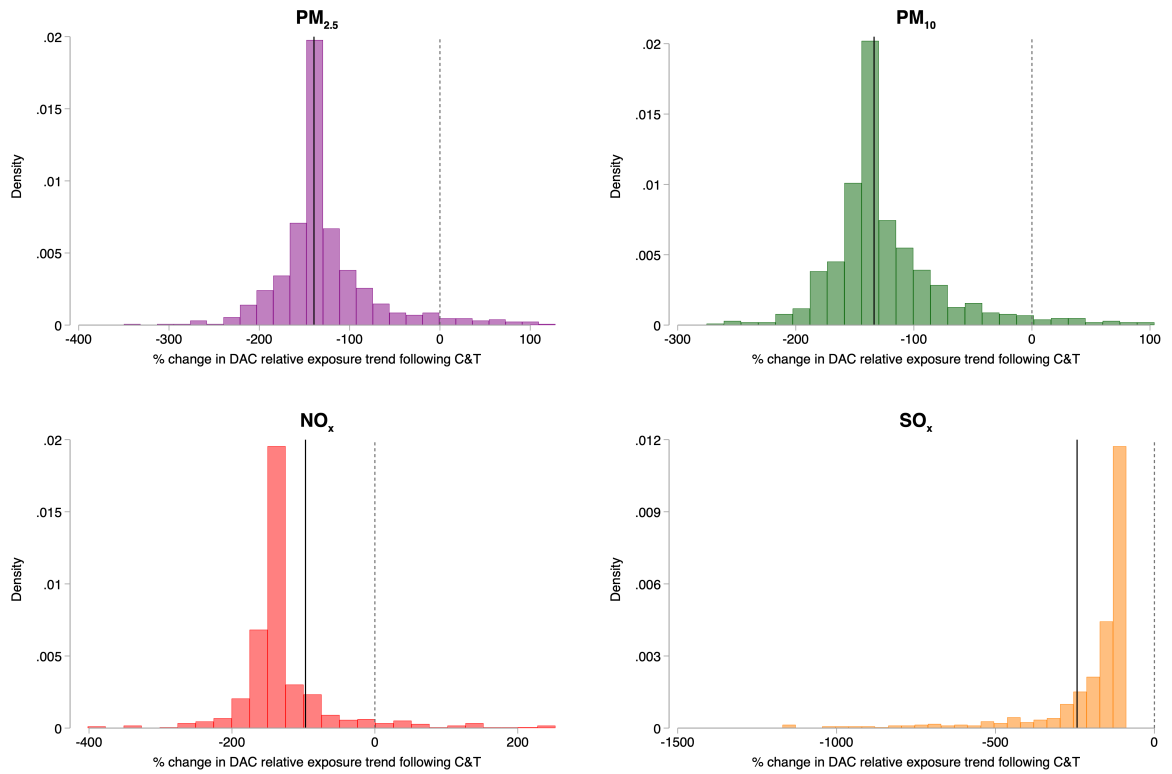
NOTES: Panels show daily concentrations (in  $\mu\text{g}/\text{m}^3/\text{day}$ ) for each zip code averaged across 2008-2017 from GHG C&T-regulated facilities as modeled in step 2 by HYSPLIT for PM<sub>2.5</sub>, PM<sub>10</sub>, NO<sub>x</sub>, and SO<sub>x</sub>, respectively.

Figure B.5: Empirical distribution of  $\beta_1^p$  and  $\beta_2^p$  from bootstrapping step 1



NOTES: Panels show the empirical distribution of  $\beta_1^p$  and  $\beta_2^p$  from equation (2.1) (across columns) for PM<sub>2.5</sub>, PM<sub>10</sub>, NO<sub>x</sub>, and SO<sub>x</sub> (across rows) using the bootstrap procedure detailed in Section B.1.1 with 250 draws. Solid black line shows parameter from directly estimating equation (2.1). Solid colored line shows the mean parameter value from the empirical bootstrapped distribution. Dotted colored lines show the 2.5% and 97.5% percentiles of the empirical bootstrap distributions.

Figure B.6: Zip code-level percent change in EJ gap trend following C&amp;T



NOTES: Panels show the distribution of zip code-level percentage change in the EJ gap trend following the introduction of the C&T program, for each disadvantaged zip code across PM<sub>2.5</sub>, PM<sub>10</sub>, NO<sub>x</sub>, and SO<sub>x</sub>. Solid line shows the average percentage change across disadvantaged zip codes, or  $\frac{\beta_2^p}{\beta_1^p} * 100$  from equation (2.2). Dashed line marks zero.

Table B.1: GHG cap-and-trade regulated and non-regulated facilities

	C&T regulated facilities	non-C&T regulated facilities
Number of facilities	106	226
Avg. 2008-2012 emissions (in metric tons):		
CO <sub>2</sub>	38192.62	17566.48
PM <sub>2.5</sub>	8.08	3.74
PM <sub>10</sub>	14.47	6.25
NO <sub>x</sub>	53.42	16.03
SO <sub>x</sub>	10.86	2.8
Shares by sector:		
Agriculture	0	.018
Manufacturing	.623	.5
Mining, oil and gas extraction	.151	.097
Services	.066	.23
Transportation	.075	.053
Utilities	.075	.093
Wholesale	.009	.009

NOTES: Sample C&T regulated and non-regulated facilities by count, average 2008-2012 GHG and criteria air pollution emissions, and by sector shares. Sectors shown adhere to the following definitions: Agriculture: NAICS 11; Manufacturing: NAICS 31-33; Mining, oil, and gas extraction: NAICS 21; Services: NAICS 51, 54, 56, 61, 62, 71, 81, 92; Transportation: NAICS 48, 49; Utilities: NAICS 22; Wholesale: NAICS 42.

Table B.2: Emissions robustness: specification and sample restrictions

	(1) sector-year FEs	(2) Drop switchers	(3) Baseline CO <sub>2e</sub> 70	(4) cutoff (%) 80
Outcome is asinh(CO <sub>2e</sub> ) emissions				
$\kappa_1^p$	0.172 (0.058) [0.005]	0.220 (0.054) [0.000]	0.194 (0.055) [0.001]	0.174 (0.050) [0.001]
$\kappa_2^p$	-0.273 (0.095) [0.006]	-0.317 (0.079) [0.000]	-0.307 (0.085) [0.001]	-0.260 (0.072) [0.001]
Facilities	315	298	294	337
Observations	2,052	1,924	1,863	2,234
Outcome is asinh(PM <sub>2.5</sub> ) emissions				
$\kappa_1^p$	0.059 (0.043) [0.176]	0.065 (0.045) [0.156]	0.071 (0.043) [0.111]	0.046 (0.043) [0.298]
$\kappa_2^p$	-0.099 (0.048) [0.046]	-0.092 (0.051) [0.081]	-0.105 (0.050) [0.044]	-0.079 (0.050) [0.121]
Facilities	301	285	281	323
Observations	1,966	1,847	1,780	2,147
Outcome is asinh(PM <sub>10</sub> ) emissions				
$\kappa_1^p$	0.086 (0.034) [0.014]	0.088 (0.035) [0.016]	0.097 (0.034) [0.008]	0.075 (0.035) [0.039]
$\kappa_2^p$	-0.124 (0.040) [0.003]	-0.108 (0.043) [0.017]	-0.129 (0.043) [0.005]	-0.103 (0.042) [0.018]
Facilities	301	285	281	323
Observations	1,966	1,847	1,780	2,147
Outcome is asinh(NO <sub>x</sub> ) emissions				
$\kappa_1^p$	0.085 (0.042) [0.048]	0.057 (0.039) [0.158]	0.085 (0.033) [0.015]	0.058 (0.037) [0.128]
$\kappa_2^p$	-0.117 (0.053) [0.035]	-0.079 (0.050) [0.123]	-0.126 (0.047) [0.010]	-0.091 (0.048) [0.066]
Facilities	302	286	282	324
Observations	1,968	1,849	1,782	2,149
Outcome is asinh(SO <sub>x</sub> ) emissions				
$\kappa_1^p$	0.005 (0.038) [0.902]	0.008 (0.036) [0.817]	-0.005 (0.038) [0.890]	-0.004 (0.035) [0.912]
$\kappa_2^p$	-0.040 (0.048) [0.407]	-0.040 (0.046) [0.386]	-0.025 (0.048) [0.600]	-0.020 (0.045) [0.657]
Facilities	302	286	282	324
Observations	1,961	1,847	1,777	2,142

NOTES: Estimates of pre-C&T differential emissions trend (i.e.,  $\kappa_1^p$  from equation (2.1)) and post-C&T differential emissions trend break (i.e.,  $\kappa_2^p$  from equation (2.1)) for GHG, PM<sub>2.5</sub>, PM<sub>10</sub>, NO<sub>x</sub>, and SO<sub>x</sub> across panels. All models include facility-specific and year-specific dummy variables (except for column 1). Column 1 replaces year fixed effects with sector-by-year fixed effects with sectors defined as shown in Table B.1. Column 2 drops facilities that switched C&T regulatory status in 2017. Columns 3 and 4 restrict facilities to those with sample average annual GHG emissions below the 70th and 80th percentile, respectively. Standard errors clustered at the county-level in parentheses, p-value in brackets.



Table B.3: Emissions effect robustness: heterogeneity by average emissions

	(1)	(2)	(3)
	Outcome is asinh(GHG) emissions		
$\kappa_1^p$	0.187 (0.052) [0.001]	0.176 (0.052) [0.002]	0.172 (0.052) [0.002]
$\kappa_2^p$	-0.297 (0.077) [0.000]	-0.361 (0.092) [0.000]	-0.354 (0.097) [0.001]
trend break $\times$ avg. emissions		0.000 (0.000) [0.053]	0.000 (0.000) [0.090]
trend break $\times$ avg. emissions <sup>2</sup>			-0.000 (0.000) [0.158]
	Outcome is asinh(PM <sub>2.5</sub> ) emissions		
$\kappa_1^p$	0.058 (0.043) [0.183]	0.060 (0.042) [0.167]	0.060 (0.043) [0.165]
$\kappa_2^p$	-0.097 (0.048) [0.053]	-0.133 (0.051) [0.012]	-0.146 (0.068) [0.040]
trend break $\times$ avg. emissions		-0.004 (0.003) [0.197]	-0.005 (0.004) [0.249]
trend break $\times$ avg. emissions <sup>2</sup>			0.000 (0.000) [0.661]
	Outcome is asinh(PM <sub>10</sub> ) emissions		
$\kappa_1^p$	0.083 (0.033) [0.016]	0.084 (0.033) [0.015]	0.086 (0.033) [0.012]
$\kappa_2^p$	-0.117 (0.039) [0.005]	-0.143 (0.042) [0.002]	-0.172 (0.048) [0.001]
trend break $\times$ avg. emissions		-0.002 (0.001) [0.080]	-0.003 (0.002) [0.073]
trend break $\times$ avg. emissions <sup>2</sup>			0.000 (0.000) [0.197]
	Outcome is asinh(NO <sub>x</sub> ) emissions		
$\kappa_1^p$	0.075 (0.039) [0.061]	0.079 (0.038) [0.046]	0.080 (0.039) [0.046]
$\kappa_2^p$	-0.104 (0.050) [0.042]	-0.143 (0.045) [0.003]	-0.157 (0.079) [0.054]
trend break $\times$ avg. emissions		-0.001 (0.000) [0.002]	-0.001 (0.001) [0.294]
trend break $\times$ avg. emissions <sup>2</sup>			0.000 (0.000) [0.793]
	Outcome is asinh(SO <sub>x</sub> ) emissions		
$\kappa_1^p$	0.006 (0.035) [0.875]	0.013 (0.035) [0.715]	0.013 (0.035) [0.705]
$\kappa_2^p$	-0.037 (0.043) [0.393]	-0.110 (0.048) [0.026]	-0.074 (0.077) [0.345]
trend break $\times$ avg. emissions		-0.004 (0.002) [0.017]	-0.002 (0.003) [0.455]
trend break $\times$ avg. emissions <sup>2</sup>			-0.000 (0.000) [0.438]

NOTES: Estimates of pre-C&T differential emissions trend (i.e.,  $\kappa_1^p$  from equation (2.1)) and and post-C&T differential emissions trend break (i.e.,  $\kappa_2^p$  from equation (2.1)) for GHG, PM<sub>2.5</sub>, PM<sub>10</sub>, NO<sub>x</sub>, and SO<sub>x</sub> across panels. Column 1 shows benchmark model. Column 2 (3) further interacts post C&T differential trend break with a linear (quadratic) function of sample average annual emissions. All models include facility-specific and year-specific dummy variables. Standard errors clustered at the county-level in parentheses, p-value in brackets.

Table B.4: Emissions effect robustness: restricting treatment spillovers

	(1)	(2)	(3)
	Benchmark	Nonattainment	Single facilities
Outcome is asinh(GHG) emissions			
$\kappa_1^p$	0.187 (0.052) [0.001]	- - -	0.210 (0.053) [0.000]
$\kappa_2^p$	-0.297 (0.077) [0.000]	- - -	-0.322 (0.078) [0.000]
Facilities	316	-	310
Observations	2,054	-	2,029
Outcome is asinh(PM <sub>2.5</sub> ) emissions			
$\kappa_1^p$	0.058 (0.043) [0.183]	0.085 (0.049) [0.092]	0.066 (0.043) [0.137]
$\kappa_2^p$	-0.097 (0.048) [0.053]	-0.119 (0.052) [0.029]	-0.101 (0.049) [0.046]
Facilities	302	260	299
Observations	1,968	1,729	1,952
Outcome is asinh(PM <sub>10</sub> ) emissions			
$\kappa_1^p$	0.083 (0.033) [0.016]	0.101 (0.034) [0.006]	0.091 (0.033) [0.008]
$\kappa_2^p$	-0.117 (0.039) [0.005]	-0.145 (0.054) [0.012]	-0.121 (0.040) [0.004]
Facilities	302	140	299
Observations	1,968	1,080	1,952
Outcome is asinh(NO <sub>x</sub> ) emissions			
$\kappa_1^p$	0.075 (0.039) [0.061]	0.057 (0.041) [0.173]	0.065 (0.039) [0.101]
$\kappa_2^p$	-0.104 (0.050) [0.042]	-0.090 (0.054) [0.102]	-0.098 (0.050) [0.060]
Facilities	303	287	300
Observations	1,970	1,879	1,954
Outcome is asinh(SO <sub>x</sub> ) emissions			
$\kappa_1^p$	0.006 (0.035) [0.875]	- - -	0.005 (0.036) [0.892]
$\kappa_2^p$	-0.037 (0.043) [0.393]	- - -	-0.036 (0.044) [0.423]
Facilities	303	-	300
Observations	1,965	-	1,950

NOTES: Estimates of pre-C&T differential emissions trend (i.e.,  $\kappa_1^p$  from equation (2.1)) and and post-C&T differential emissions trend break (i.e.,  $\kappa_2^p$  from equation (2.1)) for GHG, PM<sub>2.5</sub>, PM<sub>10</sub>, NO<sub>x</sub>, and SO<sub>x</sub> across panels. Column 1 shows benchmark model. Column 2 restricts unregulated facilities to those in counties under Clear Air Act nonattainment for pollutant of interest. Nonattainment does not apply for GHG emissions and there were no counties under SO<sub>x</sub> nonattainment during our sample period. For NO<sub>x</sub>, we use nonattainment in the one-hour ozone standard, for which NO<sub>x</sub> is a precursor pollutant. Column 3 restricts unregulated facilities to those whose parent company only operates a single facility. All models include facility-specific and year-specific dummy variables. Standard errors clustered at the county-level in parentheses, p-value in brackets.

Table B.5: Correlation between HYSPLIT-driven and ambient pollution concentrations

	(1)	(2)	(3)	(4)
	Outcome is ambient asinh(concentration)			
	PM <sub>2.5</sub>	PM <sub>10</sub>	NO <sub>x</sub>	SO <sub>x</sub>
HYSPLIT-driven asinh(concentration)	0.860 (0.154) [0.000]	0.625 (0.137) [0.000]	0.436 (0.148) [0.004]	0.231 (0.207) [0.272]
Zip codes	133	160	121	39

NOTES: Linear coefficient from zip code-level regressions of asinh daily HYSPLIT-driven pollution concentrations (in  $\mu\text{g}/\text{m}^3/\text{day}$ ) averaged across 2008-2017 on asinh daily pollution concentrations from ambient pollution monitors (in  $\mu\text{g}/\text{m}^3/\text{day}$ ) averaged across 2008-2017. We employ a asinh-asinh specification because ambient pollution readings, which capture the average daily instantaneous stock of pollution, are not directly comparable to our concentration measure, which capture average daily pollution flow from C&T-driven emissions. Ambient pollution are assumed to be uniformly distributed within a monitor's zip code. Standard errors clustered at the county-level in parentheses, p-value in brackets.

Table B.6: Pollution concentration difference between disadvantaged and other zip codes in 2008

	(1) Disadvantaged	(2) Other	(3) Difference
PM <sub>2.5</sub>	0.256 (0.888)	0.093 (0.572)	0.163 (0.038) [0.000]
PM <sub>10</sub>	0.322 (1.066)	0.109 (0.532)	0.214 (0.043) [0.000]
NO <sub>x</sub>	0.451 (2.842)	0.387 (6.856)	0.064 (0.243) [0.792]
SO <sub>x</sub>	0.364 (1.092)	0.091 (0.217)	0.273 (0.041) [0.000]
Zip codes	722	984	1,706

NOTES: Column 1 shows average 2008 pollution concentration ( $\mu\text{g}/\text{m}^3/\text{day}$ ) across disadvantaged zip codes, with standard deviation in parentheses. Column 2 shows average 2008 pollution concentration ( $\mu\text{g}/\text{m}^3/\text{day}$ ) across other zip codes, with standard deviation in parentheses. Column 3 shows the average difference in 2008 pollution concentrations between disadvantaged and other zip codes, with standard error in parentheses and p-value in brackets. All pollution concentrations generated by HYSPLIT from facilities that would eventually be regulated by the GHG C&T program.

Table B.7: EJ gap effect robustness: step 1

	(1) Year-specific effects	(2) Sector-year FEs	(3) Drop switchers	(4) GHG cutoff: 70%	(5) GHG cutoff: 80%	(6) Hetero by avg. emissions	(7) SUTVA NA	(8) SUTVA Single fac.
Panel a: PM <sub>2.5</sub>								
$\beta_1^p$	0.040 (0.011) [0.001]	0.041 (0.011) [0.001]	0.040 (0.013) [0.003]	0.025 (0.006) [0.000]	0.043 (0.010) [0.000]	0.041 (0.012) [0.001]	0.048 (0.012) [0.000]	0.043 (0.012) [0.000]
$\beta_2^p$	-0.061 (0.019) [0.003]	-0.061 (0.019) [0.002]	-0.058 (0.021) [0.007]	-0.031 (0.008) [0.000]	-0.063 (0.019) [0.001]	-0.075 (0.021) [0.001]	-0.067 (0.021) [0.002]	-0.064 (0.020) [0.002]
$(\beta_2^p/\beta_1^p) * 100$	-152.583	-148.723	-144.528	-125.385	-146.581	-182.096	-141.543	-146.262
Observations	16,416	16,416	16,413	16,387	16,426	16,416	16,416	16,416
Panel b: PM <sub>10</sub>								
$\beta_1^p$	0.062 (0.014) [0.000]	0.063 (0.014) [0.000]	0.059 (0.017) [0.001]	0.038 (0.008) [0.000]	0.069 (0.013) [0.000]	0.064 (0.014) [0.000]	0.074 (0.016) [0.000]	0.066 (0.015) [0.000]
$\beta_2^p$	-0.089 (0.027) [0.002]	-0.089 (0.026) [0.001]	-0.079 (0.028) [0.007]	-0.046 (0.009) [0.000]	-0.093 (0.026) [0.001]	-0.100 (0.028) [0.001]	-0.105 (0.030) [0.001]	-0.091 (0.028) [0.002]
$(\beta_2^p/\beta_1^p) * 100$	-142.447	-140.455	-134.110	-121.310	-134.948	-156.155	-141.932	-136.905
Observations	16,416	16,416	16,413	16,387	16,426	16,416	16,416	16,416
Panel c: NO <sub>x</sub>								
$\beta_1^p$	0.079 (0.033) [0.019]	0.091 (0.037) [0.015]	0.077 (0.032) [0.021]	0.043 (0.026) [0.108]	0.087 (0.031) [0.006]	0.079 (0.033) [0.021]	0.079 (0.032) [0.018]	0.082 (0.034) [0.018]
$\beta_2^p$	-0.132 (0.066) [0.051]	-0.145 (0.070) [0.043]	-0.132 (0.069) [0.061]	-0.055 (0.031) [0.084]	-0.149 (0.069) [0.035]	-0.142 (0.075) [0.062]	-0.138 (0.070) [0.052]	-0.141 (0.071) [0.053]
$(\beta_2^p/\beta_1^p) * 100$	-167.212	-158.315	-170.919	-128.157	-170.878	-180.760	-175.096	-172.408
Observations	16,416	16,416	16,413	16,387	16,426	16,416	16,416	16,416
Panel d: SO <sub>x</sub>								
$\beta_1^p$	0.036 (0.022) [0.108]	0.036 (0.022) [0.109]	0.038 (0.023) [0.104]	0.023 (0.015) [0.141]	0.037 (0.020) [0.077]	0.011 (0.012) [0.349]	- - -	0.037 (0.023) [0.108]
$\beta_2^p$	-0.103 (0.050) [0.045]	-0.099 (0.049) [0.047]	-0.102 (0.050) [0.046]	-0.080 (0.045) [0.084]	-0.099 (0.046) [0.037]	-0.114 (0.058) [0.054]	- - -	-0.100 (0.049) [0.047]
$(\beta_2^p/\beta_1^p) * 100$	-284.826	-275.129	-268.202	-353.380	-267.896	-1003.707	-	-272.630
Observations	16,416	16,416	16,413	16,387	16,426	16,416	-	16,416

NOTES: Estimates of the pre-C&T EJ gap trend (i.e.,  $\beta_1^p$  from equation (2.2)), post-C&T EJ gap trend break (i.e.,  $\beta_2^p$  from equation (2.2)), and the percentage change in the EJ gap trend following the introduction of the C&T program (i.e.,  $\frac{\beta_2^p}{\beta_1^p} * 100$ ) for PM<sub>2.5</sub>, PM<sub>10</sub>, NO<sub>x</sub>, and SO<sub>x</sub> down panels. All models include zip code-specific and year-specific dummy variables. Observations weighted by zip code-level average population during 2008-2012. Column 1 uses year-specific effects to estimate C&T-driven emissions. Column 2 estimates C&T-driven emissions with sector-by-year fixed effects (see column 1 of Table B.2). Column 3 estimates C&T-driven emissions after dropping facilities that switched regulatory status in 2017 (see column 2 of Table B.2). Columns 4 and 5 restrict facilities to those with sample average GHG emissions below the 70th and 80th percentile, respectively to estimate C&T-driven emissions (see columns 3 and 5 of Table B.2). Column 6 uses C&T-driven emissions that allow the C&T differential trend break to vary as a linear function of sample average emissions (see column 2 of Table B.3). Column 7 restricts unregulated facilities to those in counties under Clear Air Act nonattainment for pollutant of interest (see column 2 of Table B.4). Column 8 restricts unregulated facilities to those whose parent company only operates a single facility (see column 3 of Table B.4). Standard errors, in parentheses, cluster  $e_{it}^p$  from equation (2.2) at the county-level but are not adjusted for statistical uncertainty from equation (2.1). P-value in brackets. Observations apply to all panels.

Table B.8: EJ gap effect robustness: steps 2 and 3

	(1) Slower decay	(2) Faster decay	(3) Lower boundary	(4) Higher boundary	(5) Spatial corr. err.	(6) Pollution corr. err.
Panel a: PM <sub>2.5</sub>						
$\beta_1^p$	0.043 (0.011) [0.000]	0.041 (0.011) [0.000]	0.037 (0.010) [0.001]	0.043 (0.011) [0.000]	0.042 (0.004) [0.000]	0.042 (0.006) [0.000]
$\beta_2^p$	-0.064 (0.020) [0.002]	-0.062 (0.020) [0.003]	-0.055 (0.019) [0.007]	-0.064 (0.020) [0.002]	-0.063 (0.009) [0.000]	-0.063 (0.010) [0.000]
$(\beta_2^p/\beta_1^p) * 100$	-149.007	-150.533	-148.764	-149.992	-149.699	-149.699
Panel b: PM <sub>10</sub>						
$\beta_1^p$	0.066 (0.015) [0.000]	0.063 (0.014) [0.000]	0.057 (0.013) [0.000]	0.066 (0.014) [0.000]	0.065 (0.006) [0.000]	0.065 (0.008) [0.000]
$\beta_2^p$	-0.092 (0.027) [0.001]	-0.089 (0.027) [0.002]	-0.079 (0.027) [0.005]	-0.092 (0.027) [0.001]	-0.090 (0.011) [0.000]	-0.090 (0.013) [0.000]
$(\beta_2^p/\beta_1^p) * 100$	-139.150	-140.448	-137.785	-140.161	-139.739	-139.739
Panel c: NO <sub>x</sub>						
$\beta_1^p$	0.089 (0.036) [0.018]	0.081 (0.034) [0.020]	0.083 (0.035) [0.020]	0.085 (0.035) [0.018]	0.085 (0.039) [0.030]	0.085 (0.021) [0.000]
$\beta_2^p$	-0.148 (0.073) [0.048]	-0.139 (0.073) [0.063]	-0.140 (0.073) [0.060]	-0.144 (0.073) [0.054]	-0.143 (0.050) [0.004]	-0.143 (0.033) [0.000]
$(\beta_2^p/\beta_1^p) * 100$	-166.117	-170.804	-168.674	-168.261	-168.282	-168.282
Panel d: SO <sub>x</sub>						
$\beta_1^p$	0.037 (0.023) [0.109]	0.037 (0.022) [0.107]	0.030 (0.019) [0.133]	0.038 (0.023) [0.103]	0.037 (0.007) [0.000]	0.037 (0.006) [0.000]
$\beta_2^p$	-0.102 (0.050) [0.047]	-0.100 (0.049) [0.047]	-0.087 (0.044) [0.053]	-0.102 (0.050) [0.045]	-0.101 (0.012) [0.000]	-0.101 (0.010) [0.000]
$(\beta_2^p/\beta_1^p) * 100$	-271.967	-272.688	-295.166	-270.107	-272.291	-272.291
Observations	16,416	16,416	16,359	16,430	16,417	16,417

NOTES: Estimates of the pre-C&T EJ gap trend (i.e.,  $\beta_1^p$  from equation (2.2)), post-C&T EJ gap trend break (i.e.,  $\beta_2^p$  from equation (2.2)), and the percentage change in the EJ gap trend following the introduction of the C&T program (i.e.,  $\frac{\beta_2^p}{\beta_1^p} * 100$ ) for PM<sub>2.5</sub>, PM<sub>10</sub>, NO<sub>x</sub>, and SO<sub>x</sub> down panels. All models include zip code-specific and year-specific dummy variables. Observations weighted by zip code-level average population during 2008-2012. Column 1 applies a slower pollution decay to HYSPLIT pollution trajectories (i.e., 10% larger half-life parameter). Column 2 applies a faster pollution decay to HYSPLIT pollution trajectories (i.e., 10% smaller half-life parameter). Column 3 applies a lower planetary boundary layer set at 0.5 km. Column 4 applies a higher planetary boundary layer set at 2 km. Column 5 adjusts standard errors for spatial (500 km uniform kernel) and serial correlation (5 years). Column 6 adjusts standard errors allowing correlation across pollutants using a Seemingly Unrelated Regression (SUR) procedure. Standard errors, in parentheses, cluster  $\epsilon_{it}^p$  from equation (2.2) at the county-level but are not adjusted for statistical uncertainty from equation (2.1). P-value in brackets. Observations apply to all panels.

Table B.9: EJ gap effect robustness: asinh concentration

	(1)	(2)	(3)	(4)
	Outcome is (asinh) concentration			
	PM <sub>2.5</sub>	PM <sub>10</sub>	NO <sub>x</sub>	SO <sub>x</sub>
$\beta_1^p$	0.027 (0.013) [0.045]	0.037 (0.014) [0.009]	0.032 (0.021) [0.137]	0.017 (0.017) [0.336]
$\beta_2^p$	-0.032 (0.014) [0.026]	-0.042 (0.015) [0.009]	-0.038 (0.023) [0.102]	-0.051 (0.030) [0.095]
$\beta_1^p + \beta_2^p$	-0.006 (0.005) [0.302]	-0.004 (0.007) [0.551]	-0.005 (0.008) [0.487]	-0.034 (0.015) [0.029]
Zip codes	1649	1649	1649	1649
Counties	58	58	58	58
Observations	16,416	16,416	16,416	16,416

NOTES: Estimates of the pre-C&T EJ gap trend (i.e.,  $\beta_1^p$  from equation (2.2)), the post-C&T EJ gap trend break (i.e.,  $\beta_2^p$  from equation (2.2)), and the post-C&T EJ gap trend (i.e.,  $\beta_1^p + \beta_2^p$ ) for asinh(PM<sub>2.5</sub>), asinh(PM<sub>10</sub>), asinh(NO<sub>x</sub>), and asinh(SO<sub>x</sub>), across columns. All models include zip code-specific and year-specific dummy variables. Observations weighted by zip code-level average population during 2008-2012. Parentheses indicate standard errors that account for statistical uncertainty in C&T predicted emissions ( $\nu_{it}^p$  from equation (2.1) via the bootstrap procedure in Appendix B.1.1) and county-level heterogeneity in EJ gap effects of arbitrary form ( $\epsilon_{it}^p$  from equation (2.2)). P-value in brackets.

Table B.10: EJ gap effect robustness: total PM<sub>2.5</sub> concentration using InMAP

	(1)	(2)
	Primary PM <sub>2.5</sub>	Total PM <sub>2.5</sub>
$\beta_1^p$	0.002 (0.001) [0.001]	0.003 (0.001) [0.001]
$\beta_2^p$	-0.003 (0.001) [0.000]	-0.004 (0.001) [0.000]
$\beta_1^p + \beta_2^p$	-0.001 (0.000) [0.004]	-0.002 (0.001) [0.001]
$(\beta_2^p/\beta_1^p) * 100$	-150.559 (16.261) [0.000]	-172.948 (16.415) [0.000]
Zip codes	1648	1648
Counties	58	58
Observations	16,480	16,480

NOTES: Estimates of the pre-C&T EJ gap trend (i.e.,  $\beta_1^p$  from equation (2.2)), the post-C&T EJ gap trend break (i.e.,  $\beta_2^p$  from equation (2.2)), the post-C&T EJ gap trend (i.e.,  $\beta_1^p + \beta_2^p$ ), and the percentage change in the EJ gap trend following the introduction of the C&T program (i.e.,  $\frac{\beta_2^p}{\beta_1^p} * 100$ ) for InMAP-modeled primary PM<sub>2.5</sub> concentration (column 1) and for InMAP-modeled total (i.e., primary and secondary) PM<sub>2.5</sub> concentration (column 2). InMAP employs dispersal patterns for 2005 and not for the 2008-2017 sample period. All models include zip code-specific and year-specific dummy variables. Observations weighted by zip code-level average population during 2008-2012. Standard errors, in parentheses, cluster  $\epsilon_{it}^p$  from equation (2.2) at the county-level but are not adjusted for statistical uncertainty from equation (2.1). P-value in brackets.



Table B.11: Importance of modeling pollution dispersal

	(1)	(2)	(3)	(4)
	Facility zip code	1.6 km circle	4 km circle	10 km circle
	Panel a: PM <sub>2.5</sub>			
$\beta_1^p$	0.052 (0.036) [0.157]	-0.017 (0.026) [0.527]	-0.075 (0.040) [0.075]	-0.140 (0.079) [0.084]
$\beta_2^p$	-0.076 (0.049) [0.134]	-0.003 (0.023) [0.912]	0.067 (0.036) [0.075]	0.132 (0.072) [0.076]
Observations	785	1,831	3,573	7,545
	Panel b: PM <sub>10</sub>			
$\beta_1^p$	0.105 (0.070) [0.142]	0.020 (0.030) [0.509]	-0.069 (0.047) [0.155]	-0.143 (0.089) [0.116]
$\beta_2^p$	-0.142 (0.091) [0.132]	-0.049 (0.036) [0.177]	0.059 (0.055) [0.294]	0.137 (0.095) [0.157]
Observations	785	1,831	3,573	7,545
	Panel c: NO <sub>x</sub>			
$\beta_1^p$	0.163 (0.188) [0.391]	-0.120 (0.110) [0.285]	-0.292 (0.096) [0.005]	-0.417 (0.175) [0.022]
$\beta_2^p$	-0.213 (0.247) [0.396]	0.103 (0.132) [0.442]	0.311 (0.110) [0.008]	0.480 (0.179) [0.011]
Observations	785	1,831	3,573	7,545
	Panel d: SO <sub>x</sub>			
$\beta_1^p$	0.001 (0.004) [0.688]	-0.156 (0.122) [0.210]	-0.273 (0.183) [0.145]	-0.433 (0.250) [0.091]
$\beta_2^p$	-0.014 (0.009) [0.125]	-0.007 (0.030) [0.813]	0.128 (0.103) [0.223]	0.253 (0.143) [0.085]
Observations	783	1,823	3,553	7,535

NOTES: Estimates of the pre-C&T EJ gap trend (i.e.,  $\beta_1^p$  from equation (2.2)) and the post-C&T EJ gap trend break (i.e.,  $\beta_2^p$  from equation (2.2)) for PM<sub>2.5</sub>, PM<sub>10</sub>, NO<sub>x</sub>, and SO<sub>x</sub> down panels. All models include zip code-specific and year-specific dummy variables. Observations weighted by zip code-level average population during 2008-2012. Column 1 assigns pollution concentration to only the zip code of the emitting facility. Columns 2-4 assign pollution concentration to zip codes with centroid within a 1.6, 4 km and 10 km circle of emitting facility, respectively. Standard errors in parentheses cluster  $\epsilon_{it}^p$  from equation (2.2) at the county-level but are not adjusted for statistical uncertainty from equation (2.1). P-value in brackets.

# Bibliography

- [1] M. Gibson, *Regulation-induced pollution substitution*, *Review of Economics and Statistics* (2018), no. 0.
- [2] M. Fowlie, *Incomplete environmental regulation, imperfect competition, and emissions leakage*, *American Economic Journal: Economic Policy* **1** (2009), no. 2 72–112.
- [3] M. Fowlie and M. Reguant, *Mitigating emissions leakage in incomplete carbon markets*, .
- [4] M. A. Rangel and T. S. Vogl, *Agricultural fires and health at birth*, *Review of Economics and Statistics* **101** (2019), no. 4 616–630.
- [5] J. Graff Zivin and M. Neidell, *Environment, health, and human capital*, *Journal of Economic Literature* **51** (2013), no. 3 689–730.
- [6] J. Currie, J. G. Zivin, J. Mullins, and M. Neidell, *What do we know about short-and long-term effects of early-life exposure to pollution?*, *Annu. Rev. Resour. Econ.* **6** (2014), no. 1 217–247.
- [7] M. A. Rangel and T. S. Vogl, *Agricultural fires and health at birth*, *Review of Economics and Statistics* (2018), no. 0.
- [8] K. Baylis, D. Fullerton, and D. H. Karney, *Negative leakage*, *Journal of the Association of Environmental and Resource Economists* **1** (2014), no. 1/2 51–73.
- [9] C. Hansman, J. Hjort, and G. León, *Interlinked firms and the consequences of piecemeal regulation*, *Journal of the European Economic Association* **17** (2019), no. 3 876–916.
- [10] B. Rijal and N. Khanna, *High priority violations and intra-firm pollution substitution*, *Journal of Environmental Economics and Management* (2020) 102359.
- [11] R. Hanna, *Us environmental regulation and fdi: Evidence from a panel of US-based multinational firms*, *American Economic Journal: Applied Economics* **2** (2010), no. 3 158–89.

- [12] I. Ben-David, S. Kleimeier, and M. Viehs, *Exporting pollution*, tech. rep., National Bureau of Economic Research, 2018.
- [13] J. S. Shortle and R. D. Horan, *The economics of nonpoint pollution control*, *Journal of economic surveys* **15** (2001), no. 3 255–289.
- [14] P. Carrillo, D. Pomeranz, and M. Singhal, *Dodging the taxman: Firm misreporting and limits to tax enforcement*, *American Economic Journal: Applied Economics* **9** (2017), no. 2 144–64.
- [15] D. Yang, *Can enforcement backfire? Crime displacement in the context of customs reform in the Philippines*, *The Review of Economics and Statistics* **90** (2008), no. 1 1–14.
- [16] P. Mohai, D. Pellow, and J. T. Roberts, *Environmental justice*, *Annual review of environment and resources* **34** (2009) 405–430.
- [17] R. D. Bullard, *Dumping in Dixie: Race, class, and environmental quality*. Avalon Publishing-(Westview Press), 2008.
- [18] R. Morello-Frosch, *Separate but unequal? residential segregation and air quality in us metropolitan areas*, *Epidemiology* **15** (2004), no. 4 S134.
- [19] S. Banzhaf, L. Ma, and C. Timmins, *Environmental justice: The economics of race, place, and pollution*, *Journal of Economic Perspectives* **33** (2019), no. 1 185–208.
- [20] M. Pastor, J. Sadd, and J. Hipp, *Which came first? Toxic facilities, minority move-in, and environmental justice*, *Journal of urban affairs* **23** (2001), no. 1 1–21.
- [21] R. Bullard and B. H. Wright, *Environmentalism and the politics of equity: emergent trends in the black community*, *Mid-American Review of Sociology* **12** (1987), no. 2 21–37.
- [22] D. Fullerton and E. Muehlegger, *Who bears the economic burdens of environmental regulations?*, *Review of Environmental Economics and Policy* **13** (2019), no. 1 62–82.
- [23] S. Hsiang, P. Oliva, and R. Walker, *The distribution of environmental damages*, *Review of Environmental Economics and Policy* **13** (2019), no. 1 83–103.
- [24] S. P. Holland, E. T. Mansur, N. Z. Muller, and A. J. Yates, *Distributional effects of air pollution from electric vehicle adoption*, *Journal of the Association of Environmental and Resource Economists* **6** (2019), no. S1 S65–S94.

- [25] J. Currie, J. Voorheis, and R. Walker, *What caused racial disparities in particulate exposure to fall? New evidence from the Clean Air Act and satellite-based measures of air quality*, tech. rep., National Bureau of Economic Research, 2020.
- [26] L. Chakraborti, *Environmental justice and toxic releases in urban Mexico*, .
- [27] L. Chakraborti and J. P. Shimshack, *Environmental disparities in the global south: Evidence from toxic water pollution in urban Mexico*, .
- [28] C. Hausman and S. Stolper, *Inequality, information failures, and air pollution*, tech. rep., National Bureau of Economic Research, 2020.
- [29] J. von der Goltz and P. Barnwal, *Mines: The local wealth and health effects of mineral mining in developing countries*, *Journal of Development Economics* **139** (2019) 1–16.
- [30] R. Heilmayr, K. M. Carlson, and J. J. Benedict, *Deforestation spillovers from oil palm sustainability certification*, *Environmental Research Letters* **15** (2020), no. 7 075002.
- [31] M. Dell and B. A. Olken, *The development effects of the extractive colonial economy: The dutch cultivation system in java*, *The Review of Economic Studies* **87** (2020), no. 1 164–203.
- [32] D. d. A. França, K. M. Longo, T. G. S. Neto, J. C. Santos, S. R. Freitas, B. F. Rudorff, E. V. Cortez, E. Anselmo, and J. A. Carvalho, *Pre-harvest sugarcane burning: Determination of emission factors through laboratory measurements*, *Atmosphere* **3** (2012), no. 1 164–180.
- [33] S. Jayachandran, *Air quality and early-life mortality evidence from Indonesia’s wildfires*, *Journal of Human resources* **44** (2009), no. 4 916–954.
- [34] H. Pullabhotla, *Fires, wind, and smoke: Air pollution and infant mortality*, *Job Market Paper*. Available here (2018).
- [35] J. Graff-Zivin, T. Liu, Y. Song, Q. Tang, and P. Zhang, *The unintended impacts of agricultural fires: Human capital in China*, *Journal of Development Economics* **147** (2020) 102560.
- [36] G. He, T. Liu, and M. Zhou, *Straw burning, PM<sub>2.5</sub>, and death: Evidence from China*, *Journal of Development Economics* (2020) 102468.
- [37] F. Campos Ortiz and M. Oviedo Pacheco, *Extensión de los predios agrícolas y productividad. El caso del campo cañero en México*, *El trimestre económico* **82** (2015), no. 325 147–181.

- [38] V. Buchard, A. da Silva, C. Randles, P. Colarco, R. Ferrare, J. Hair, C. Hostetler, J. Tackett, and D. Winker, *Evaluation of the surface PM<sub>2.5</sub> in Version 1 of the NASA MERRA aerosol reanalysis over the United States*, *Atmospheric environment* **125** (2016) 100–111.
- [39] S. Chen, P. Oliva, and P. Zhang, *The effect of air pollution on migration: evidence from China*, tech. rep., National Bureau of Economic Research, 2017.
- [40] M. S. Hammer, A. van Donkelaar, C. Li, A. Lyapustin, A. M. Sayer, N. C. Hsu, R. C. Levy, M. Garay, O. Kalashnikova, R. A. Kahn, *et. al.*, *Global estimates and long-term trends of fine particulate matter concentrations (1998-2018)*, *Environmental Science & Technology* (2020).
- [41] M. Fowlie, E. Rubin, and R. Walker, *Bringing satellite-based air quality estimates down to earth*, in *AEA Papers and Proceedings*, vol. 109, pp. 283–88, 2019.
- [42] J. Currie, M. Neidell, and J. F. Schmieder, *Air pollution and infant health: Lessons from New Jersey*, *Journal of health economics* **28** (2009), no. 3 688–703.
- [43] A. C. Cameron, J. B. Gelbach, and D. L. Miller, *Robust inference with multiway clustering*, *Journal of Business & Economic Statistics* (2012).
- [44] K. Y. Chay and M. Greenstone, *The impact of air pollution on infant mortality: Evidence from geographic variation in pollution shocks induced by a recession*, *The quarterly journal of economics* **118** (2003), no. 3 1121–1167.
- [45] T. Deryugina, G. Heutel, N. H. Miller, D. Molitor, and J. Reif, *The mortality and medical costs of air pollution: Evidence from changes in wind direction*, *American Economic Review* **109** (2019), no. 12 4178–4219.
- [46] E. Arceo, R. Hanna, and P. Oliva, *Does the effect of pollution on infant mortality differ between developing and developed countries? Evidence from Mexico City*, *The Economic Journal* **126** (2016), no. 591 257–280.
- [47] M. Fowlie, S. P. Holland, and E. T. Mansur, *What do emissions markets deliver and to whom? Evidence from Southern California’s NO<sub>x</sub> trading program*, *American Economic Review* **102** (2012), no. 2 965–93.
- [48] C. Grainger and T. Ruangmas, *Who wins from emissions trading? Evidence from California*, *Environmental and resource economics* **71** (2018), no. 3 703–727.
- [49] D. Hernandez-Cortes and K. C. Meng, *Do environmental markets cause environmental injustice?*, tech. rep., mimeo, 2020.
- [50] M. Ash and J. K. Boyce, *Racial disparities in pollution exposure and employment at us industrial facilities*, *Proceedings of the National Academy of Sciences* **115** (2018), no. 42 10636–10641.

- [51] T. Garg, M. Jagnani, and H. Pullabhotla, *Agricultural labor exits increase crop fires*, .
- [52] O. Deschênes, M. Greenstone, and J. S. Shapiro, *Defensive investments and the demand for air quality: Evidence from the NOx budget program*, *American Economic Review* **107** (2017), no. 10 2958–89.
- [53] R. Schmalensee and R. N. Stavins, *Policy evolution under the clean air act*, *Journal of Economic Perspectives* **33** (November, 2019) 27–50.
- [54] C. Costello, D. Ovando, T. Clavelle, C. K. Strauss, R. Hilborn, M. C. Melnychuk, T. A. Branch, S. D. Gaines, C. S. Szuwalski, R. B. Cabral, D. N. Rader, and A. Leland, *Global Fishery Prospects under Contrasting Management Regimes*, *Proceedings of the National Academy of Sciences* **113** (2016), no. 18 5125–5129.
- [55] J. Salzman, G. Bennett, N. Carroll, A. Goldstein, and M. Jenkins, *The Global Status and Trends of Payments for Ecosystem Services*, *Nature Sustainability* **1** (2018), no. 3 136–144.
- [56] World Bank Group, *State and Trends of Carbon Pricing*, .
- [57] T. Crocker, *The structuring of atmospheric pollution control systems. the economics of air pollution*, *The economics of air pollution*. New York, WW Norton & Co (1966) 61–86.
- [58] J. H. Dales, *Pollution, Property and Prices: An Essay in Policy*. Toronto: University of Toronto Press, 1968.
- [59] W. D. Montgomery, *Markets in Licenses and Efficient Pollution Control Programs*, *Journal of Economic Theory* **5** (1972), no. 3 395 – 418.
- [60] R. Bullard, *Dumping in Dixie: Race, Class, and Environmental Quality*. Westview Press, 2000.
- [61] W. Bowen, *An Analytical Review of Environmental Justice Research: What do we Really Know?*, *Environmental Management* **29** (2002), no. 1 3–15.
- [62] E. J. Ringquist, *Assessing Evidence of Environmental Inequities: A Meta-analysis*, *Journal of Policy Analysis and Management* **24** (2005), no. 2 223–247.
- [63] P. Mohai, D. Pellow, and J. T. Roberts, *Environmental Justice*, *Annual Review of Environment and Resources* **34** (2009), no. 1 405–430.
- [64] S. Banzhaf, L. Ma, and C. Timmins, *Environmental Justice: The Economics of Race, Place, and Pollution*, *Journal of Economic Perspectives* **33** (February, 2019) 185–208.

- [65] C. W. Tessum, J. S. Apte, A. L. Goodkind, N. Z. Muller, K. A. Mullins, D. A. Paoletta, S. Polasky, N. P. Springer, S. K. Thakrar, J. D. Marshall, and J. D. Hill, *Inequity in consumption of goods and services adds to racial–ethnic disparities in air pollution exposure*, *Proceedings of the National Academy of Sciences* **116** (2019), no. 13 6001–6006, [<https://www.pnas.org/content/116/13/6001.full.pdf>].
- [66] J. Colmer, R. Martin, M. Muûls, U. J. Wagner, *et. al.*, *Does pricing carbon mitigate climate change? firm-level evidence from the european union emissions trading scheme*, *Center for Economic Performance Discussion Paper* (2020), no. 1728.
- [67] J. Currie, J. Voorheis, and R. Walker, *What caused racial disparities in particulate exposure to fall? new evidence from the clean air act and satellite-based measures of air quality*, Working Paper 26659, National Bureau of Economic Research, January, 2020.
- [68] D. Burtraw, D. A. Evans, A. Krupnick, K. Palmer, and R. Toth, *Economics of pollution trading for so2 and no x*, *Annu. Rev. Environ. Resour.* **30** (2005) 253–289.
- [69] M. Fowlie, S. P. Holland, and E. T. Mansur, *What Do Emissions Markets Deliver and to Whom? Evidence from Southern California’s NO<sub>x</sub> Trading Program*, *American Economic Review* **102** (2012), no. 2 965–93.
- [70] C. Grainger and T. Ruangmas, *Who Wins from Emissions Trading? Evidence from California*, *Environmental and Resource Economics* **71** (Nov, 2018) 703–727.
- [71] J. S. Shapiro and R. Walker, *Where is pollution moving? environmental markets and environmental justice*, Working Paper 28389, National Bureau of Economic Research, January, 2021.
- [72] R. Leber, *The most Dramatic Climate Fight of the Election is in Washington State*, *Grist* (2016).
- [73] E. Herron, *Oregon Clean Energy Jobs Bill Has Mixed Support From Environmental Justice Groups*, *Willamette Week* (2019).
- [74] Transnational Institute, *It is Time to Scrap the ETS!* , .
- [75] S. Petrick and U. J. Wagner, *The impact of carbon trading on industry: Evidence from german manufacturing firms*, Available at SSRN 2389800 (2014).
- [76] R. Martin, M. Muûls, and U. J. Wagner, *The impact of the european union emissions trading scheme on regulated firms: what is the evidence after ten years?*, *Review of environmental economics and policy* **10** (2016), no. 1 129–148.

- [77] D. Burtraw, A. Carlson, D. Cullenward, Q. Foster, and M. Fowlie, *2018 annual report of the independent emissions market advisory committee*, 2018.
- [78] S. Borenstein, J. Bushnell, F. A. Wolak, and M. Zaragoza-Watkins, *Expecting the unexpected: Emissions uncertainty and environmental market design*, *American Economic Review* **109** (November, 2019) 3953–77.
- [79] W. J. Baumol and W. E. Oates, *The Theory of Environmental Policy, Second Edition*. Cambridge University Press, 1988.
- [80] O. Deschenes and K. C. Meng, *Quasi-experimental Methods in Environmental Economics: Challenges and Opportunities*, *Handbook of Environmental Economics* **4** (2018) 285.
- [81] D. M. Sullivan, *The True Cost of Air Pollution: Evidence from the Housing Market*, *mimeo* (2017).
- [82] M. Greenstone and T. Gayer, *Quasi-experimental and experimental approaches to environmental economics*, *Journal of Environmental Economics and Management* **57** (2009), no. 1 21 – 44. *Frontiers of Environmental and Resource Economics*.
- [83] J. Graff Zivin and M. Neidell, *Environment, health, and human capital*, *Journal of Economic Literature* **51** (2013), no. 3 689–730.
- [84] J. H. Dale, *Pollution, property, and prices: An essay in policy-making*, .
- [85] E. T. Mansur and G. Sheriff, *Do Pollution Markets Harm Low Income and Minority Communities? Ranking Emissions Distributions Generated by California’s RECLAIM Program*, Working Paper 25666, National Bureau of Economic Research, March, 2019.
- [86] M. F. Bellemare and C. J. Wichman, *Elasticities and the inverse hyperbolic sine transformation*, *Oxford Bulletin of Economics and Statistics* **82** (2020), no. 1 50–61.
- [87] L. Davis and C. Hausman, *Market Impacts of a Nuclear Power Plant Closure*, *American Economic Journal: Applied Economics* **8** (April, 2016) 92–122.
- [88] R. R. Draxler and G. Hess, *An Overview of the HYSPLIT<sub>4</sub> Modelling System for Trajectories*, *Australian Meteorological Magazine* **47** (1998), no. 4 295–308.
- [89] L. R. Henneman, L. J. Mickley, and C. M. Zigler, *Air pollution accountability of energy transitions: the relative importance of point source emissions and wind fields in exposure changes*, *Environmental Research Letters* **14** (2019), no. 11 115003.



- [90] J. A. Casey, J. G. Su, L. R. Henneman, C. Zigler, A. M. Neophytou, R. Catalano, R. Gondalia, Y.-T. Chen, L. Kaye, S. S. Moyer, *et. al.*, *Improved asthma outcomes observed in the vicinity of coal power plant retirement, retrofit and conversion to natural gas*, *Nature Energy* **5** (2020), no. 5 398–408.
- [91] U. EPA, *Revision to the Guideline on Air Quality Models: Enhancements to the AERMOD Dispersion Modeling System and Incorporation of Approaches to Address Ozone and Fine Particulate Matter*, Working Paper 2060-AS54, US Environmental Protection Agency, 2015.
- [92] L. R. Henneman, C. Choirat, C. E. Ivey, K. Cummiskey, and C. M. Zigler, *Characterizing population exposure to coal emissions sources in the united states using the hyads model*, *Atmospheric Environment* **203** (2019), no. 203 271–280.
- [93] U.S. EPA, *User’s Guide for the AMS/EPA Regulatory Model AERMOD*, .
- [94] F. Liu, S. Beirle, Q. Zhang, S. Dörner, K. He, and T. Wagner, *NO<sub>x</sub> Lifetimes and Emissions of Cities and Power Plants in Polluted Background Estimated by Satellite Observations*, *Atmospheric Chemistry and Physics* **16** (2016), no. 8 5283–5298.
- [95] C. Lee, R. V. Martin, A. van Donkelaar, H. Lee, R. R. Dickerson, J. C. Hains, N. Krotkov, A. Richter, K. Vinnikov, and J. J. Schwab, *SO<sub>2</sub> Emissions and Lifetimes: Estimates from Inverse Modeling using in situ and global, space-based (SCIAMACHY and OMI) Observations*, *Journal of Geophysical Research: Atmospheres* **116** (2011), no. D6.
- [96] D. A. Rahn and C. J. Mitchell, *Diurnal Climatology of the Boundary Layer in Southern California Using AMDAR Temperature and Wind Profiles*, *Journal of Applied Meteorology and Climatology* **55** (2016), no. 5 1123–1137.
- [97] L. R. Henneman, C. Choirat, and C. M. Zigler, *Accountability assessment of health improvements in the united states associated with reduced coal emissions between 2005 and 2012*, *Epidemiology* **30** (2019), no. 4 477–485.
- [98] C. W. Tessum, J. D. Hill, and J. D. Marshall, *Inmap: A model for air pollution interventions*, *PLOS ONE* **12** (04, 2017) 1–26.
- [99] M. Ash and T. R. Fetter, *Who Lives on the Wrong Side of the Environmental Tracks? Evidence from the EPA’s Risk-Screening Environmental Indicators Model*, *Social Science Quarterly* **85** (2004), no. 2 441–462.
- [100] R. Morello-Frosch and B. M. Jesdale, *Separate and Unequal: Residential Segregation and Estimated Cancer Risks Associated with Ambient Air Toxics in US Metropolitan Areas*, *Environmental Health Perspectives* **114** (2006), no. 3 386.

- [101] K. Cummiskey, C. Kim, C. Choirat, L. R. F. Henneman, J. Schwartz, and C. Zigler, *A source-oriented approach to coal power plant emissions health effects*, 2019.
- [102] C. Kim, L. R. Henneman, C. Choirat, and C. M. Zigler, *Health effects of power plant emissions through ambient air quality*, *Journal of the Royal Statistical Society: Series A (Statistics in Society)* (2020).
- [103] C. A. R. Board, *California Greenhouse Gas Emissions for 2000 to 2018: Trends of Emissions and Other Indicators*, tech. rep., 2020.
- [104] L. Cushing, D. Blaustein-Rejto, M. Wander, M. Pastor, J. Sadd, A. Zhu, and R. Morello-Frosch, *Carbon Trading, Co-pollutants, and Environmental Equity: Evidence from California’s cap-and-trade program (2011–2015)*, *PLoS medicine* **15** (2018), no. 7 e1002604.
- [105] T. G. Conley, *GMM Estimation with Cross Sectional Dependence*, *Journal of Econometrics* **92** (Jan, 1999) 1–45.
- [106] W. K. Newey and K. D. West, *A Simple, Positive Semi-Definite, Heteroskedasticity and Autocorrelation Consistent Covariance Matrix*, *Econometrica* **55** (1987), no. 3 703–708.
- [107] B. Depro, C. Timmins, and M. O’Neil, *White flight and coming to the nuisance: Can residential mobility explain environmental injustice?*, *Journal of the Association of Environmental and Resource Economists* **2** (2015), no. 3 439–468, [<https://doi.org/10.1086/682716>].
- [108] P. Weber, *Dynamic response to carbon pricing in the electricity sector*, tech. rep., mimeo, 2020.
- [109] M. Fowlie, R. Walker, and D. Wooley, *Climate policy, environmental justice, and local air pollution*, tech. rep., Brookings Economic Studies, 2020.
- [110] IPCC, *Summary for policymakers. in: Global warming of 1.5c. an ipcc special report on the impacts of global warming of 1.5c above pre-industrial levels and related global greenhouse gas emission pathways, in the context of strengthening the global response to the threat of climate change, sustainable development, and efforts to eradicate poverty [masson-delmotte, v., p. zhai, h.-o. pörtner, d. roberts, j. skea, p.r. shukla, a. pirani, w. moufouma-okia, c. péan, r. pidcock, s. connors, j.b.r. matthews, y. chen, x. zhou, m.i. gomis, e. lonnoy, t. maycock, m. tignor, and t. waterfield (eds.)].*, *In Press* (2018).
- [111] C. B. Field and V. R. Barros, *Climate change 2014–Impacts, adaptation and vulnerability: Regional aspects*. Cambridge University Press, 2014.

- [112] S. Seneviratne, N. Nicholls, D. Easterling, C. Goodess, S. Kanae, J. Kossin, Y. Luo, J. Marengo, K. McInnes, M. Rahimi, *et. al.*, *Changes in climate extremes and their impacts on the natural physical environment*, .
- [113] K. E. Trenberth, A. Dai, G. Van Der Schrier, P. D. Jones, J. Barichivich, K. R. Briffa, and J. Sheffield, *Global warming and changes in drought*, *Nature Climate Change* **4** (2014), no. 1 17–22.
- [114] M. A. Altieri and C. I. Nicholls, *The adaptation and mitigation potential of traditional agriculture in a changing climate*, *Climatic Change* **140** (2017), no. 1 33–45.
- [115] G. Fischer, M. Shah, F. N. Tubiello, and H. Van Velhuizen, *Socio-economic and climate change impacts on agriculture: an integrated assessment, 1990–2080*, *Philosophical Transactions of the Royal Society B: Biological Sciences* **360** (2005), no. 1463 2067–2083.
- [116] R. Mendelsohn, J. Arellano-Gonzalez, and P. Christensen, *A ricardian analysis of mexican farms*, *Environment and Development Economics* (2010) 153–171.
- [117] P. S. BIRTHAL, T. Khan, D. S. Negi, and S. Agarwal, *Impact of climate change on yields of major food crops in india: Implications for food security*, *Agricultural Economics Research Review* **27** (2014), no. 347-2016-17126 145–155.
- [118] P. Dasgupta, J. Morton, D. Dodman, B. Karapinar, F. Meza, M. G. Rivera-Ferre, A. Toure Sarr, and K. E. Vincent, *Rural areas*, .
- [119] J. E. Baez, D. Kronick, and A. D. Mason, *Rural households in a changing climate*. The World Bank, 2013.
- [120] H. Kazianga and C. Udry, *Consumption smoothing? livestock, insurance and drought in rural burkina faso*, *Journal of Development economics* **79** (2006), no. 2 413–446.
- [121] A. Wineman, N. M. Mason, J. Ochieng, and L. Kirimi, *Weather extremes and household welfare in rural kenya*, *Food security* **9** (2017), no. 2 281–300.
- [122] J. E. Baez, L. Lucchetti, M. E. Genoni, and M. Salazar, *Gone with the storm: Rainfall shocks and household well-being in guatemala*, 2015.
- [123] M. C. Acevedo, *The effect of extreme hydro-meteorological events on labor market outcomes: evidence from the colombian caribbean*, *Unpublished paper*, *World Bank, Washington, DC* (2016).
- [124] M. Rosales-Rueda, *The impact of early life shocks on human capital formation: Evidence from el niño floods in ecuador*, *Journal of health economics* **62** (2018) 13–44.

- [125] Mahajan, *Blame it on the rain?: Gender differentiated impacts of drought on agricultural wage and work in india*, 2014.
- [126] S. Lohmann and T. Lechtenfeld, *The effect of drought on health outcomes and health expenditures in rural vietnam*, *World development* **72** (2015) 432–448.
- [127] K. Joshi, *The impact of drought on human capital in rural india*, *Environment and Development Economics* **24** (2019), no. 4 413–436.
- [128] DOF, *Programa especial de cambio climático 2014-2018. publicado en el diario oficial de la federación el 28 de abril de 2014.*, .
- [129] L. M. Hunter, S. Murray, and F. Riosmena, *Rainfall patterns and us migration from rural mexico*, *International Migration Review* **47** (2013), no. 4 874–909.
- [130] SEMARNAT, *Estadísticas del agua en méxico, edición 2008. gobierno de la república mexicana*, .
- [131] INECC, *México: Sexta comunicación nacional y segundo informe bienal de actualización ante la convención marco de las naciones unidas sobre el cambio climático*, 2018.
- [132] S. Mardero, B. Schmook, J. O. López-Martínez, L. Cicero, C. Radel, and Z. Christman, *The uneven influence of climate trends and agricultural policies on maize production in the yucatan peninsula, mexico*, *Land* **7** (2018), no. 3 80.
- [133] G. N. Murray-Tortarolo and V. J. Jaramillo, *The impact of extreme weather events on livestock populations: the case of the 2011 drought in mexico*, *Climatic Change* **153** (2019), no. 1 79–89.
- [134] A. Monterroso, C. Conde, C. Gay, D. Gómez, and J. López, *Two methods to assess vulnerability to climate change in the mexican agricultural sector*, *Mitigation and Adaptation Strategies for Global Change* **19** (2014), no. 4 445–461.
- [135] INEGI, *Volumen y crecimiento. población total según tamaño de localidad para cada entidad federativa*, *Instituto Nacional de Estadística y Geografía* (2010).
- [136] CONEVAL, *Diez años de medición de pobreza multidimensional en méxico: avances y desafíos en política socialmedición de la pobreza serie 2008-2018*. [https://www.coneval.org.mx/Medicion/MP/Documents/Pobreza\\_18/Pobreza\\_2018\\_CONEVAL.pdf](https://www.coneval.org.mx/Medicion/MP/Documents/Pobreza_18/Pobreza_2018_CONEVAL.pdf), .
- [137] C. Conde, R. Ferrer, and S. Orozco, *Climate change and climate variability impacts on rainfed agricultural activities and possible adaptation measures. a mexican case study*, *Atmósfera* **19** (2006), no. 3 181–194.

- [138] R. Guerrero Compeán *et. al.*, *Weather and welfare: Health and agricultural impacts of climate extremes, evidence from mexico*, tech. rep., Inter-American Development Bank, 2013.
- [139] K. Jessoe, D. T. Manning, and J. E. Taylor, *Climate change and labour allocation in rural mexico: Evidence from annual fluctuations in weather*, *The Economic Journal* **128** (2018), no. 608 230–261.
- [140] A. Lopez-Feldman *et. al.*, *Climate change, agriculture, and poverty: A household level analysis for rural mexico*, *Economics Bulletin* **33** (2013), no. 2 1126–1139.
- [141] E. Rodriguez-Oreggia, A. De La Fuente, R. De La Torre, and H. A. Moreno, *Natural disasters, human development and poverty at the municipal level in mexico*, *The Journal of Development Studies* **49** (2013), no. 3 442–455.
- [142] R. J. Nawrotzki, J. DeWaard, M. Bakhtsiyarava, and J. T. Ha, *Climate shocks and rural-urban migration in mexico: exploring nonlinearities and thresholds*, *Climatic change* **140** (2017), no. 2 243–258.
- [143] S. Feng, A. B. Krueger, and M. Oppenheimer, *Linkages among climate change, crop yields and mexico–us cross-border migration*, *Proceedings of the national academy of sciences* **107** (2010), no. 32 14257–14262.
- [144] D. M. Liverman, *Drought impacts in mexico: climate, agriculture, technology, and land tenure in sonora and puebla*, *Annals of the Association of American Geographers* **80** (1990), no. 1 49–72.
- [145] D. W. Stahle, J. V. Diaz, D. J. Burnette, J. C. Paredes, R. R. Heim, F. K. Fye, R. A. Soto, M. D. Therrell, M. K. Cleaveland, and D. K. Stahle, *Major mesoamerican droughts of the past millennium*, *Geophysical Research Letters* **38** (2011), no. 5.
- [146] M. Dell, *Path dependence in development: Evidence from the mexican revolution*, *Harvard University, mimeograph* (2012).
- [147] D. W. Stahle, E. R. Cook, D. J. Burnette, J. Villanueva, J. Cerano, J. N. Burns, D. Griffin, B. I. Cook, R. Acuna, M. C. Torbenson, *et. al.*, *The mexican drought atlas: Tree-ring reconstructions of the soil moisture balance during the late pre-hispanic, colonial, and modern eras*, *Quaternary Science Reviews* **149** (2016) 34–60.
- [148] J. Tutino, *From insurrection to revolution in Mexico: social bases of agrarian violence, 1750-1940*. Princeton University Press, 1986.
- [149] D. Acemoglu, L. Fergusson, and S. Johnson, *Population and conflict*, *The Review of Economic Studies* **87** (2020), no. 4 1565–1604.

- [150] C. I. Speranza, B. Kiteme, P. Ambenje, U. Wiesmann, and S. Makali, *Indigenous knowledge related to climate variability and change: insights from droughts in semi-arid areas of former makueni district, kenya*, *Climatic change* **100** (2010), no. 2 295–315.
- [151] E. Skoufias and K. Vinha, *The impacts of climate variability on household welfare in rural mexico*, *Population and Environment* **34** (2013), no. 3 370–399.
- [152] R. Lobato-Sanchez, R. Pascual-Ramirez, and A. Albanil-Encarnacion, *[regional climates] mexico [in “state of the climate in 2011”].*, *Bull. Amer. Meteor. Soc.* **93(7)**, **S167-169** (2012).
- [153] F. Arreguín Cortés, M. López Pérez, D. Korenfeld Federman, D. Ortega Gaucin, *et. al.*, *The national drought policy in mexico*, .
- [154] D. Ortega Gaucin, I. Velasco Velasco, *et. al.*, *Aspectos socioeconómicos y ambientales de las sequías en méxico*, .
- [155] P. Martínez Austria, C. Patiño Gómez, *et. al.*, *Efectos del cambio climático en los recursos hídricos de méxico: volumen iii: atlas de vulnerabilidad hídrica en méxico ante el cambio climático*, 2010.
- [156] B. Orlowsky and S. I. Seneviratne, *Elusive drought: uncertainty in observed trends and short-and long-term cmip5 projections*, *Hydrology and Earth System Sciences* **17** (2013), no. 5 1765–1781.
- [157] P. Romero-Lankao, J. Smith, D. D.J., N. Diffenbaugh, P. Kinney, P. Kirshen, P. Kovacs, and L. Villers Ruiz, *Changes in climate extremes and their impacts on the natural physical environment*, .
- [158] G. Murray-Tortarolo, P. Friedlingstein, S. Sitch, V. J. Jaramillo, F. Murguía-Flores, A. Anav, Y. Liu, A. Arneth, A. Arvanitis, A. Harper, *et. al.*, *The carbon cycle in mexico: past, present and future of c stocks and fluxes*, *Biogeosciences* **13** (2016), no. 1 223–238.
- [159] R. Prieto-González, V. Cortés-Hernández, and M. Montero-Martínez, *Variability of the standardized precipitation index over méxico under the a2 climate change scenario*, *Atmósfera* **24** (2011), no. 3 243–249.
- [160] M. Wehner, D. R. Easterling, J. H. Lawrimore, R. R. Heim, R. S. Vose, and B. D. Santer, *Projections of future drought in the continental united states and mexico*, *Journal of Hydrometeorology* **12** (2011), no. 6 1359–1377.
- [161] G. N. Murray-Tortarolo, *Seven decades of climate change across mexico*, *Atmósfera* **34** (2021), no. 2 217–226.

- [162] CONEVAL, *Coneval informa la evolución de la pobreza 2010-2016. dirección de información y comunicación social. comunicado de prensa no. 09.*  
<https://www.coneval.org.mx/SalaPrensa/Comunicadosprensa/Documents/Comunicado-09-Medicion-pobreza-2016.pdf>, .
- [163] Y. Kusunose and T. J. Lybbert, *Coping with drought by adjusting land tenancy contracts: A model and evidence from rural morocco*, *World Development* **61** (2014) 114–126.
- [164] E. F. Wood, S. D. Schubert, A. W. Wood, C. D. Peters-Lidard, K. C. Mo, A. Mariotti, and R. S. Pulwarty, *Prospects for advancing drought understanding, monitoring, and prediction*, *Journal of Hydrometeorology* **16** (2015), no. 4 1636–1657.
- [165] V. Magaña, B. Méndez, C. Neri, and G. Vázquez, *El riesgo ante la sequía meteorológica en México*, *Realidad, Datos y Espacio. Revista Internacional de Estadística y Geografía* **9** (2018) 35–48.
- [166] J. D. Angrist and J.-S. Pischke, *Mostly harmless econometrics: An empiricist's companion*. Princeton university press, 2008.
- [167] J. M. Wooldridge, *Econometric analysis of cross section and panel data*. MIT press, 2010.
- [168] CONEVAL, *Anexo técnico para la construcción del Índice de la tendencia laboral de la pobreza (itlp)*, .
- [169] P. D. Udmale, Y. Ichikawa, S. Manandhar, H. Ishidaira, A. S. Kiem, N. Shaowei, and S. N. Panda, *How did the 2012 drought affect rural livelihoods in vulnerable areas? empirical evidence from india*, *International Journal of Disaster Risk Reduction* **13** (2015) 454–469.
- [170] M. Horridge, J. Madden, and G. Wittwer, *The impact of the 2002–2003 drought on australia*, *Journal of Policy Modeling* **27** (2005), no. 3 285–308.
- [171] D. Gautier, D. Denis, and B. Locatelli, *Impacts of drought and responses of rural populations in west africa: A systematic review*, *Wiley Interdisciplinary Reviews: Climate Change* **7** (2016), no. 5 666–681.
- [172] E. Skoufias and S. W. Parker, *Job loss and family adjustments in work and schooling during the mexican peso crisis*, *Journal of Population Economics* **19** (2006), no. 1 163–181.
- [173] A. Kochar, *Explaining household vulnerability to idiosyncratic income shocks*, *The American Economic Review* **85** (1995), no. 2 159–164.

- [174] A. Kochar, *Smoothing consumption by smoothing income: hours-of-work responses to idiosyncratic agricultural shocks in rural india*, *Review of Economics and Statistics* **81** (1999), no. 1 50–61.
- [175] S. W. Parker and E. Skoufias\*, *The added worker effect over the business cycle: evidence from urban mexico*, *Applied Economics Letters* **11** (2004), no. 10 625–630.
- [176] J. A. Pagán and S. M. Sánchez, *Gender differences in labor market decisions: Evidence from rural mexico*, *Economic Development and Cultural Change* **48** (2000), no. 3 619–637.
- [177] D. Cogneau and R. Jedwab, *Commodity price shocks and child outcomes: the 1990 cocoa crisis in cote d'ivoire*, *Economic Development and Cultural Change* **60** (2012), no. 3 507–534.
- [178] DOF, *Acuerdo por el que se emiten las reglas de operación del programa de desarrollo humano oportunidades, para el ejercicio fiscal 2012. publicado en el diario oficial de la federación el 30 de diciembre de 2011.*, .
- [179] D. M. Liverman, *Vulnerability and adaptation to drought in mexico*, *Nat. Resources J.* **39** (1999) 99.